

Delft University of Technology
Faculty of Civil Engineering and Geosciences

**Reservoir stratigraphy and architecture of glacial tunnel
valleys reservoirs: Examples from Ordovician of North
Africa and Pleistocene of North America.**

MSc Thesis by Pablo Barros



Delft, 25th of August 2011

Graduation committee:

- *Prof. Dr. Andrea Moscariello – Delft University of Technology and University of Geneva*
- *Mr. Adriaan Janszen- Delft University of Technology*
- *Dr. Neil McDougall – Repsol YPF*
- *Prof. Dr. Giovanni Bertotti - Delft University of Technology*

1 Abstract

Upper Ordovician glaciogenic rocks from Block-NC186, in the Murzuq Basin, SW Libya, represent important hydrocarbon reservoirs. The producing reservoirs are found in glacial incisions filled by the Melaz Shuqran and Mamuniyat formations. These formations present complex reservoir architecture and high sediment heterogeneity. Understanding the morphology and internal reservoir architecture in these incisions is important in order to improve prediction in such complex reservoir systems.

This study describes the Upper Ordovician formations from Block-NC186 (Libya) using an integrated approach based on seismic, isopach maps, well logs, core and chemostratigraphic data. The results are compared and contrasted with the infill of a Pleistocene glacial incision from Lake Simcoe (Ontario, Canada) inferred from high-resolution seismic data.

Results show differences in the infilling history of the two systems. Sedimentological records from the Upper Ordovician show different phases of ice-sheet advance, retreat and glacio-isostatic rebound infilling a complex network of mainly fault-controlled incisions, of very variable widths and depths, cut under the pre-glacial Middle Ordovician Hawaz Formation. In the other hand, the Pleistocene infill from the Lake Simcoe shows a similar incised valley, filled during small fluctuations of the ice front in a single episode of ice-sheet retreat within low energy lacustrine environment.

The comparison of these two systems highlights the variability of the glaciogenic infill and the need to incorporate influencing parameters such as regional tectonic trend, bedrock types, glaciations amplitudes and geographical environments into the geological models aimed to reconstruct and predict reservoir distribution within these glacial sedimentary systems.

2 Acknowledgments

I would like to thank:

Professor Andrea Moscariello, my supervisor, for giving me the opportunity to participate in this interesting research subject and for his help and advices during the last 7 months.

Adriaan Janszen, for being my daily supervisor, for his patience, guidance, help and comments in the different topics of the research.

Neil McDougall and Repsol, for providing the data necessary for the study.

My classmates, Efe Kermen, Koen van Tooreenburg, Kevin Bisdom, Jonatan Flores, Rahul-Mark Fonseca, Dorien Frequien, Siavash Kahrobaie and all others present daily during this 7 months.

My friends and neighbours from Marcushof, which made these 7 months so special and for being my second family in The Netherlands.

Finally, I would like to specially thank my family for supporting me during my Master studies in Delft.

Table of contents

1	Abstract.....	2
2	Acknowledgments.....	3
3	Introduction	6
3.1	Definition of tunnels valley	6
3.2	Problem	6
3.3	Study Approach and Objectives	6
4	Short review of sedimentary architecture and sequence stratigraphy of Ordovician glacial deposits	8
4.1	Sequence Stratigraphy in glaciated continental shelves	8
4.1.1	System tracts and unconformities	8
4.2	Facies association	9
4.2.1	Glacial Maximum (GMaST)	9
4.2.2	Ice-sheet retreat (GRST)	9
4.2.3	Glacial minimum periods (GMiST)	10
4.2.4	Ice-sheet advance (GAST)	10
4.3	Stratigraphic framework	11
PART 1: Block NC186, Murzuq Basin, SW Lybia		
5	Introduction	13
6	Location.....	13
7	Geological setting	14
7.1	Geological evolution of the Murzuq Basin during the Palaeozoic.....	14
7.2	The Ordovician glaciations.....	15
7.3	Ordovician Stratigraphy.....	17
7.3.1	The Hawaz Formation	17
7.3.2	The Melaz Shuqran Formation.....	18
7.3.3	The Mamuniyat Formation.....	19
7.4	Sedimentary architecture of the Upper Ordovician deposits in analogues from the Murzuq Basin.....	22
8	Data set.....	25
8.1	Study Approach	25
8.1.1	Structural framework.....	25
8.1.2	Well data	31
8.1.3	Core descriptions	32
8.1.4	Chemostrat data.....	32
9	Results	33
9.1	Description	33
9.1.1	Chemostrat data.....	33
9.1.2	Core descriptions	39

9.1.3	Seismic Lines description and interpretation	43
9.2	Interpretation of the results	55
9.2.1	Chemostrat results.....	55
9.2.2	Interpretation of the formations and depositional environments	64
9.2.3	Cross-sections.....	67
9.2.4	Infilling history.....	70

PART 2: Lake Simcoe, Ontario, Canada

10	Introduction.....	71
11	Location.....	71
12	Geological setting.....	72
13	Data set.....	74
13.1	Study Approach	76
13.1.1	Lake Simcoe : seismostratigraphic sequences.....	76
13.1.2	Seismic facies	78
14	Results.....	80
14.1	Description	80
14.1.1	Seismic stratigraphy.....	81
14.1.2	Internal reflection characteristics	87
14.2	Interpretation and infilling history.....	88
15	Discussion.....	91
16	Conclusions.....	94
17	References	95
18	Appendixes.....	97

3 Introduction

3.1 Definition of tunnels valley

Glacial tunnel valleys are large U-shaped depressions originally cut under the glacial ice near the margin of continental ice sheets. Their dimensions can be several kilometres wide, tens of kilometres long and hundreds of meters deep (O Cofaigh, 1996). These morphological structures may be filled with large thickness of sandy deposits that create good quality reservoirs (see Figure 1).

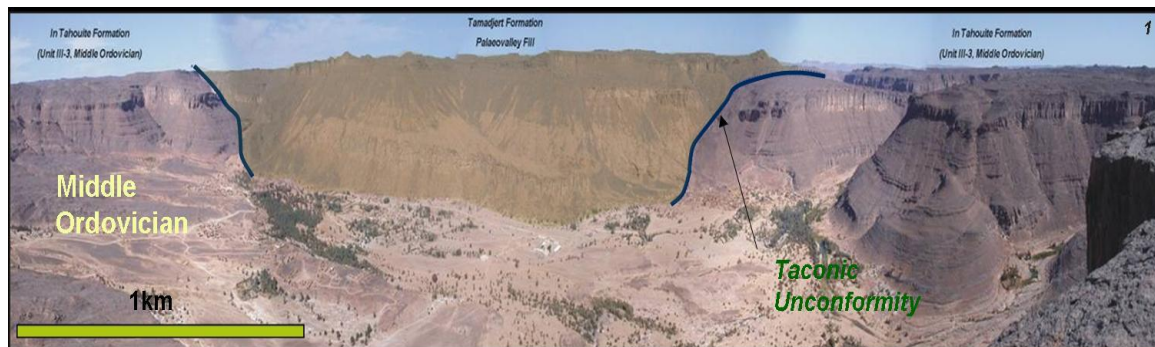


Figure 1 Erosively-bounded, steep-sided, narrow palaeovalley exposed at Iherir village, Tassili N Ajjers; SE Algeria; the valley fill is >250m thick. After Neil McDougal et al., 2008.

3.2 Problem

These glaciogenic reservoirs can contain natural resources; in Europe and North America they are important water reservoirs whereas in North Africa they represent important hydrocarbons reservoirs.

In both cases, their high sediment heterogeneity and complex internal architecture make these reservoirs very difficult to model, therefore hard to predict.

For this reason, despite the relatively large amount of studies carried out on this matter, large uncertainties still remain. Therefore it is important to improve the understanding on the genesis, architecture and the nature of the subsequent infilling processes.

3.3 Study Approach and Objectives

In this study we propose to examine two cases studies in two different settings: the deep subsurface hydrocarbon reservoirs from the Upper Ordovician Mamuniyat Formation in licence Block NC186, Murzuq Basin (SW Libya) and the shallow Quaternary glacial deposits from Lake Simcoe, Ontario, Canada (Figure 3 and Figure 46).

Based on the available data provided by Repsol (Block NC186) and the Geological Survey of Canada (Lake Simcoe), an integrated approach based on seismic, isopach maps, well logs, core and chemostratigraphic data, was used in order to compare and contrast valley geometries and infill architecture.

In particular, the study aimed to compare different geological settings and understand the effects of different parameters such as the influence of the bedrock type, its age, the timing of infilling and the scale of the depositional setting (shelf margin vs. continental lake).

The ultimate objectives of this study is to capture any communalities and differences between these two locations which can be then used to assist modelling and prediction of subsurface glacial tunnel valley reservoirs.

4 Short review of sedimentary architecture and sequence stratigraphy of Ordovician glacial deposits

Here, the major characteristics of glacial sedimentary architecture combined with notions of glacial sequence stratigraphy are described. These elements are important in order to understand the facies distribution and the sequence of events in time responsible for the deposition of the Upper Ordovician formations found in our area of study.

First, basic notions from proposed sequence stratigraphic model in temperate, glaciated continental shelves by Powell & Cooper (2002) will be presented. Later, a description of the deposits types associated with their glacial regime by Sutcliffe et al. (2000) will be integrated into this sequence stratigraphic framework.

4.1 Sequence Stratigraphy in glaciated continental shelves

Powell & Cooper (2002) describe the different systems tracts found in a glacially influenced environment and they define the general principles that differentiate sequence stratigraphy frameworks affecting low latitudes margins from high latitude glaciated continental margins.

4.1.1 System tracts and unconformities

The glacial system tracts defined by Powell and Cooper (2002) are related to glacial advance and retreat signatures:

GMaST: Glacial maximum

GRST: Glacial retreat

GMiST: Glacial minimum

GAST: Glacial advance

Furthermore, the authors describe the disconformities bounding each of these system tracts as follow:

GRS: Grounding-line retreat surface

MRS: Maximum (glacial) retreat surface

GAS: Glacial advance surface

They define a regional significant unconformity that bounds each glacial advance and: a glacial erosion surface (GES).

4.2 Facies association

Sutcliffe et al. (2000) divide the glacial deposits in two parts: deposits associated to glacial advance and deposits associated to glacial retreat. Powell & Cooper (2002) define more in detail the transitional periods between both regimes.

Here we describe the deposits and elements architecture formed during the glacial maximum stage, the elements related to the ice-sheet retreat periods, the glacial minimum stage and finally the remains of a glacial advance stage.

4.2.1 Glacial Maximum (GMaST)

The main facies deposited during glacial maximum system tracts (GMaST) are subglacial till. These deposits are usually deposited above a glacial erosion surface (GES) although commonly absent.

4.2.2 Ice-sheet retreat (GRST)

They are the dominant glacial deposits found in glacio-marine rocks. Sutcliffe et al. (2000) divide these deposits into three categories: ice-contact deposits, glacial-marine shelf deposits and post-glacial isostatic rebound elements.

Sutcliffe et al. (2000) describe the ice-contact elements as intraformational conglomerates composed of “matrix-supported, polymictic pebble sized clasts (or larger) in a granule-rich sandstone matrix” in fining upwards sequences. They interpret the conglomeratic beds as “subaqueous debris flows generated at the grounding line of an ice-sheet”. Powell et al. (2002) add that the deposition of such sediments is dominated by the effects of glacial meltwater. These gravel deposits can be “replaced laterally and vertically by cross-stratified, coarsening-upward sandstones”, which they interpret as “subaqueous ice-contact fans in front of an ice sheet ending in tidewater” deposited during a stillstand period of the ice-sheet retreat.

Glacial-marine shelf deposits are described by Sutcliffe et al. (2000) as more laterally extensive deposits with a higher mudstone fraction. These deposits are usually well sorted, but the authors indicate that they can be some exceptions such as “sandy diamictites” or “shales with outsized clasts”, which would be related to ice-rafted debris. Other glacial-marine shelf deposits can correspond to interbedded sandstones and claystone. These deposits can present hummocky and swaley cross-stratification, implying shelf sedimentation and forming fining upward sequences. Geometries of such deposits are described by Powell & Cooper (2000). They describe the geometry of the deposits as “banks or wedges/fans forming the offlap-break at the outer continental shelf and also form the retrogradational stacking of bank systems on the shelf”.

Finally, the postglacial isostatic rebound is described by Sutcliffe et al. (2000) as dependent on the rebound speed. Erosion characterises fast isostatic rebounds whereas slow isostatic rebound will be characterise by coarsening/shallowing upward successions. Furthermore, they suggest that ice-retreating conditions could be accompanied by bioturbation due to “recolonization by infaunal communities”.

Examples of dimensions and maximum height for uplifts can be found in a paper from Walcott (1973). These values vary according to the extension of the glaciations. In general terms, the wavelength is measured in a kilometeric scale (1000 to 4000 km) and uplift in a metric scale (maximum uplifts ranging from 45 to 115 m).

4.2.3 Glacial minimum periods (GMiST)

These occur with glacial retreat onto continental areas. It is represented in nearshore by progradational deposits of paralic systems dominated by deltaic and siliciclastic shelf systems, and in the offshore areas by condensed sections.

4.2.4 Ice-sheet advance (GAST)

They are represented by the inversed GRST facies succession, but are also the most likely interval to be eroded during readvance.

In a glacialmarine shelf environment, the sections deposited are mainly coarsening upward sections characterised by erosional and syn-sedimentary deformations.

Syn-sedimentary deformation features due to ice-sheet loading can be present as “stress pillars” formed by partial fluidization of sediments and “loadlike synclines” (meters to tens of meter) formed beneath subglacial erosion surfaces in unlithified sediments. Syn-sedimentary deformation can also be directly related to the ice movement and its shearing action, producing striated surfaces and thrusting or folding in the unlithified sediments. More subglacial deformation results in boudinage and extension of the sediment column (Sutcliffe et al. (2000)).

Figure 2 summarizes all the elements describe above.

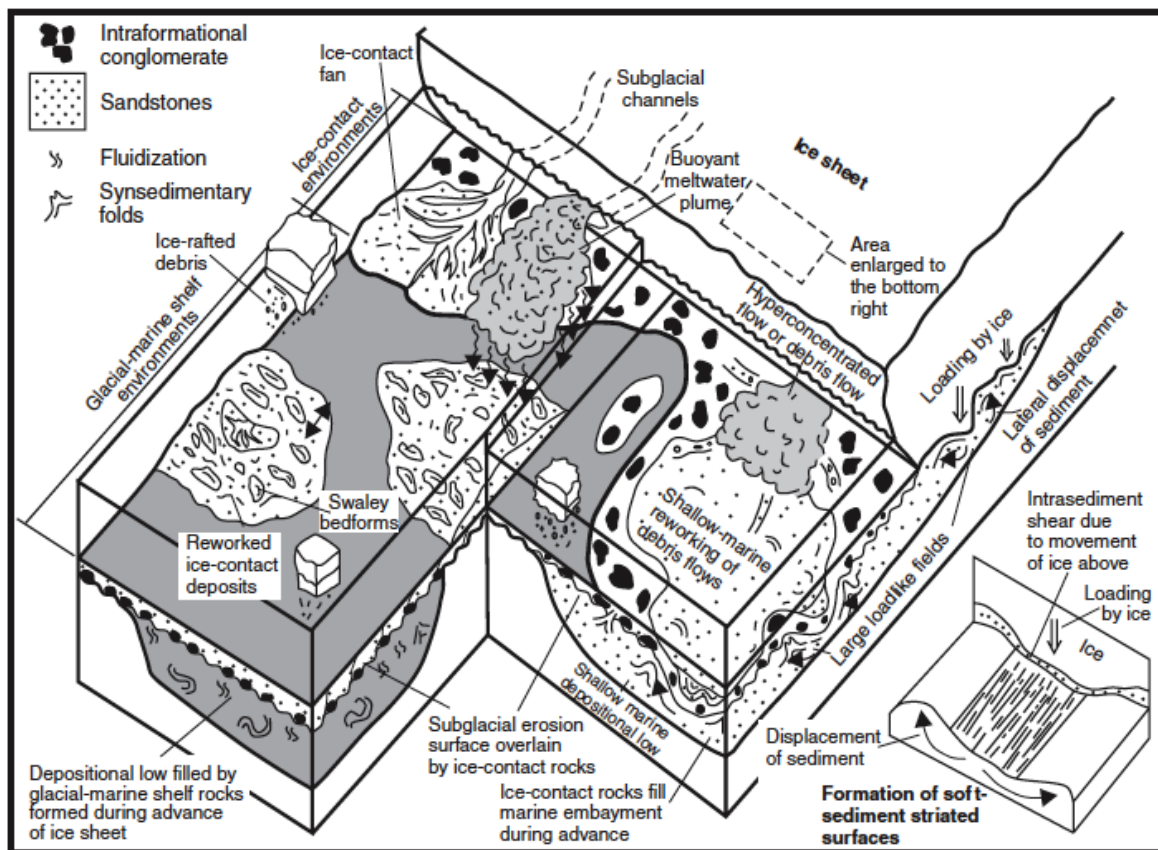


Figure 2 depositional models for Upper Ordovician glaciogenic rocks of northern Africa (left) and South Africa (right) and models for formation of soft sediment striated surfaces and synsedimentary deformation. The model is extracted from Sutcliffe et al. (2000).

4.3 Stratigraphic framework

A stratigraphic framework on which to interpret temperate glaciated continental margins is more complex to define than for lower latitude margins. The main problems are the uncertainties concerning the number of forces controlling accommodation space and being able to identify the causes of water depth variations.

Powell and Cooper (2002) establish that cycles of glacial advance and retreat could control sedimentation and the genesis of system tracts more than other forces such as relative sea level. They defined the principles of sequence stratigraphy for glaciated continental shelves but they insist in 5 different points that play an important role in understanding these system:

1. Glaciers and ice streams within major ice-sheets may fluctuate and behave independently of major global eustatic events;
2. The rapid accumulation rate of sediments at the glacial grounding lines may reduce water depth without changes in relative sea-level;
3. Facies changes vary as a function of water depth changes due to a combination of the magnitude of glacial loading, and the relative timing of glacial fluctuation versus relative sea-level change;
4. Active tectonism can influence sedimentation during icehouse period or glacial events and be responsible for the shelves glaciations;

5. Cross-shelf erosional surfaces on temperate glaciated shelves may appear due to subglacial erosion during glacial advance and not due to exposure during a lowstand in sea level.

To sum up, in glacial contexts, relative sea-level variations are not the major factor controlling sedimentation and genesis of system tracts.

PART 1: The Murzuq Basin, Libya

5 Introduction

The Murzuq Basin is a prolific basin in Libya, North Africa. Major hydrocarbons accumulations are found in the Upper Ordovician glaciogenic succession that infill palaeovalley shaped structures. These reservoirs are now a day the main target of exploration by energy companies.

Studies by many authors, such as Daniel Le Heron, Owen Sutcliffe, Mohamed Ali Kalefa El-ghali and others, describe the sedimentological evolution and architecture of the valley-fill in order to provide models that improve prediction in sedimentary architecture in the subsurface.

In this chapter we compile the basic literature knowledge about these sedimentary types of deposits and apply it to Block-NC186. This block, operated by Repsol SA, presents different fields producing from such reservoir types. Large-scale seismic, log data, core description and more recently chemostrat data has been acquire in those field, giving us different tools for tempting an integrate approach study of the glaciogenic reservoirs.

6 Location

The Murzuq Basin is located on the southwest of Libya, about 800 km south of the capital Tripoli (Figure 3). The basin is bounded by the Gargaf Arch to the north, by the Tihembeka high and the Hoggar Massif in Algeria to the west, the Tibesti Uplift to the east and extends into Niger to the south. The basin has an extension of about 450 km for north to south and from east to west.

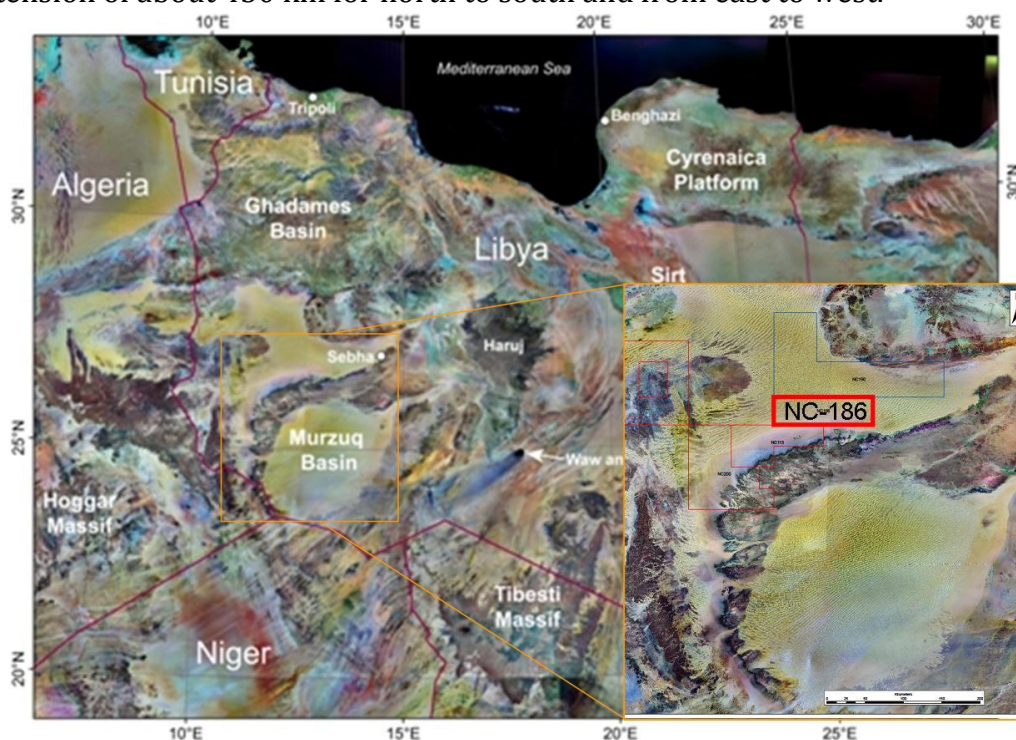


Figure 3 Satellite view of Libya. The Murzuq Basin located in the SW part of Libya and parts of Algeria, Niger and Chad. The zoomed square shows the location of Block NC-186.

7 Geological setting

The Murzuq Basin was initiated during the Palaeozoic era. It is considered a large intracratonic basin with up to 3000m of sedimentary fill extending its boundaries into the neighbouring countries of Algeria, Niger and Chad.

The geological history of the Murzuq Basin has been explained using palaeo-geographic plate reconstruction of the African region.

7.1 Geological evolution of the Murzuq Basin during the Palaeozoic

During the early Palaeozoic, the African craton was part of the Gondwana supercontinent. Ramos et al. (2005) show that palaeo-geographic reconstructions of Gondwana during Ordovician times by several authors, such as Matte (2001), Cocks and Torsvik (2002) and Kuhn and Barnes (2005), place the now a day's North Africa region in the western boundary of Gondwana forming a passive margin (Figure 4).

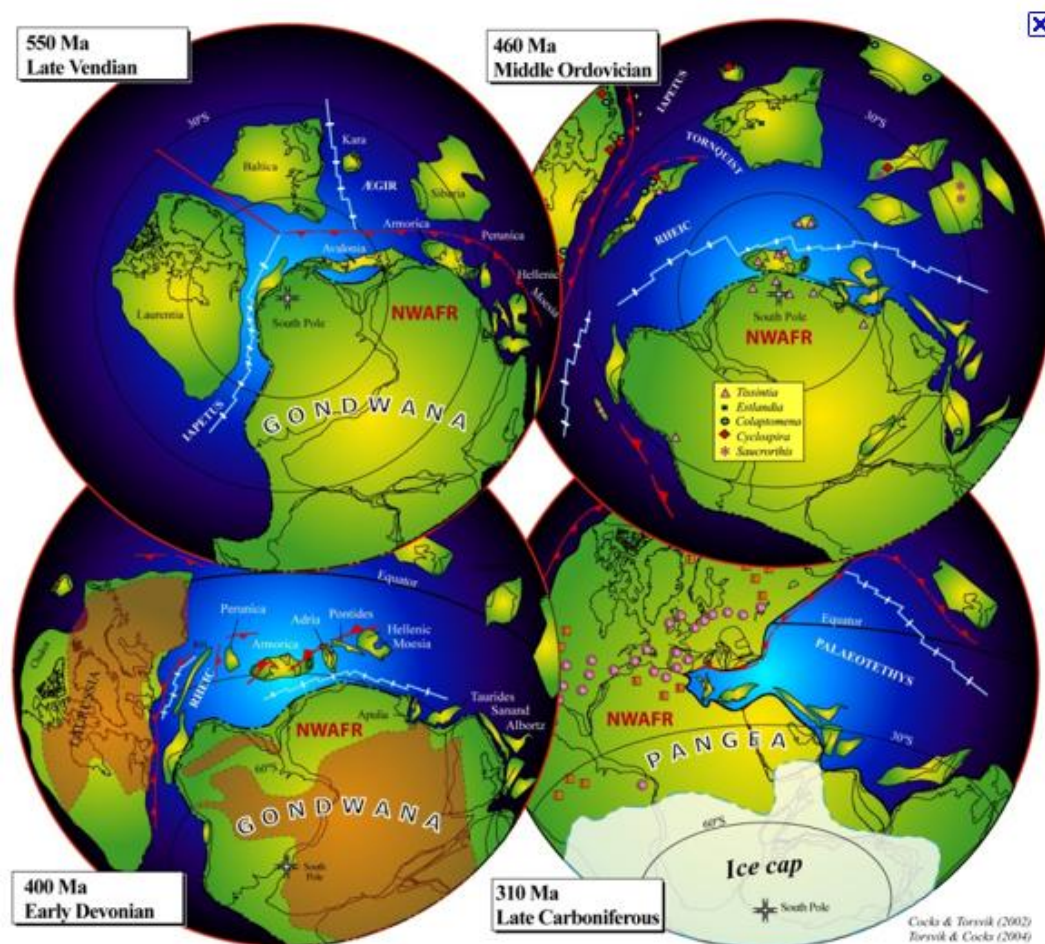


Figure 4 Paleogeographic reconstruction centred in the South Pole, showing the evolution of the African Plate from the late Precambrian to the Palaeozoic times. In the Late Precambrian to Cambrian times, North Africa was dominated by subduction followed by a rifting phase of Avalonia that created the Rheic Ocean. During late Ordovician, NW Africa drifted into south polar latitudes depositing all the sandy glacial to periglacial sediments in the region. Passive margin conditions

dominated during most of the Palaeozoic times. After Carmen Gaina from *The African Plate Project (TAP)* (2009). Picture modified after TH Torsvik.

During the Early to Middle Ordovician, the passive margin was subjected to an extensional regime, leading to the separation of the Avalonia and Baltica terranes (Badalini et al., 2002). The local intensity of this tectonic event is critical to understand the thickness variations of the sedimentary infill of the intracratonic basins of the north Sahara region such as the Murzuq Basin.

The sedimentary record indicates that maximum tectonic activity must have happen during the Middle Ordovician (Darriwilian to Sandbian times) (Echikh and Sola, 2000).

Furthermore, Boote et al. (1998) and Klitzch (2000) state that sedimentation in the eastern Sahara zone was controlled by the development, during the Cambrian and the Early-Middle Ordovician, of a north-south to north-northwest—south-southeast-oriented system of horst and grabens forming wide elongated troughs and basinal areas.

Echikh and Sola (2000) add that the influences of glacial events during that period are responsible for the enhancement of the faulted topography. Topography and the related glacial erosion formed the oriented NW-SE palaeo-valleys, which are now filled by the Hirnantian sediments of the Mamuniyat Formation.

Later stages of the basin formation correspond to an important increase in subsidence from Silurian to Early Devonian times, which is characterised by a regional transgressional event which overlapped the Silurian shales over the Ordovician erosional relief.

7.2 The Ordovician glaciations

The geological history and the sedimentary infill of the Murzuq basin's main reservoir formations are greatly influenced by the glacial events that took place during Late Ordovician times. Deposits related to such events are the now a days main objectives for energy companies in the region.

Hambrey (1985) summarized the evidences of Ordovician glacial deposits and describe the Late Ordovician-Early Silurian period.

The author lists the glaciations records from the Ordovician time, continent by continent, showing records in Africa, Asia, Europe and North and South America. Evidence of glaciations appears in form of several types of landforms (terrestrial glacial, fluvio-glacial and periglacial).

The glacial deposits are characterised by being deposited unconformably over older Ordovician deposits. Each glacial formation can be further divided into different sequences corresponding to episodes of advance and retreat of the ice-sheets and are internally bounded by erosional unconformities.

The author gives what should be the time-span of such glaciations in each continent by dating the stratas containing such deposits. The glaciations appears worldwide to have taken place during Katian to Hirnantian times (Late Ordovician) and finished during the Early to Middle Llandovery age (Early

Silurian), when the Silurian Shales were deposited by a widespread marine transgression. This would suggest that the glaciations occurred intermittently over a period of 35 Ma. However, it's important to notice that authors like Le Heron (2004), using studies from Sutcliffe et al. (2000) suggest a much shorter duration of the glaciations restricting it to the Extraordinarius Zone of the Hirnantian stage (Late Ordovician), of 0.2 to 0.5 Ma in duration.

Causes for the Ordovician glaciations are mainly explained with paleocontinental reconstructions using paleomagnetic data as suggested by Hambrey (1985), but Le Heron (2004) also suggests an important sensitivity of the global climate to the Earth's orbital eccentricity cycles influence during that period.

Plate reconstructions (Figure 5 and Figure 6) show that North Africa was centred over the South Pole in Late Ordovician times. Le Heron et al. (2004) adds that the drift of Gondwana over the South Pole influenced climate change and promoted the growth of an ice-sheet covering up to 65° of palaeolatitude (Scotese et al., 1999). Hambrey (1985) also suggest that the ice moved radially from a point near the pole covering most areas of Africa and the Arabian Peninsula.

The result of such glaciations was the second largest mass extinction in Earth's history and a eustatic sea level drop of about 60m that lead to a significant increase in sediment supply to glacierised continental shelves (Brenchley et al., 1994; 1995; Sutcliffe et al., 2000a, b, 2001).

The glaciations episodes in the region ended by the movement of South America, that gradually replaced Africa over the South Pole (Hambrey, 1985), ending the glacial period over this region.

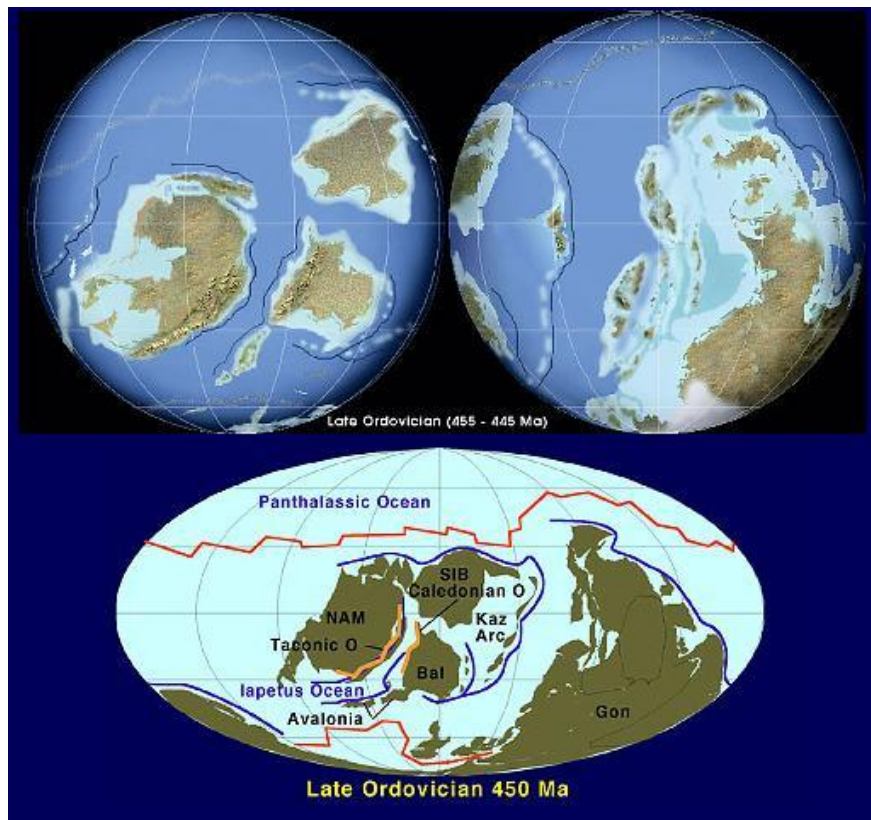


Figure 5 Hemisphere views and mellewide projection indicating first order tectonic elements for the late Ordovician (450 Ma). Ron Blakey, earthscienceworld.org

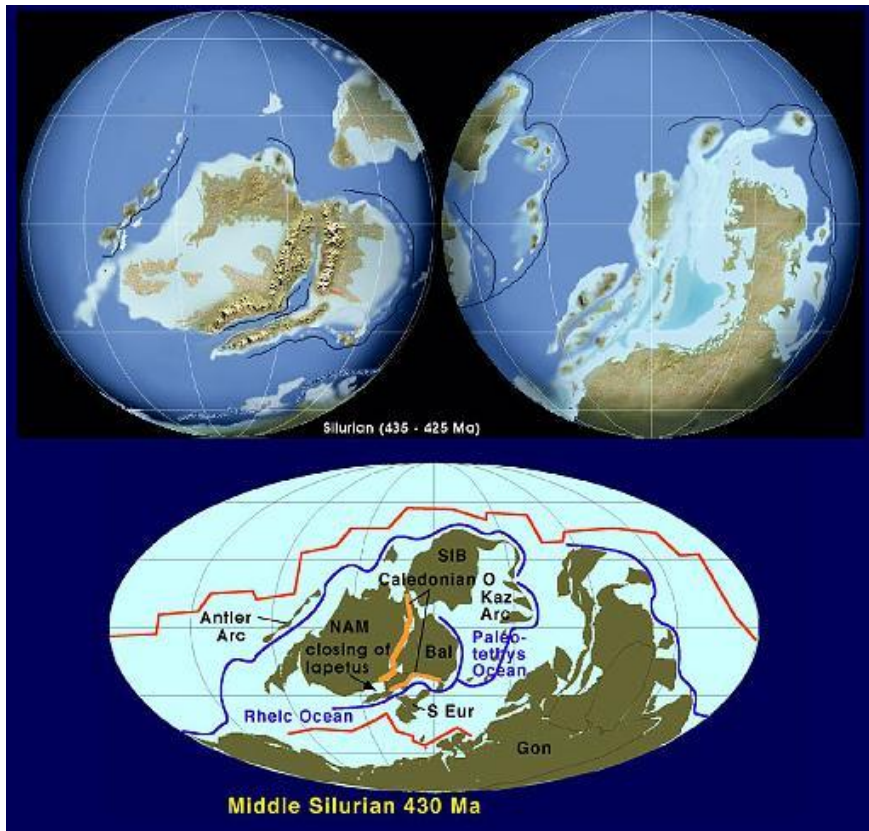


Figure 6 Hemisphere views and mellewide projection indicating first order tectonic elements for the Silurian. Ron Blakey, earthscienceworld.org

7.3 Ordovician Stratigraphy

The Ordovician stratigraphy has been divided into three different formations on the Murzuq Basin: The Hawaz Formation, the Melaz Shuqran Formation and the Mamuniyat Formation; The Bir Tlacin Formation being a transitional formation towards the Silurian Shales (Figure 7).

Furthermore, the uppermost Ordovician succession, Melaz Shuqran formation and Mamuniyat formation, have been subdivided by many authors into four unconformity-bound rock units, which comprise the Melaz Shuqran, the Lower, Middle and Upper Mamuniyat Units.

7.3.1 The Hawaz Formation

Echikh and Sola (2000) describe the Hawaz as the onset of the first major Palaeozoic marine transgression, consisting of alternating fine to medium grained, often quartzitic, semi lithified sandstones with silty shales. The authors describe the presence of Tigillites fossils and traces of bioturbation as one of the formation characteristics. The formation records deposition in a large-scale, with low-gradient estuaries partially controlled by tectonic extension (Ramos et al., 2006). Ramos et al. (2006) explain that the upper boundary of the formation is marked by two erosion surfaces related to the Late Ordovician glaciations. These

important erosion surfaces are responsible for the palaeo-topography that will control the accommodation space available for the following formations deposition (see Figure 8).

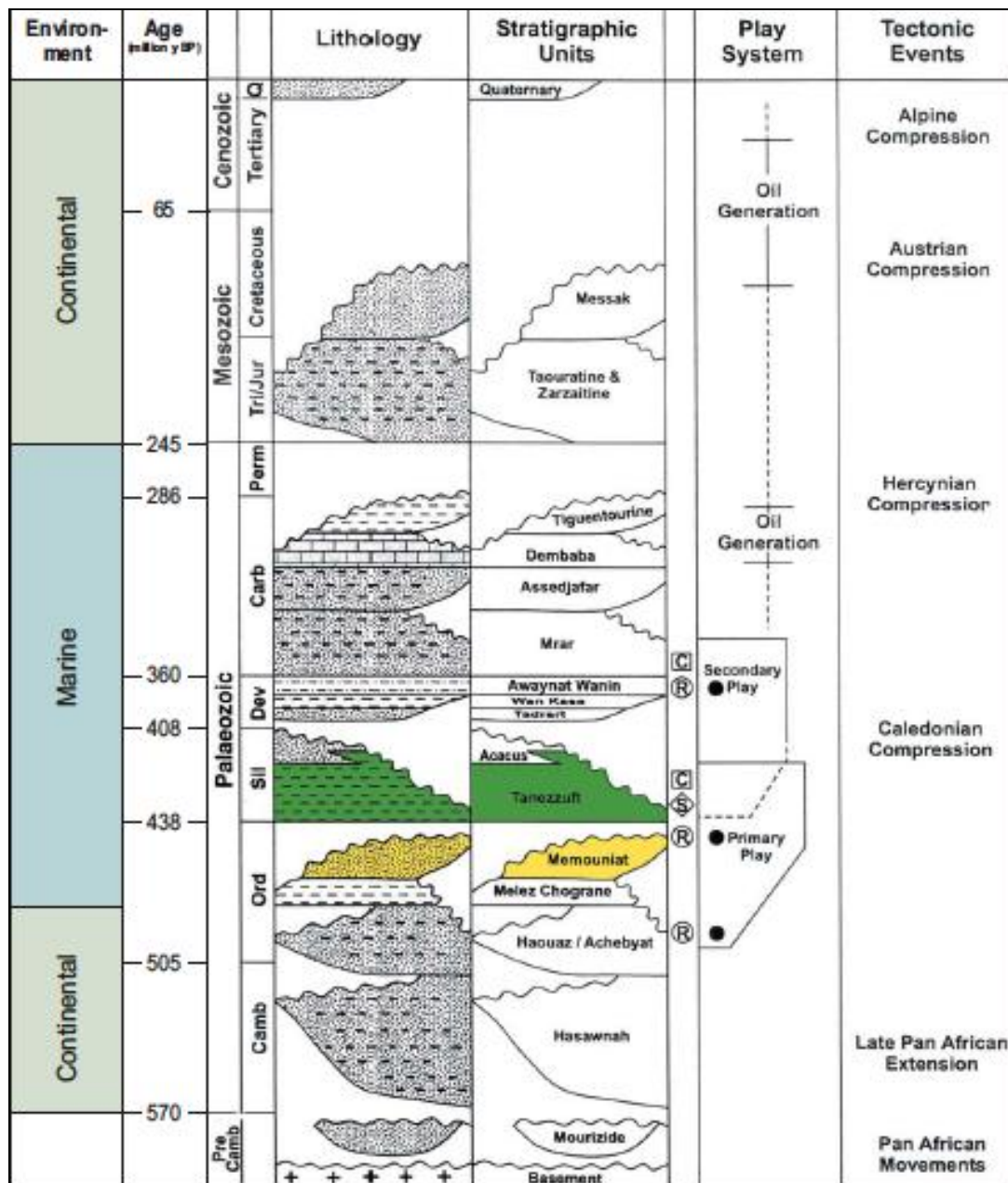


Figure 7 Stratigraphic table from the Murzuq Basin showing the main lithologies from each formation, the formations, the play systems and main tectonic events associated. Note that the nomenclature changes, Hauouaz being the Hawaz Formation, Melez Chegrane the Melaz Shuqran and the Memouniat the Mamuniyat. Picture taken from Rakhit Petroleum Consulting Ltd., "Petroleum migration and charge modelling Murzuq Basin Libya".

7.3.2 The Melaz Shuqran Formation

The Melaz Shuqran formation represents the highstand of the marine transgression initiated during the deposition of the Hawaz Formation (Echikh &

Sola, 2000) as a response to a major glacial retreat following the initial platform-wide incision event marking the onset of the end-Ordovician glaciations (McDougall et al., 2008). The formation is therefore mainly composed of shale deposits. McDougall and Martin (2000) propose that the sediments can be differentiated into glacially and non-glacially influenced facies. Glacially influenced deposits are characterized by presence of dropstones within argillaceous siltstones that have been interpreted by Benn and Evans in 1998 as rain out diamictites and/or ice margin density underflows. Non-glacial sediments are composed of heterolithic deposits, represented by silty mudstones containing wave or current rippled sand lenses (McDougall and Martin, 2000). McDougall et al. (2008) interpreted the environment of deposition to be a combination of glaciomarine processes such as iceberg rainout, diluted debris flows and density underflows derived from tidewater glaciers (see Figure 8).

7.3.3 The Mamuniyat Formation

The Mamuniyat Formation is mainly composed of thick sandstones successions and by quick lateral changes in thickness. It is commonly divided and sub-divided into individual units and sub-units (Figure 8).

Lower Mamuniyat Unit

The Lower Mamuniyat is the most widespread unit from the Mamuniyat formation. This sand dominated formation appears to erosively truncate the underlying argillaceous sediments, locally resting directly on the older pre-glacial sediments of Middle Ordovician age (McDougall et al., 2008). The Lower Mamuniyat is characterized by a predominantly fine-grained, sand-prone succession with a maximum thickness of at least 100m (McDougall and Martin, 2000). The lower part of the formation is described by McDougall et al. (2008) as having locally conglomeratic channel sandstones, climbing megaripples and debrites. In contrast, they describe the upper part of the formation as comprising fine sheetflood sandstones changing laterally into thick and more extensive shallow marine sandsheets. Previously, McDougall and Martin (2000) found a total of 5 facies associations and 25 lithofacies which they associate to different palaeo-environments with a predominance of deposition in a storm-influenced shallow marine setting, sand flats and braided plains. These environments of depositions occurred in pro-glacial or peri-glacial areas during a period of retreat of the glacial ice sheets (McDougall et al., 2008).

Middle Mamuniyat Unit

McDougall and Martin (2000) describe this unit as “the most varied unit in terms of facies characteristics”. They describe it as a variably argillaceous and generally fine-grained package, up to 100m thick, that can be clearly distinguish from the sand-prone Lower Mamuniyat Unit. The Middle Mamuniyat unit is characterized by often occurrences of large-scale syndepositional deformation features such as

slumps, meter-scale load balls, slides and growth faults. These authors found a total of 7 facies associations and 18 lithofacies deposited in a wide range of environments such as in an unstable or destructive delta front, slope and shelf environments and sometimes deposition in a more continental environment such as a braided delta plain. These palaeo-environments are associated to an episode of glacial advance and incision later followed by a post-glacial flooding event when the glaciers retreated.

Upper Mamuniyat Unit

The Upper Mamuniyat unit is described by McDougall and Martin (2000) as a “typically coarse-grained, locally conglomeratic and almost shale free unit”. These characteristics make this unit “the key Upper Ordovician reservoir horizon across the Saharan Platform” (McDougall et al., 2008). According to these authors, common thicknesses are of a couple of ten meters, but thickness variations are important and can exceed 100m in some areas. McDougall and Martin (2000) assigned 6 facies associations and 13 lithofacies mainly deposited in braid plains, sand flat and what they call “bedrock-confined anastomosed high energy fluvial systems”. Others depositional environments have been interpreted in a more local setting with depositions in braid-delta clinofolds and Gilbert deltas. They are interpreted as being formed by subglacial to proglacial flooding events reflecting a further episode of base level fall and ice advance (McDougall et al. 2008).

Furthermore, McDougall et al. (2008) subdivide and describe in detail the Upper Mamuniyat formation, which they call “Sequence U04”, following outcrop work where they identified three-fold subdivision where each component is bounded by significant unconformities.

They divided the Upper Mamuniyat in sub-units or sequences U04a, U04b and U04c. Note that in this report these subunits are assigned the names of UM1, UM2 and UM3 respectively corresponding to “Upper Mamuniyat”.

Sub-unit U04a (UM1) is described as an overall coarse, pebbly and locally conglomeratic sandstones sequence. The sandstones tend to fill up the palaeo-reliefs in the form of massive channel bodies containing abundant mudchips overlain by large-scale, low angle cross-stratification. The deposition is interpreted to belong to major glacial outburst associated with tunnel valleys.

Sub-unit U04b (UM2) is also described as a very coarse formation forming a single coarsening upwards package with trough cross-bedding toward the top marked by a bipolar palaeocurrent distribution. The unit was deposited during a relative sea-level fall that eroded U04a and prograded in the form of tidally-influenced braided deltas and Gilbert deltas.

Sub-unit U04c (UM3), very similar to sub-unit U04a, seems to appear more locally. The unit is composed of incising anastomosing channels deposited in highly irregular surfaces cut in response to a base level fall.

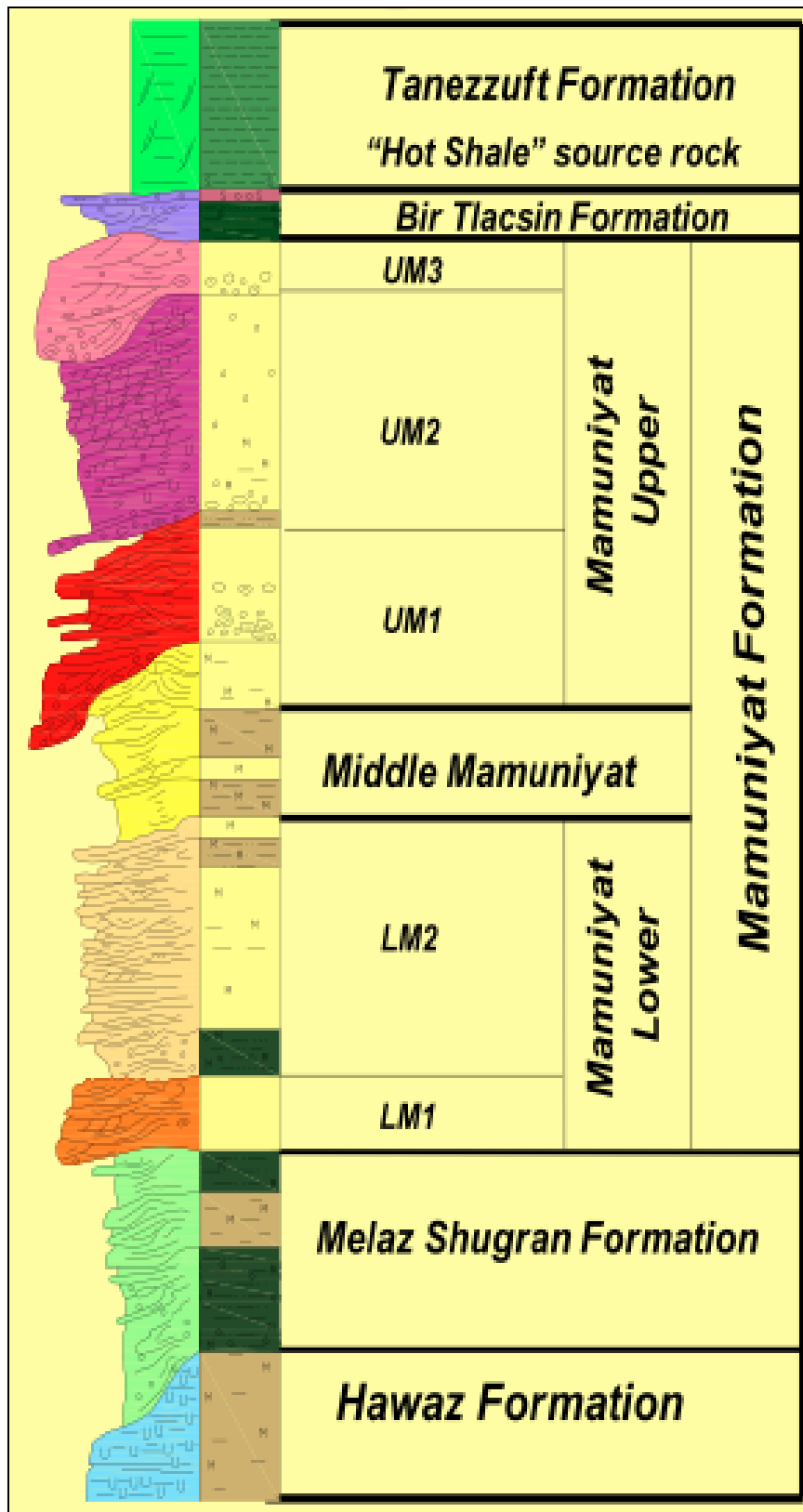


Figure 8 Synthetic type section compiled from various outcrop observations (Ghat area) and stratigraphic column of the Ordovician deposits in the Murzuq Basin. Extracted from McDougall work, Repsol S.A.

7.4 Sedimentary architecture of the Upper Ordovician deposits in analogues from the Murzuq Basin

Several authors have described and interpreted the previous Upper Ordovician formations in palaeo-valley outcrops across the Murzuq Basin (El-ghali, 2005; Le Heron et al., 2004; Le Heron, 2010).

Here we give a short overview of how the units are arranged in outcrop analogues from the Gargaf Arch following a study by Le Heron et al., 2004.

Le Heron et al. (2004) describe a palaeo-valley system 30 km long and with two 4 km tributaries cut into the Hawaz Formation and filled with the Upper Ordovician formations (Figure 9). The palaeo-valley margins are defined by beds dipping at 18-25° towards the axis (structural downbed) and overlapped by an undeformed horizontal fill.



Figure 9 interpreted LANDSAT image of the Gargaf Arch palaeo-valley, modify after Le Heron et al., 2004.

They state that the incisions were “created by subglacial meltwater erosion and glacial loading of a soft substrate during ice-sheet advance”. Furthermore, they describe the initial stage of valley-fill as localised mass-flows and the main infilling stage as northerly prograding, underflow fan-lobes, occurring during a deglaciation stage.

Figure 10 shows the stratal relationship of the Upper Ordovician rocks in the outcrop example from the Gargaf Arch. The schematic interpretation shows how the Upper Ordovician formations (Melaz Shuqran and Mamuniyat Formations) are arranged laterally and bounded by four unconformities (from UC1 eroding

the Hawaz formation to UC4 that separates the Middle and Upper Mamuniyat Fm.)

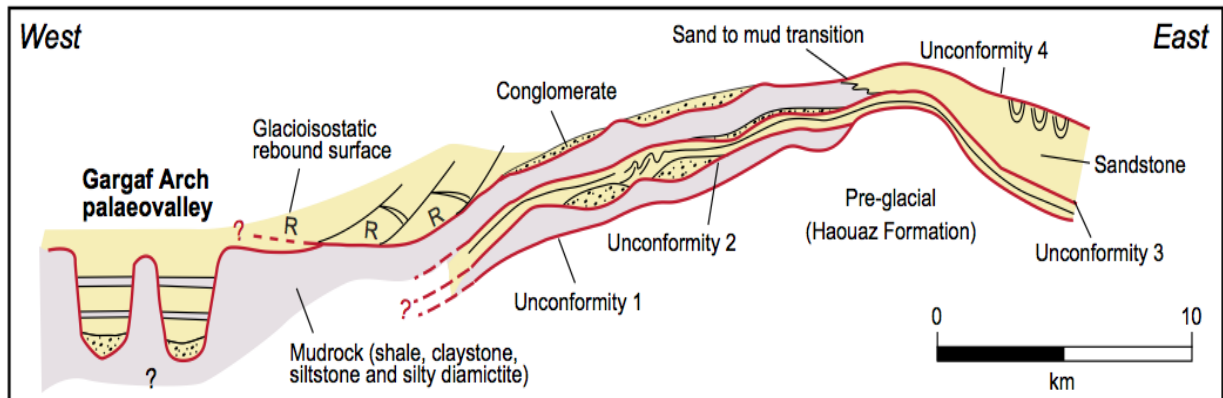
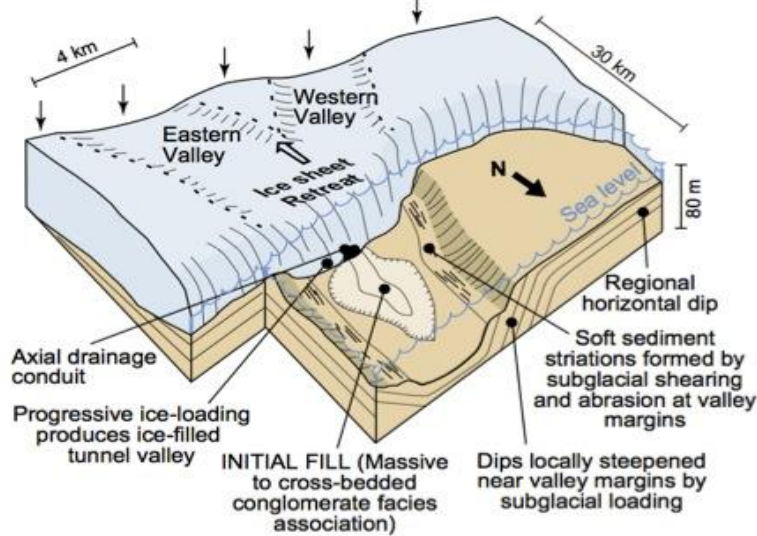


Figure 10 Stratigraphic relationships of Upper Ordovician rocks in the Gargaf Arch palaeo-valley, from Le Heron et al., 2004.

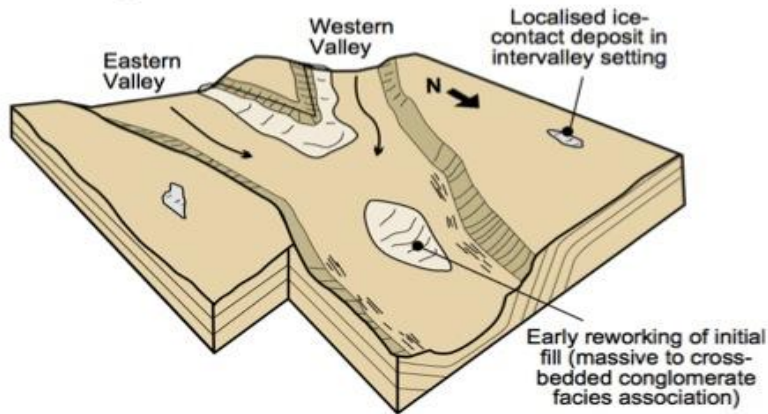
The interpretation suggests that the palaeo-valley infill corresponds only to the Upper Mamuniyat formation and shows the high lateral and vertical heterogeneity in terms of sedimentary architecture.

Finally Figure 11 shows the depositional model for the infill of the Gargaf Arch palaeo-valleys proposed by Le Heron et al., 2004.

(a) Ice sheet loading, incision and initial fill during the early phase of ice sheet retreat



(b) Meltwater underflows moving along tunnel valley axis



(c) Main fill deposited during the later stages of ice sheet retreat-prograding underflow fans

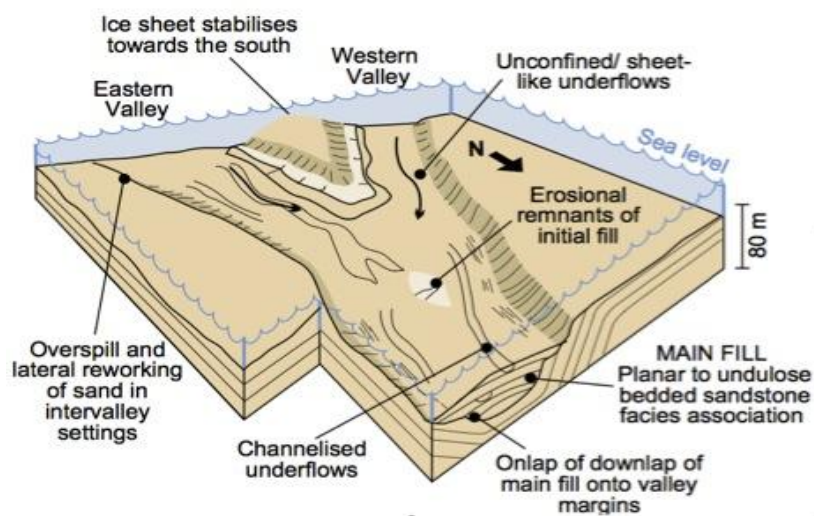


Figure 11 Proposed depositional model of the infill on the Gargaf Arch palaeo-valley, by Le Heron et al., 2004.

8 Data set

The data set available for the study of glaciogenic reservoirs in the Murzuq Basin was composed of digital and literature data.

All digital data came from block NC-186 and was provided by Repsol, the company that operates the field.

The data set was composed of:

- Two previously interpreted digital seismic surfaces,
- An isopach map of the area obtained by subtracting the Top of the Hawaz Formation from the well-defined Top Ordovician,
- Screen captures of random seismic lines passing through selected well in the area,
- Large amount of wells data (coordinates, well tops and logs),
- Quemscan analysis of 3 wells,
- Chemostrat studies in 18 wells,
- Cores descriptions of 4 wells.

Due to the large and diverse nature of the data available for the study, an integrate approach was chosen in order to study the glaciogenic reservoirs from the Murzuq Basin.

8.1 Study Approach

8.1.1 Structural framework

The first step of the integrated approach consisted in defining a structural framework in order to understand the distribution of such deposits.

The isopach map (Figure 12) provided by Repsol, gives a palaeo-geographic framework for the Upper Ordovician highlighting the distribution of palaeo-highs (red/orange) and both narrow and wide palaeo-valleys (green-blue) (McDougall and Gruenwald, 2011).

The isopach map was further simplified in order to highlights the highs and lows and to add the well data information available in the area (Figure 13).

As stated before, the isopach map was obtained by subtracting the Top Hawaz Surface from the Top Tannezuft Surface. These two surfaces are also provided in a digital format and loaded in the Petrel Software, giving the chance to observe the study area in a 3D view (Figure 14 and Figure 15).

Last step in defining the structural framework in the area consisted in studying the seismic lines obtained from a 3D seismic cube provided by Repsol. These lines run from well to well and show how the Upper Ordovician truncates, at relatively high angles, flat-lying reflectors typically associated with the Middle Ordovician Hawaz formation forming a set of palaeo-valleys (locally >300m thick in subsurface) and, locally, well defined interfluves or remnant palaeo-highs (McDougall and Gruenwald, 2011).

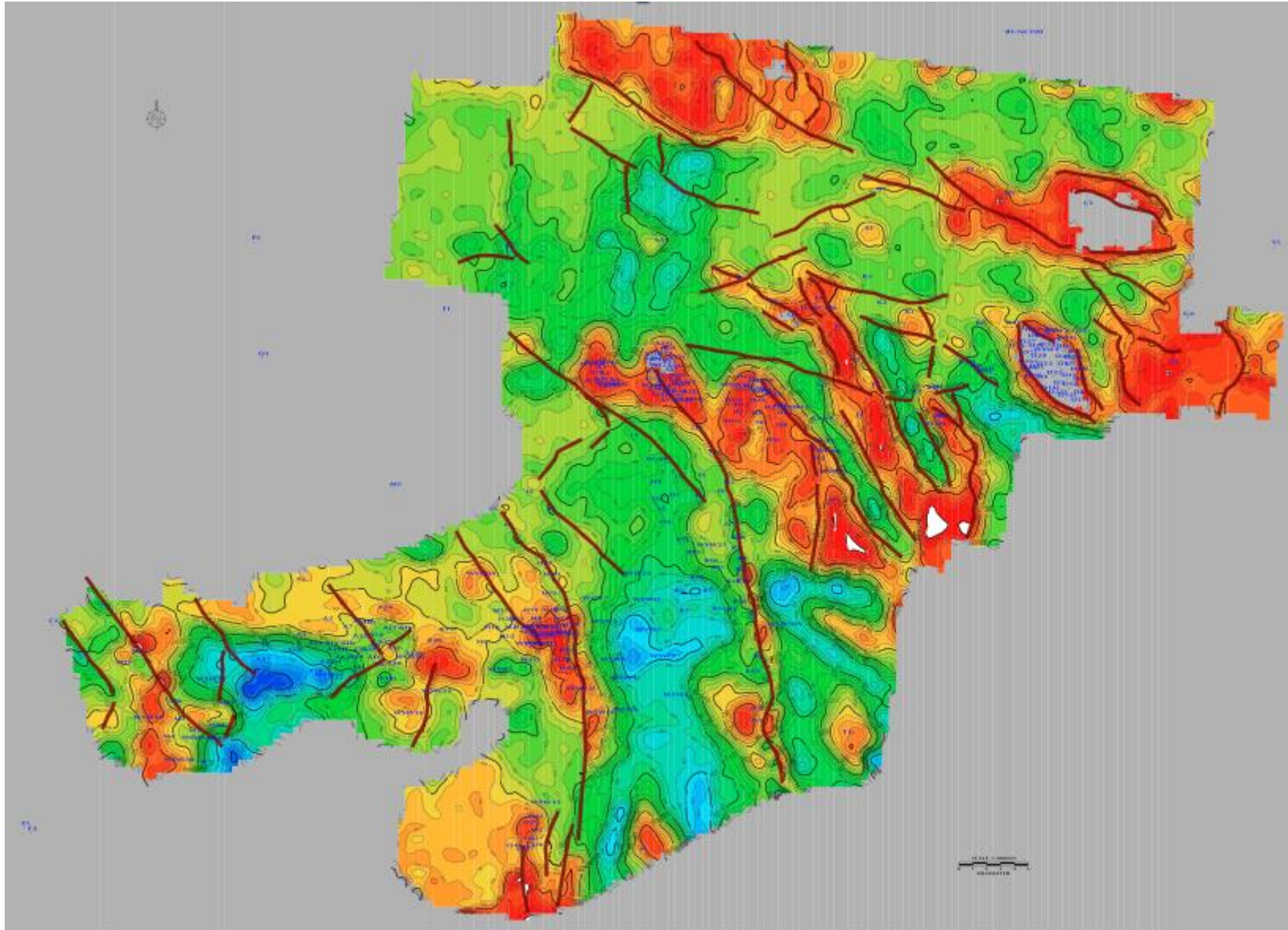


Figure 12 Isopach map of the Upper Ordovician created by subtracting the Base Tannezuft to the Top Hawaz in Block NC186 (up right) and part of NC-115 (bottom left). Warm colours (red to yellow) show thin thickness of Upper Ordovician deposits (palaeo-highs) and cold colours (green to blue) show relatively thick sections (incisions).

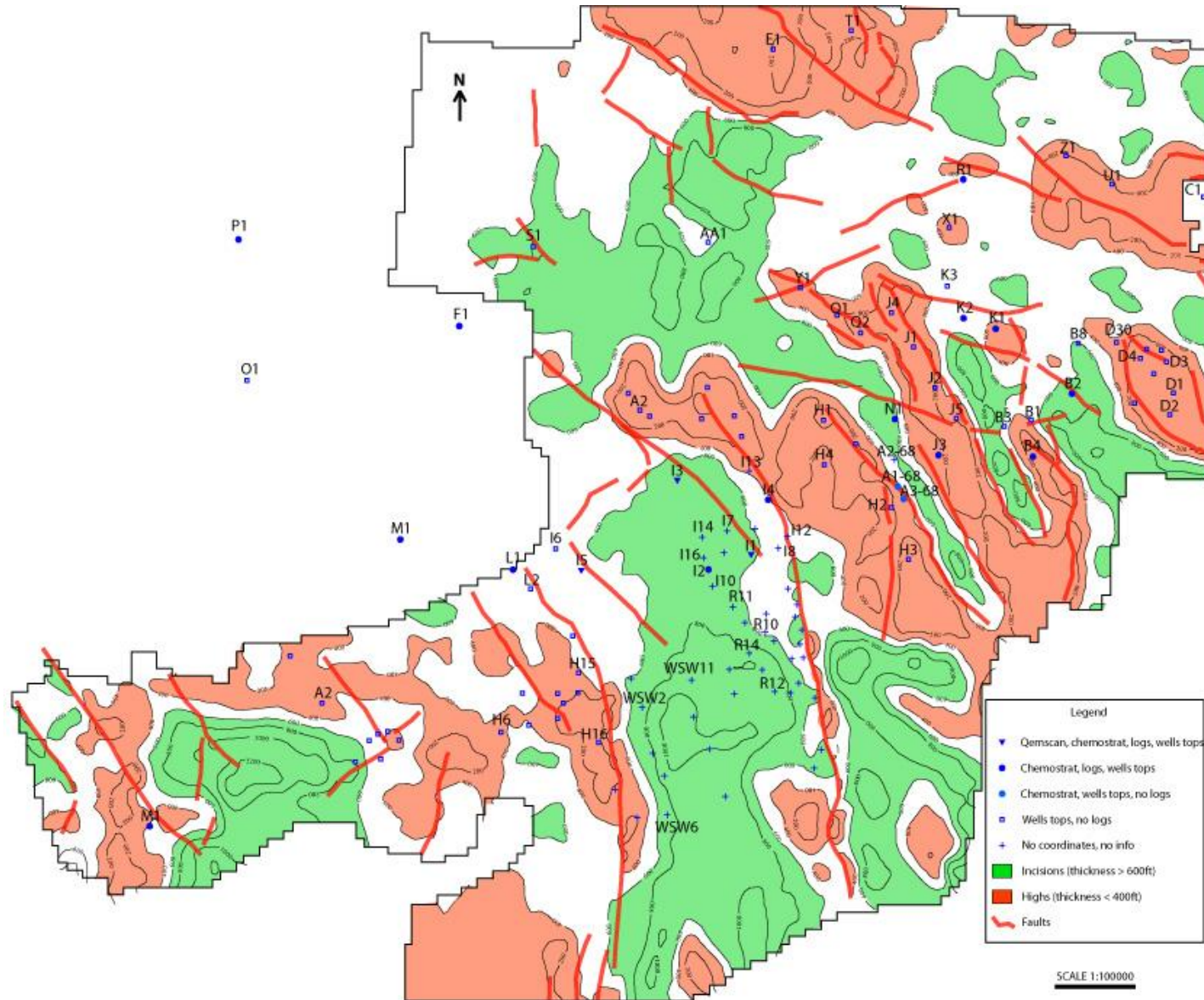


Figure 13 Simplify version of the isopach map provided by Repsol. This map shows in red thin Upper Ordovician sections (<400ft) and in green the important thicknesses of Upper Ordovician deposits (> 600ft). The map also includes well locations and the information available in each well.

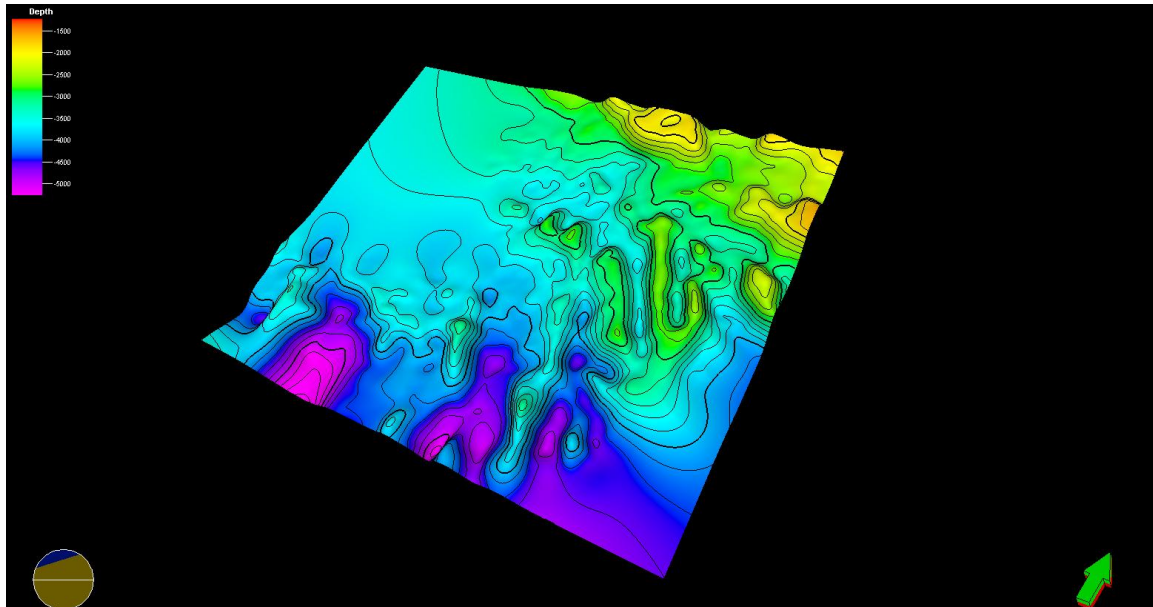


Figure 14 Top the Hawaz Formation. Seismic surface obtained by importing seismic grip points into Petrel.

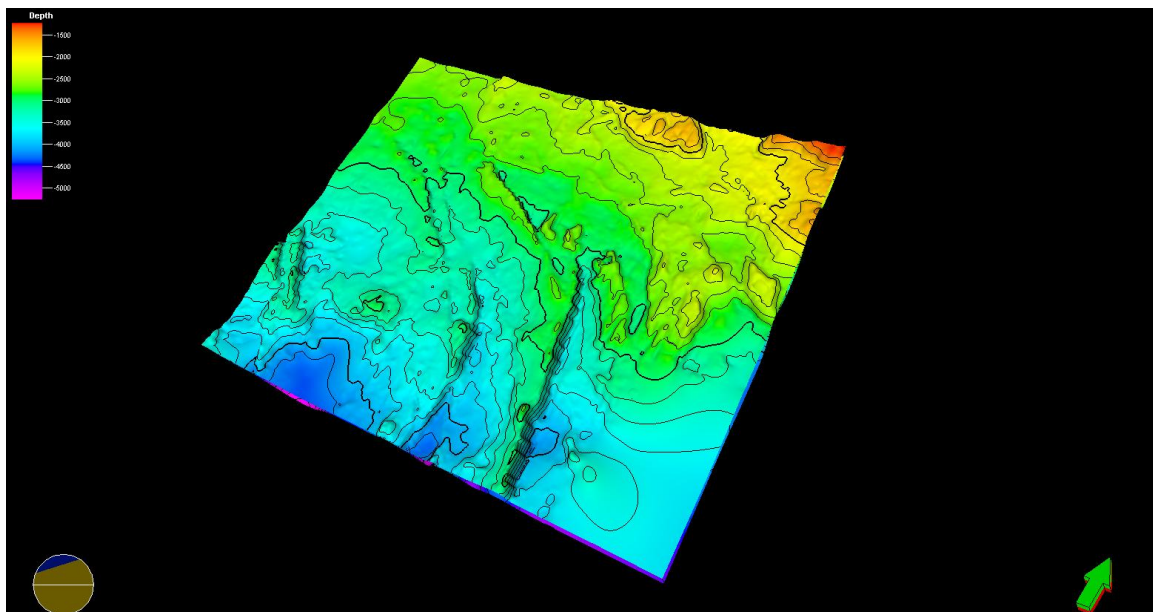


Figure 15 Base of the Tannezuft Fm. The seismic was obtained by importing into Petrel the seismic grip point given by Repsol.

The following chapter will illustrate these features with selected examples from different areas of Block NC-186.

Using this palaeo-geographic framework of palaeo-highs and valleys, Block NC-186 and part of NC-115 was further divided into different study areas: Area 1, Area 2 and Area 3 (Figure 16).

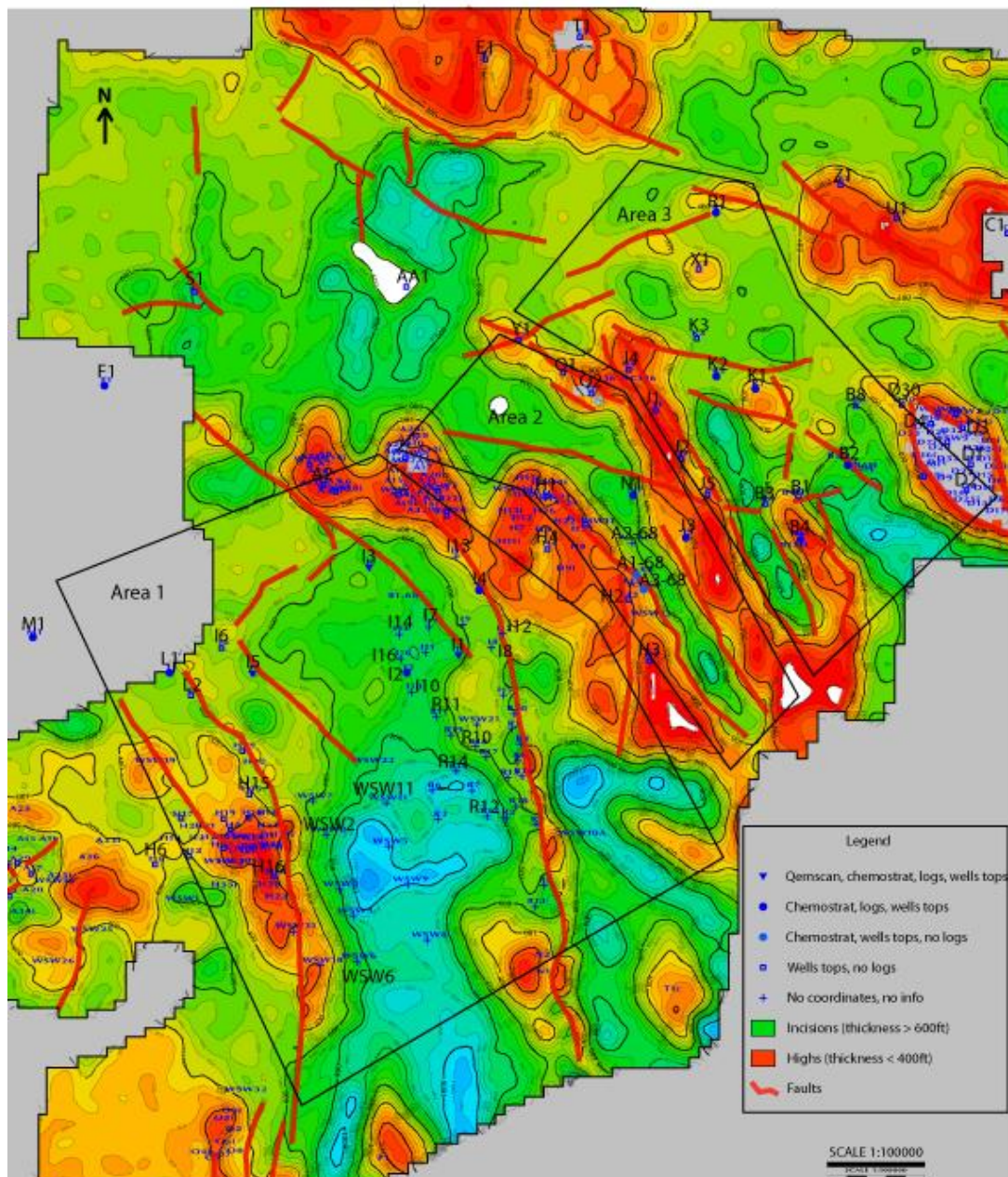


Figure 16 Isopach map showing the division of part of the Block NC186 and NC115 into 3 different areas, from west to east: Area 1, Area 2 and Area 3.

The division takes into account the different incisions and assumes that deposition of the glacial deposits in each area was not always laterally connected and therefore each area should be studied separately in the first place. If general patterns are found within each area, a large-scale correlation could be attempted.

Well data available was also divided by areas and by palaeo-geographic position; wells were assigned positions: (1) centre, (2) frontal position/tunnel valley mouth, (3) flanks and (4) proglacial (see Table 1).

Well	Area	Set
I1-NC186	AREA 1	centre
I2-NC186	AREA 1	centre
I3-NC186	AREA 1	frontal
I4-NC186	AREA 1	flanks
I5-NC186	AREA 1	frontal
I6-NC186	AREA 1	frontal
I7-NC186	AREA 1	centre
I8-NC186	AREA 1	flanks
I9-NC186	AREA 1	flanks
I10-NC186	AREA 1	centre
I11-NC186	AREA 1	centre
I12-NC186	AREA 1	flanks
I13-NC186	AREA 1	flanks
I14-NC186	AREA 1	centre
I15-NC186	AREA 1	flanks
I16-NC186	AREA 1	centre
B1-68	AREA 1	centre
L1-NC186	AREA 1	proglacial?
R2-NC186	AREA 1	flanks
R3-NC186	AREA 1	centre
R4-NC186	AREA 1	flanks
R5-NC186	AREA 1	flanks
R6-NC186	AREA 1	centre
R7-NC186	AREA 1	centre
R8-NC186	AREA 1	flanks
R9-NC186	AREA 1	flanks
R10-NC186	AREA 1	flanks
R11-NC186	AREA 1	centre
R12-NC186	AREA 1	centre
R13-NC186	AREA 1	flanks
R14-NC186	AREA 1	centre
R15-NC186	AREA 1	flanks
R16-NC186	AREA 1	flanks
R17-NC186	AREA 1	flanks
R18-NC186	AREA 1	flanks
R19-NC186	AREA 1	centre
R20-NC186	AREA 1	flanks
WSW2-NC186	AREA 1	flanks
WSW4-NC186	AREA 1	flanks
WSW5-NC186	AREA 1	centre
WSW7-NC186	AREA 1	flanks
WSW9-NC186	AREA 1	centre
WSW11-NC186	AREA 1	centre
WSW21-NC186	AREA 1	flanks
WSW22-NC186	AREA 1	centre
Q1-NC186	AREA 2	flanks
Q2-NC186	AREA 2	flanks
A1-68	AREA 2	flanks
A2-68	AREA 2	centre
A3-68	AREA 2	flanks
N2-NC186	AREA 2	centre

J3-NC186	AREA 2	flanks
B3-NC186	AREA 3	flanks
B13-NC186	AREA 3	flanks
K1-NC186	AREA 3	flanks
K2-NC186	AREA 3	frontal
K3-NC186	AREA 3	proglacial
J2-NC186	AREA 3	flanks
J5-NC186	AREA 3	flanks
B1-NC186	AREA 3	flanks
B2-NC186	AREA 3	center
B5-NC186	AREA 3	center
B6-NC186	AREA 3	center
B7-NC186	AREA 3	center
B8-NC186	AREA 3	frontal
B9-NC186	AREA 3	flanks
D19-NC186	AREA 3	flanks
D23-NC186	AREA 3	flanks

Table 1 Table showing where the wells are situated and their paleogeographic position.

8.1.2 Well data

Well data was available for a large number of wells (Figure 13 summarizes which data is available in the given wells). These data was used for structural, well correlations and sedimentological purposes in this study.

Well tops

Well tops have been assigned and provided by Repsol. These have been revised several times by Neil McDougall correlations. They provided key information when looking at log data and later for dividing the intervals for the chemostrat data.

Log data

Log data (Gamma Ray, Neutron and Density logs and others), not always combined with core descriptions, was used in order to attempt sequence stratigraphic interpretation in some wells. The procedure consisted in dividing and interpreting the log shapes in terms of grain size and their implication on sea level variations, accommodation space available, sedimentation rate, etc. and matches the results with the previous knowledge about this formation obtained by literature.

Examples of well correlations, cross-sections and more sedimentological analyses will be provided in the following chapter.

8.1.3 Core descriptions

Core descriptions provided by Repsol are key data for our sedimentological study, geological model and depositional environment study. They provided local but very detailed information about the formations and facies found in wells B1, B2, B8 and K3-NC186.

These core descriptions reports were summarized well by well and later combined with more log data in order to create local depositional environment models in the area where these were wells are present.

8.1.4 Chemostrat data

The chemostrat data represents the most unconventional data and therefore the most challenging data used in this study.

Measurements were acquired for Repsol in the latest attempt to find methods for correlations between units after palynology and biostratigraphy studies failed to give accurate results.

Furthermore, this technique could also be use to correlate formations at a regional scale were the glacial formations such as the Mamuniyat are found regionally but under different names.

The data correspond to chemical analysis of various chemical compounds, chemical elements and Rare Earth Elements (REE) from 18 different wells from block NC-186 (A1-68, A3-68, B2-NC186, B4-NC186, F1-NC186, I1-NC186, I2-NC186, I3-NC186, I4-NC186, I5-NC186, J3-NC186, K1-NC186, K2-NC186, L1-NC186, M1-NC186, N1-NC186, P1-NC186, R1-NC186).

Chemical compounds such as Al₂O₃, SiO₂, TiO₂, FeO₃, MnO, MgO, CaO, Na₂O and P₂O₅ were analyzed with ICP-OES methods, with results are expressed in weight percentage. All other chemical elements and REE were analyzed through ICP-MS methods and results were expressed in particles per million (ppm).

These analyses were done in core and cutting samples. The lithology was noted at each depth with a very simple nomenclature: (1) sandstone, (2) argillaceous sandstone, (3) siltstone, (4) silty claystone and (5) claystone. No further details in grain size are given.

It is very important to know the lithology of the analyzed sample since many elements proportion are grain-size dependent. The dependency on grain-size was clearly observed by comparing values for the same element at same depths but in different lithology types (i.e. sandstone vs. claystone).

Chemical ratios and proxies signals will be explained if the following chapters.

9 Results

9.1 Description

9.1.1 Chemostrat data

The acquired chemostrat data was used for the first time in this study, in order to depict the main characteristics of the infilling deposits of the Murzuq Basin. The study analysed large-scale features such as provenance and tectonic setting, their belonging in the sandstone classification, climate characteristic and others.

Provenance

Discrimination diagrams for clastic sediments using major elements as explained by Rollinson (1993) allowed us to identify sedimentary provenance depending on the different tectonic environments.

Rollinson (1993) shows three types of discrimination diagrams for sedimentary rocks based upon major element geochemistry.

He describes two discriminant functions for sandstones from Bhatia (1983) that are used, in a bivariate plot, in order to divide samples in four main tectonic settings: Passive Margin, Active Continental Margin, Continental Island Arc and Oceanic Island Arc. Unfortunately these functions will not be used due to the lack of measurement of the FeO chemical compound, needed in the equations.

Nevertheless, two other discriminant diagrams from Bhatia (1983) and one from Roser and Korsch (1986) can be used in order to determine the same tectonic settings. Figure 17, Figure 18 and Figure 19 show the plots for the infilling formations of Block-NC186.

These three plots show that all samples from different formations found in the wells from Block-NC186 belong to the passive margin tectonic setting.

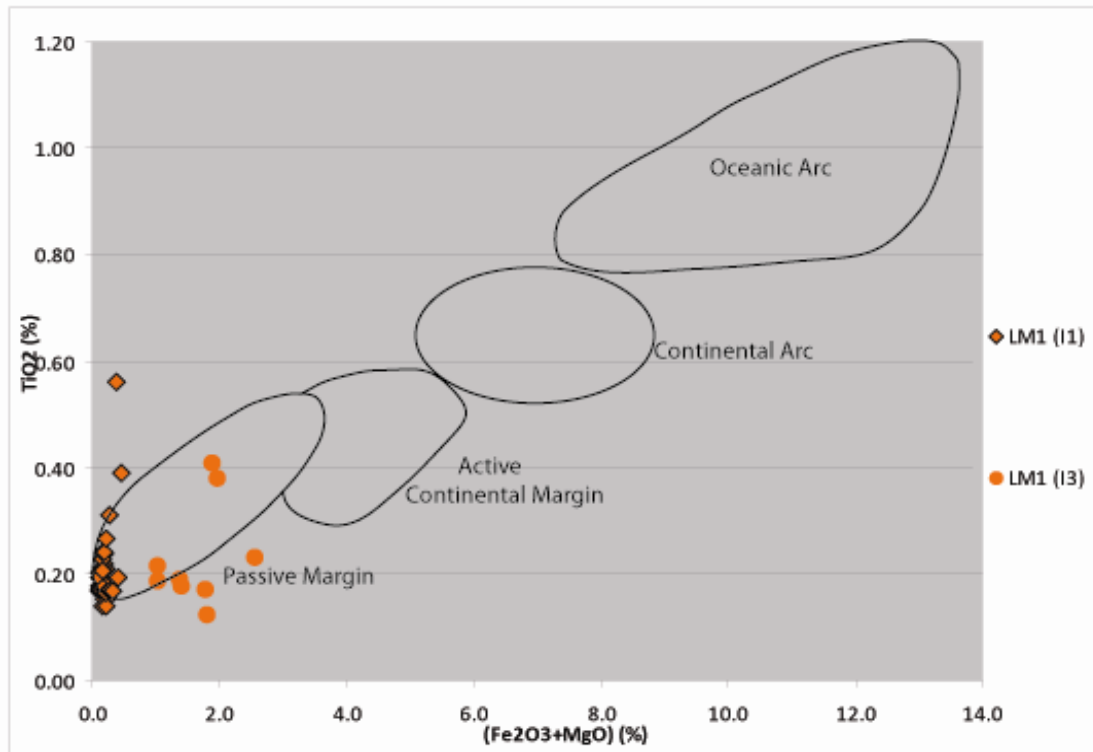


Figure 17 Discriminant diagram after Bhatia (1983) of a bivariate plot showing TiO₂ vs. Fe₂O₃+MgO. The graph shows Lower Mamuniyat samples from two different wells (I1 and I3-NC186). A Passive Margin tectonic setting is suggested.

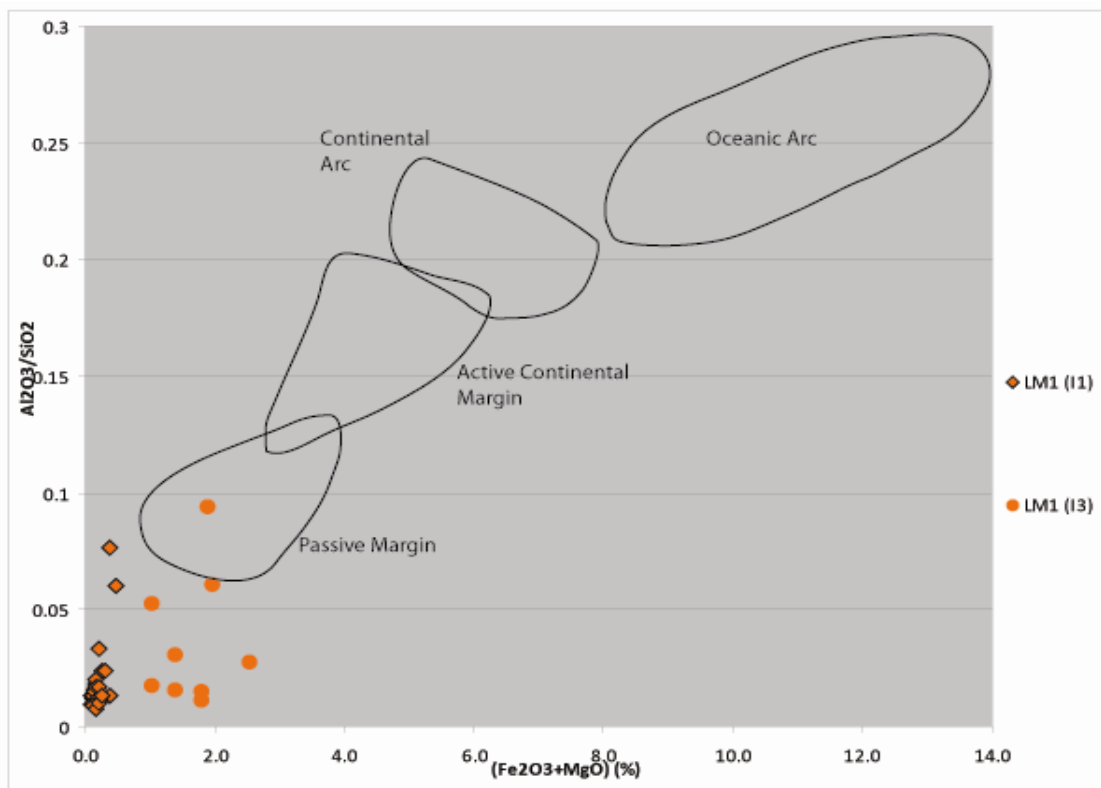


Figure 18 Discriminant diagram after Bhatia (1983) of a bivariate plot: showing Al₂O₃/SiO₂ vs. Fe₂O₃+MgO. The graph shows samples from the Lower Mamuniyat Formation. Most of the samples fall in or close of the Passive Margin setting, indicating such conditions during Upper Ordovician times.

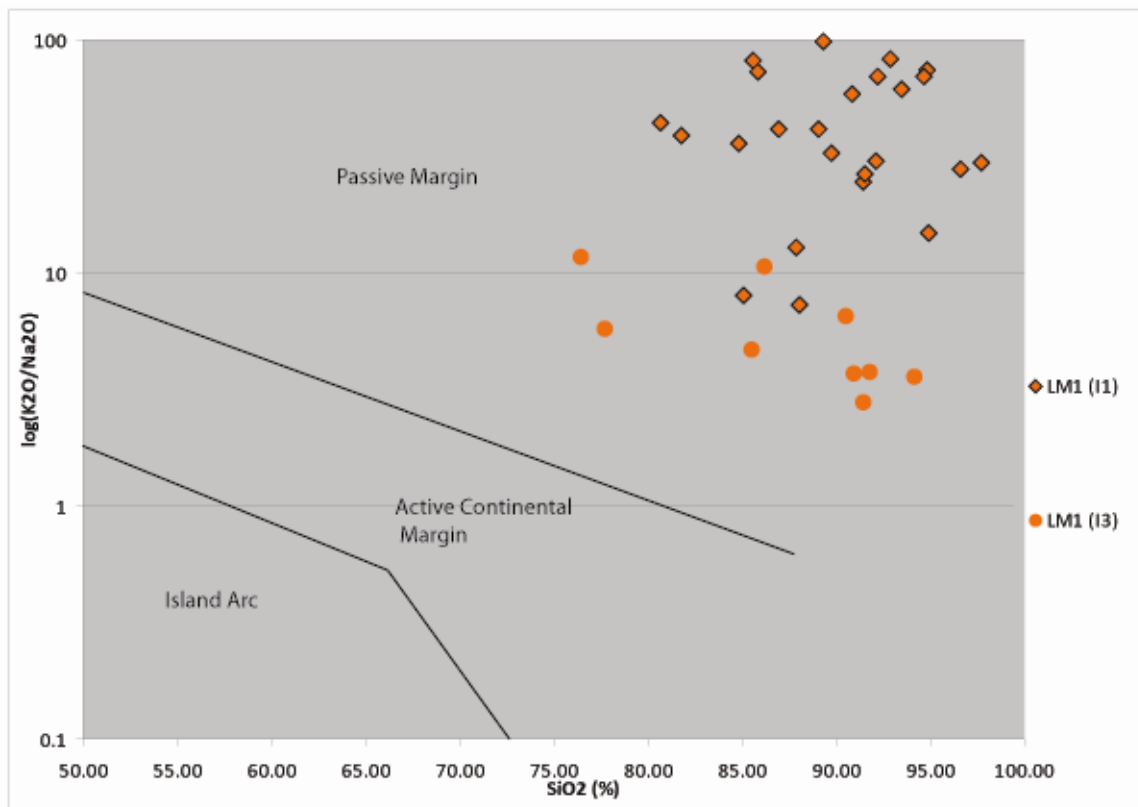


Figure 19 The K₂O/Na₂O vs. SiO₂ sandstone-mudstone discrimination diagram from Roser and Korsch (1986). Samples from the same wells have been used, suggesting again a Passive Margin tectonic setting as provenance for the deposition of these sediments.

Sandstone classification

The classification of terrigenous sandstones and shales from Herron (1988) was also used. This classification uses $\log(\text{SiO}_2/\text{Al}_2\text{O}_3)$ and $\log(\text{Fe}_2\text{O}_3/\text{K}_2\text{O})$ in a bivariate plot in order to classify samples in various categories of sedimentary rock types.

Figure 20 shows examples of plots for some formations found in the Upper Ordovician deposits.

Samples from the Mamuniyat Fm show a very siliciclastic origin. In the thick sand sequences from the Lower and Upper Mamuniyat, most of the samples show a “Quartz Arenite” sandstone type. In finer lithological formation, such as the Middle Mamuniyat, a relative increase in Fe and Al elements is visible indicating an increase in shalier components to the system.

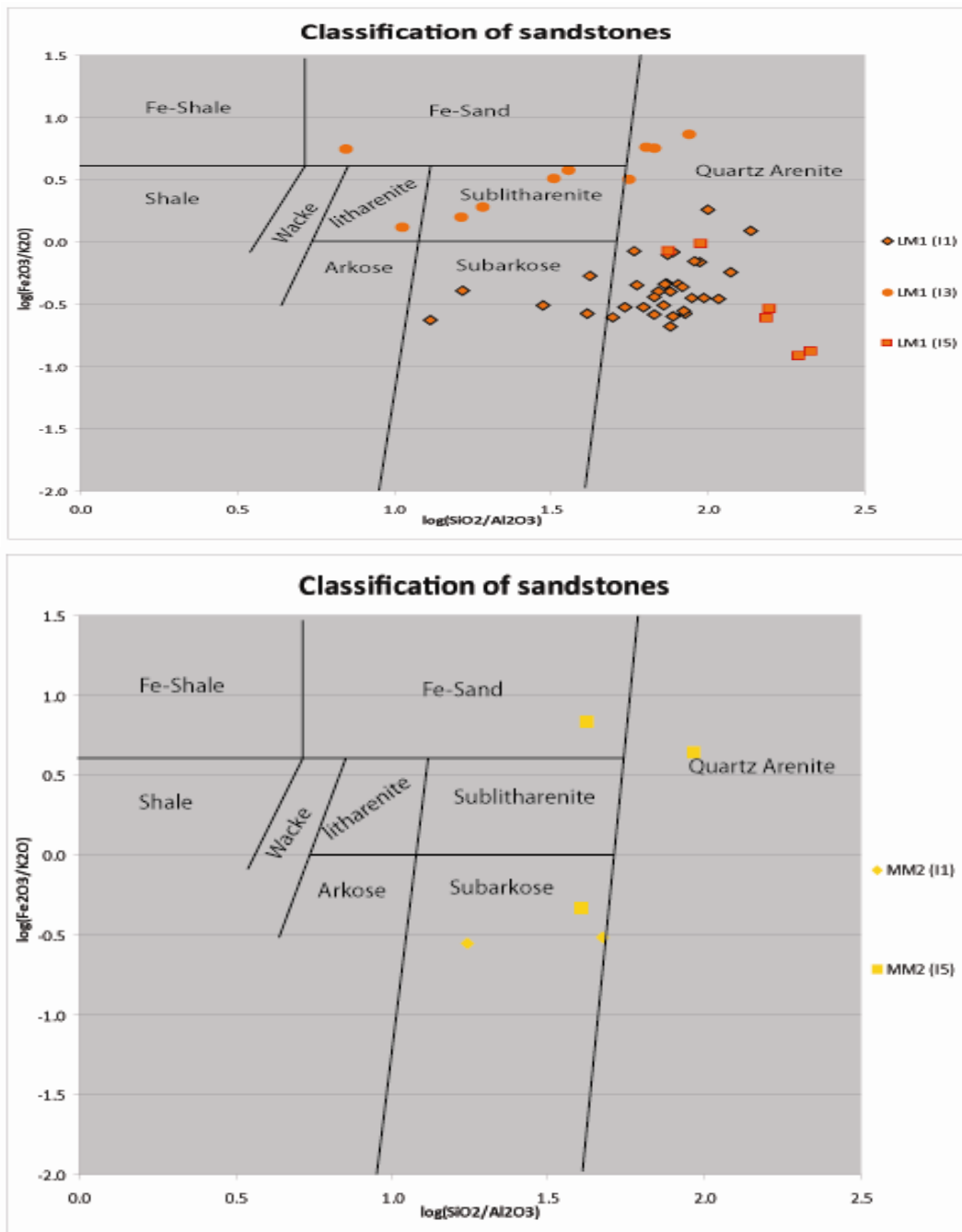


Figure 20 Plots of the classification of sandstones proposed by Herron (1988). The upper plot shows distribution of samples from the Lower Mamuniyat unit in the classification. The plot below shows the distribution of samples from the Middle Mamuniyat unit. Both show high siliciclastic content.

Proxy signals

In order to depict variations in the geochemical composition of the sedimentary formations, proxy signals were studied.

The proposed proxy signals use were choose following the example of a study carried on in South Africa by Kay Scheffler, Dieter Buehmann and Lorenz Schwark: "Analysis of Late Palaeozoic glacial to postglacial sedimentary

successions in South Africa by geochemical proxys – Response to climate evolution and sedimentary environment” (2006).

The proxy signals are:

- Zr/Ti for provenance
- Chemical Index of Alteration (CIA) as a climate indicator
- Rb/K as a salinity indicator
- U/Th, Ni/V, Ni/Co, V/Cr as redox-proxies.

The data available for this study was present as weight percentages (wt% and ppm). In order to create the above ratios, simple operations were performed. These comprise a conversion from weight percentage to molecular percentage and getting the weight percentage of a single element from a chemical compound.

It is also important to notice that this conversion and virtual disaggregation of chemical compounds might induce errors in terms of real composition values. Therefore, results will be studied in terms of chemical variations and not in function of their absolute value.

Zr/Ti

The Zirconium over Titanium ratio has been use as a provenance proxy. In fact, Zr has high field strength and is present in the heavy mineral fraction of sediments (Scheffler et al., 2006), these tend to be immobile during weathering processes. Scheffler et al. (2006) adds that “these heavy minerals are not influenced by changing climate conditions” and “their occurrence in sediments is mainly controlled by the geochemistry of the provenance rocks”. Different Zr/Ti ratio characterise provenance rocks, hence we can differentiate the origin of the sample by correlating the Zr/Ti ratio to the provenance rock value.

The following values, obtained by Scheffler et al. (2006) will be use as cut-off values in the results (Figure 37).

- Granitic or sedimentary clastic: > 0.13
- Shale: < 0.13 with values around 0.067 (average upper crust), 0.043 (North American Shale composite), 0.034 (andesites) and 0.024 (basalts).

(Ti measurements were not available, only TiO₂ values were measured. A conversion from the chemical compound to the element was achieved, introducing uncertainty and errors to ratios curves)

Chemical Index of Alteration (CIA)

The Chemical Index of Alteration (CIA) was also calculated for each sample. The CIA provides information about chemical weathering processes, which were controlled by climate (Scheffler et al. 2006). It was defined by Nesbitt and Young (1982) as $CIA = [Al_2O_3 / (Al_2O_3 + Na_2O + K_2O + CaO^*)] * 100$ using molar proportions. CaO* represents the amount of calcium incorporated in the silicate fraction (Scheffler et al. 2006).

The CIA plots show changes of proportion from feldspars minerals ($\text{Al}_2\text{O}_3 + \text{Na}_2\text{O} + \text{K}_2\text{O} + \text{CaO}$) to clay minerals (Al_2O_3). Weathering processes destroy feldspar minerals disintegrating them into clay minerals. Therefore, low CIA values will indicate unaltered rocks in cold/arid conditions, whereas high CIA values will indicate warm/humid conditions.

- Unaltered basaltic rocks: 30-45
- Fresh granites: 50 (unweathered, cold/arid)
- Shales: >70 (intense weathering, warm/humid)

Furthermore Bahlburg et al. (2009) gives values for CIA in glaciomarine deposits that will be used as visual cut-off values in the graphs shown in the results (Figure 37).

Values from 0 to 50 are considered as unweathered rocks.

Low CIA values between 50 and 70 are given for diamictite facies.

XX explains that diamictites represent either lodgement tills or moraine material which was rapidly redeposited by mass wasting in glaciomarine environments. These deposits are often associated with finer grained and laminated glaciomarine sandstones, siltstones and shales, which may include ice-rafted debris, with higher CIA values between 70 and 85.

Rb/K

Scheffler et al. (2006) explains that Campbell and Williams (1965) used the Rb/K ratio to differentiate sediments formed in fresh water, brackish or marine environment. He points out that the use of the ratio as a salinity proxy is based on the assumption that marine shales contain higher Rb content due to higher Rb⁺ concentration in the ocean water than in fresh water environment (0.12 ppm Rb in oceans to 0.0013 ppm Rb in rivers; Taylor and McLennan, 1985). When sediments enter a marine environment, elements in clay products, such as Potassium, are partially replaced by Rb due to the concentration gradient between the two contrasting environments (Scheffler et al., 2006). Therefore, marine conditions and increasing salinity will be recorded as high Rb/K ratio whereas fresh to brackish conditions will have lower ratios:

- Fresh water to brackish conditions: $<4 \cdot 10^{-3}$
- Marine environments: $>6 \cdot 10^{-3}$

These values are used as a visual cut-off in the results (Figure 37).

(K measurements were not available, only K₂O values were measured. A conversion from the chemical compound to the element was achieved, introducing uncertainty and errors to ratios curves)

Redox-proxies

Redox proxies correspond to ratios that use transition element contents in order to reconstruct palaeo-redox conditions.

In fact, environment-sensitive elements will be enriched or depleted when they are deposited in an aquatic environment with different conditions from the ones present during weathering.

For our study, the U/Th ratio has been chosen. This ratio uses the insoluble properties of Th and the solubility and extraction capacity of U from the sea. Low U/Th ratios (< 0.14) indicate continental weathering and leaching, leaving insoluble elements behind, whereas high U/Th ratios indicate extraction of U from the sea and therefore marine conditions (> 0.33). Intermediate values indicate poor weathering and rapid deposition of detritus. The values presented above will be used as cut-off values in Figure 37 when presenting the results.

A comparison between these geochemical proxies signal within representative wells from Block NC-186 will be present in the chapter below.

9.1.2 Core descriptions

Here a brief description of these cores is presented. We use the wells tops from Repsol in order to differentiate the formation described in the different reports.

Well B1-NC186

Melaz Shuqran

The Melaz Shuqran was described in well B1-NC186 although it was not cored. In this well, it reaches a thickness of 60ft. The Melaz Shuqran is composed of sandy mudstones and muddy heterolithics with abundant floating casts, thin laminations and traces of synsedimentary deformation. The authors of the report interpret the Melaz Shuqran deposits as sediments deposited in a glaciomarine ice margin environment.

Lower Mamuniyat

The Lower Mamuniyat is not completely cored in the well. The entire unit is about 73ft thick. Sand packages show fining upwards tendency of medium to fine sandstone with interclast intervals. The sandstones are dominated by sets of low angle parallel lamination (hummocky cross-stratification or hummocky megaripples). The fining upward sequences change to the top towards a coarsening upward and aggradational sequence. Localised bioturbation and scour surfaces are also present towards the top of this unit. The Lower Mamuniyat unit has been interpreted as tidal channels and shoreface to shelf deposits associated to a low gradient braid-delta that infill previously created incisions.

Middle Mamuniyat

The Middle Mamuniyat has been completely cored and is about 27ft thick. This thin unit is characterized by the fine-grained nature of its deposits (argillaceous, silty and fine grained sandstones). The deposits are well sorted and present current ripples and planar lamination with sometimes soft sediment

deformation. The sediments have been interpreted as mouth bar deposits associated to a relatively steep gradient of a constructive braid-delta front.

Upper Mamuniyat

Finally the thick Upper Mamuniyat has also been cored in its full length (296ft). The whole unit is composed of sandstones. Although Repsol has divided the unit into 3 sub-units, this division has not been taken into account in the core description. Here the different depositional environments found in each sub-unit are presented.

UM1 shows fining-upwards sequences of medium to fine sandstones. Low amount of interclasts are found, mostly at the base. The sub-unit is characterised by planar lamination. UM1 is interpreted as a retrogradational parasequence. The depositional environment consists in fluvio-glacial channels to braid-deltas. These infill deposits are mainly located in a previously incised area. Towards the top the environments of deposition change towards shoreface and shelf conditions.

The lower UM2 sandstones show fine coarsening-upward sequences with increasingly abundant mudstone interclasts. Towards the top, several stacked fining-upwards sequences are found. Mudstone interclasts horizons mark the base of each of these sequences. The top of UM2 shows cleaner sandstones with floating granules and pebbles in overall coarsening upwards sequences. These deposits are interpreted as delta plain and braid-delta front to shoreface deposits (delta front channel system).

Finally, UM3 sandstones are described as very poorly sorted coarse-grained sandstones with large interclast content. The subunit shows signs of an increase of energy in the environment of deposition with facies going from delta plain and Gilbert delta facies deposits to a fluvial conglomerate deposits associated to debris flows and hyperconcentrated flows.

Well B2-NC186

In the sedimentological study of well B2-NC186 provided by Repsol, only part of the Upper Mamuniyat was cored and analysed.

The Upper Mamuniyat is composed of sandstone deposits. Again, these deposits have been described without taking into account the subdivision proposed by Repsol. Here well tops information and core description are combined in order to have a more detailed description.

Upper Mamuniyat

UM1 is only partially cored and the sandstones that compose the subunit show stacked coarsening-upwards sequences of fine to medium sandstones with faint cross-bedding and planar lamination. They are interpreted as prograding upper shoreface deposits associated with high energy, wave dominated braid-delta environment.

UM2 sandstones are present as thick fining-upwards sequences, generally poorly to moderately well sorted with floating small pebbles and mudstones interclasts in a planar or trough cross-bedding lamination. The section is capped by thin coarsening upward sequence followed by another fining and thinning upward sequence. The sub-unit is interpreted as proximal glacial outwash channels,

braid-delta plain, distributaries channels and shoreface deposits. Finally, UM3 sandstones present the same lithological association found UM2 but changes towards the top into well sorted sandstones with trough cross-bedding and planar lamination. Facies found are therefore the same as found in UM2 but changing towards the top to a more distal braid-delta plain with distributaries channels environment.

Well B8-NC186

Well B8-NC186 cored the entire Melaz Shuqran and Mamuniyat formations.

Melaz Shuqran

The Melaz Shuqran (66ft thick) is described as sandstones interbedded by finer layers of argillaceous sandstones, heterolithics, siltstones and mudstones. This alternation of high to low energy deposits is interpreted in terms of depositional environment as alternating proximal and distal mouthbars facies.

Lower Mamuniyat

The sandy Lower Mamuniyat (104ft thick) shows an alternation between clean cross-bedded and locally high angle planar laminated sandstones and deformed and dewatered sandstones packages. These sandstones deposits are interpreted as distributaries channels, wave dominated upper shoreface and proximal mouthbars respectively.

Middle Mamuniyat

The Middle Mamuniyat (190ft thick) is characterise by the large presence of deformed and dewatered sandstones interbedded with also deformed and dewatered argillaceous sandstones, heterolithics, siltstones and mudstones. These deposits are intercalated with clean cross-bedded and planar laminated sandstones. The succession is interpreted as distal to proximal mouthbars, distributaries channels and wave dominated upper shoreface facies.

Upper Mamuniyat

Finally, the Upper Mamuniyat (UM3 only) overlies the previous deposits with a 190ft succession of sandstones deposits. These sandstones are generally clean with abundant cross-beds or low angle laminations. Intervals of deformed and dewatered sandstones are also common. The succession is interpreted as distributaries channels, proximal mouthbars and wave dominated upper shoreface deposits.

Well K3-NC186

Well K3-NC186 was drilled and cored over the whole Mamuniyat Formation without encountering the Melaz Shuqran or reaching the Hawaz formation.

Lower Mamuniyat

It has a minimum thickness of 273ft. This very sandy formation is described as an alternation of clean sandstones showing local flat planar to ripple cross lamination with some slumped intervals and thin deformed to dewatered

sandstones sections. The sediments are interpreted as deposited in a sandy slope environment or by submarine sediment flows.

Middle Mamuniyat

It is also very sandy in this area and presents a thickness of 62ft. It is composed of clean and massive sandstones with local interclast intervals presenting low to high angle cross-beds and ripple cross lamination. There are also clean to locally argillaceous sandstones with presence of deformed mudclast in massive to cross-bed laminations. Planar lamination and scoured surfaces are also common. The environments of deposition assigned to the unit are sandy slopes and submarine sediment flows.

Upper Mamuniyat

It is 213ft thick and it is divided into sub-units UM1 (144ft thick) and UM2 (69ft thick). Both sub-units are described as generally clean sandstones interbedded with slumped/dewatered intervals, mudclast deposits and floating outsized grained. The environment of deposition for the Upper Mamuniyat was again interpreted as sandy slopes and submarine sediment flows.

9.1.3 Seismic Lines description and interpretation

No digital seismic data in the Murzuq Basin was available for this project. Nevertheless, Repsol provided large amounts of seismic lines screen shots, obtained from a 3D seismic cube, which pass through numerous wells. These lines give an overview of the structural setting on the area and the lateral variability of the Upper Ordovician deposits.

Combining these seismic lines to the well tops available in the area, a series of cross-sections from the different areas of study are proposed.

Here selected seismic lines are presented. See Figure 21 for position of lines. These lines are used in order to understand what are the main factors controlling the creation of the incisions and the lateral variability of the infilling deposits in the different areas of study within Block NC-186.

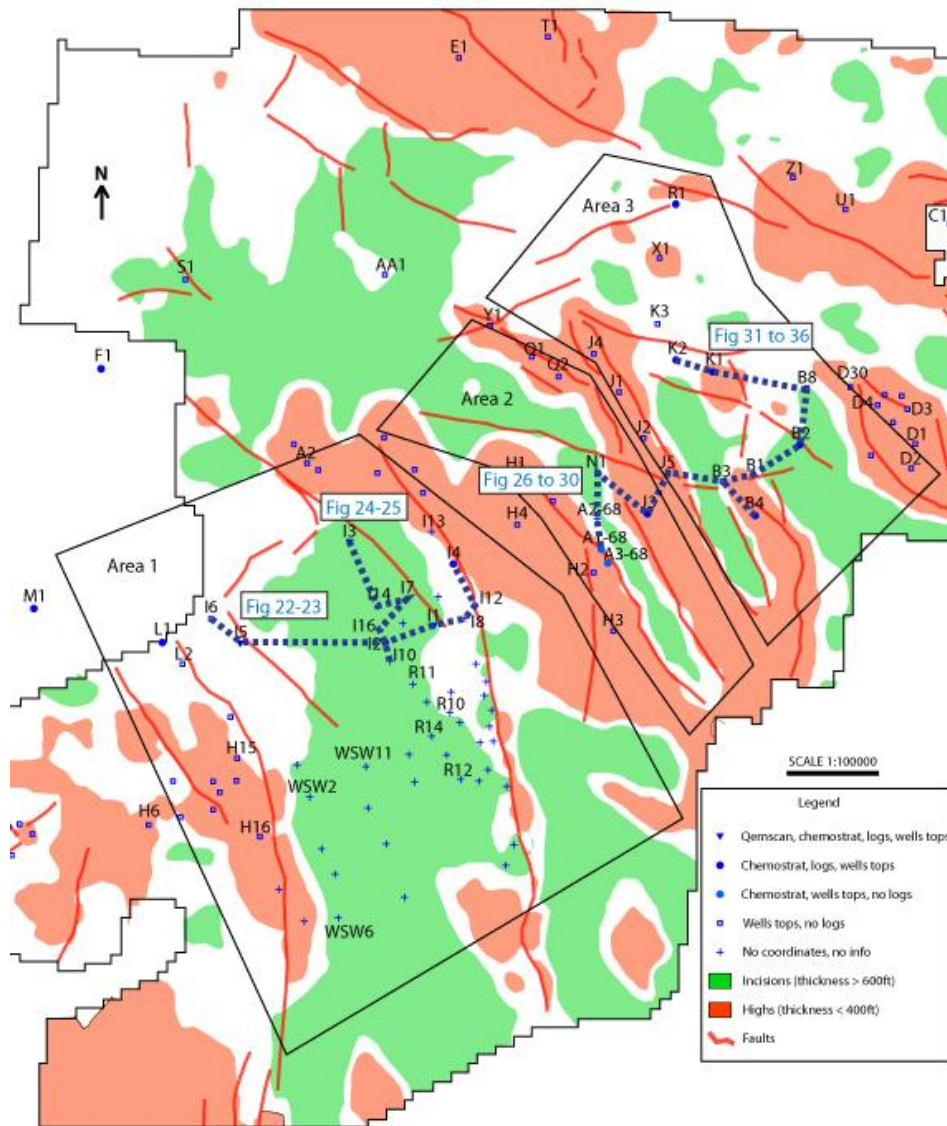


Figure 21 Simplified isopach map of part of Block NC-186. The map shows the main incisions (green), highs (red) and faults (red lines), the subdivision of the study area in 3 areas and the well data available. The dotted blue lines show the position of the selected seismic lines.

Area 1

Area 1 presents one of the largest incisions on the isopach map showing the thickness of the Upper Ordovician deposits. To illustrate the shape of the incision two lines, perpendicular to each other, have been chosen: seismic line "I6I5I2I1I8I12I4FlattenedDembzoomgrey" oriented WSW-ENE (Figure 22 and Figure 23) and seismic line "I3I14I7I16I2I10altgreyflatondembada" oriented NNW-SSE (Figure 24 and Figure 25).

The WSW-ENE section (Figure 22 and Figure 23) show how the incision is found in an area of intense structural control, with presence of pre depositional normal faults rarely affecting the Upper Ordovician deposits. These faults are probably responsible for the creation of accommodation space in the area and favouring ice-streams incisions that will later deposit the infilling formations.

The NNW-SSE section (Figure 24 and Figure 25) shows a decrease in thickness of the Upper Ordovician formations towards the north (left). The isopach map shows the presence of a palaeo-high in that area responsible for the termination of the incision and the decrease in thickness of the infilling deposits.

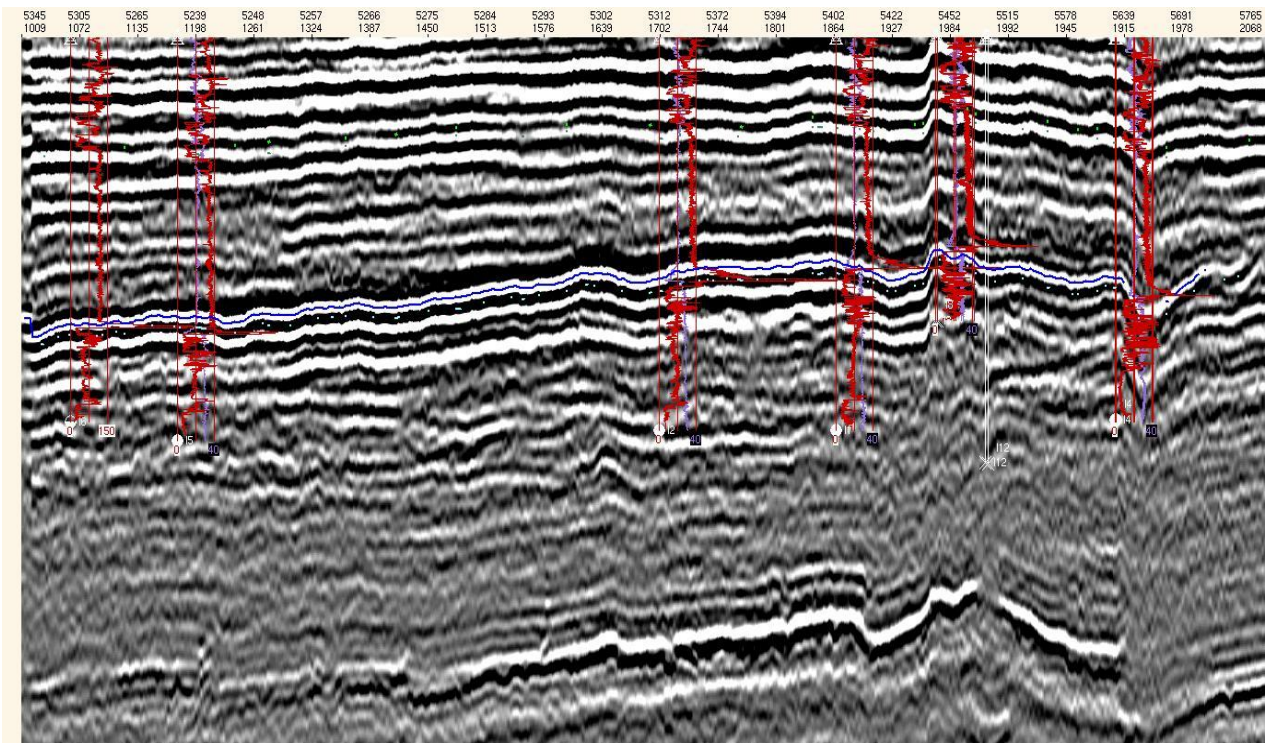


Figure 22 Seismic line "I615I21118I1214FlattenedDembzoomgrey" oriented WSW-ENE.

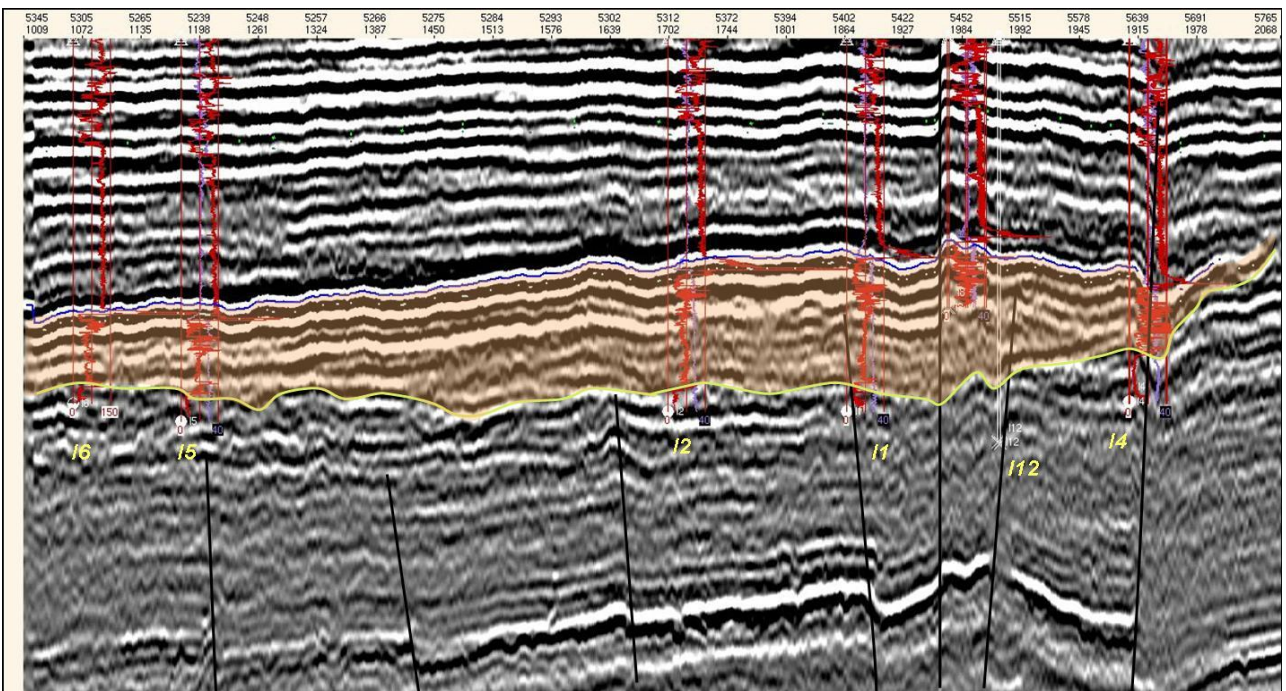


Figure 23 Seismic line "I615I21118I1214FlattenedDembzoomgrey" interpreted by Neil McDougall.

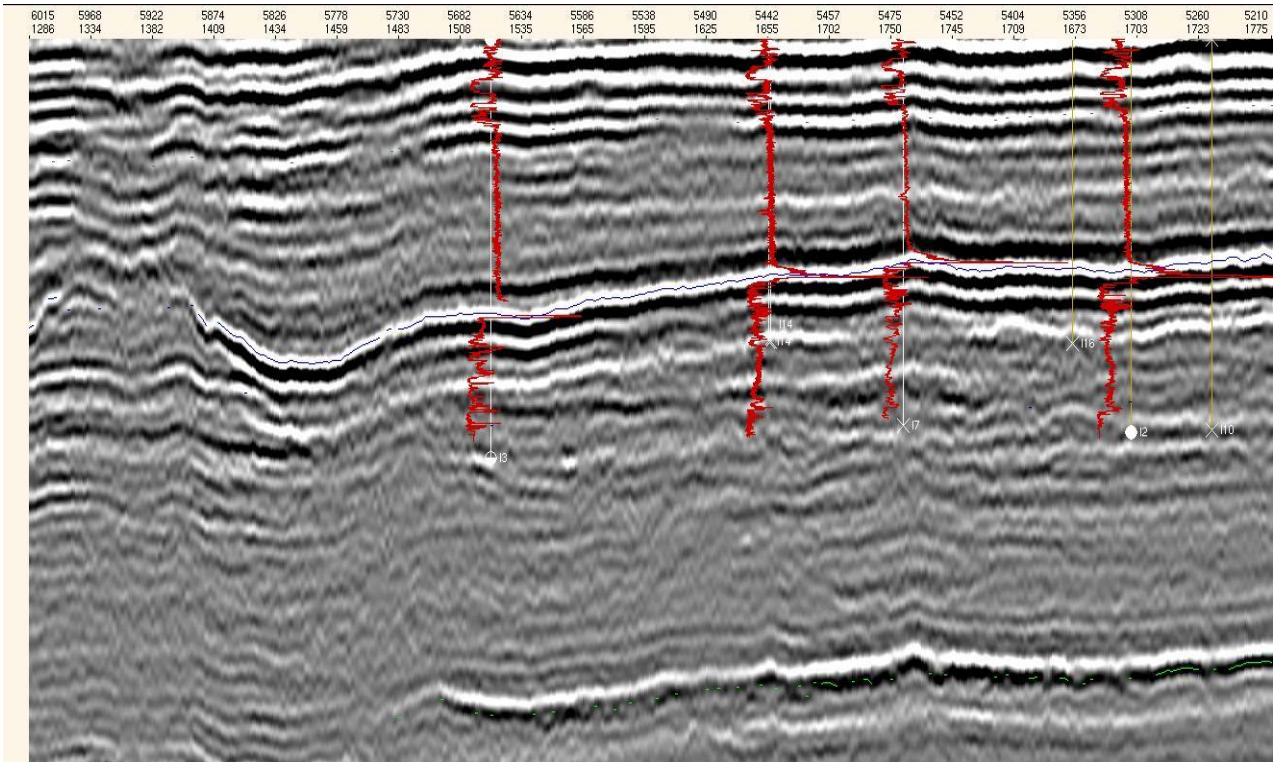


Figure 24 Seismic line "I3114I7116I2I10altgreyflatondembada" oriented NNW-SSE.

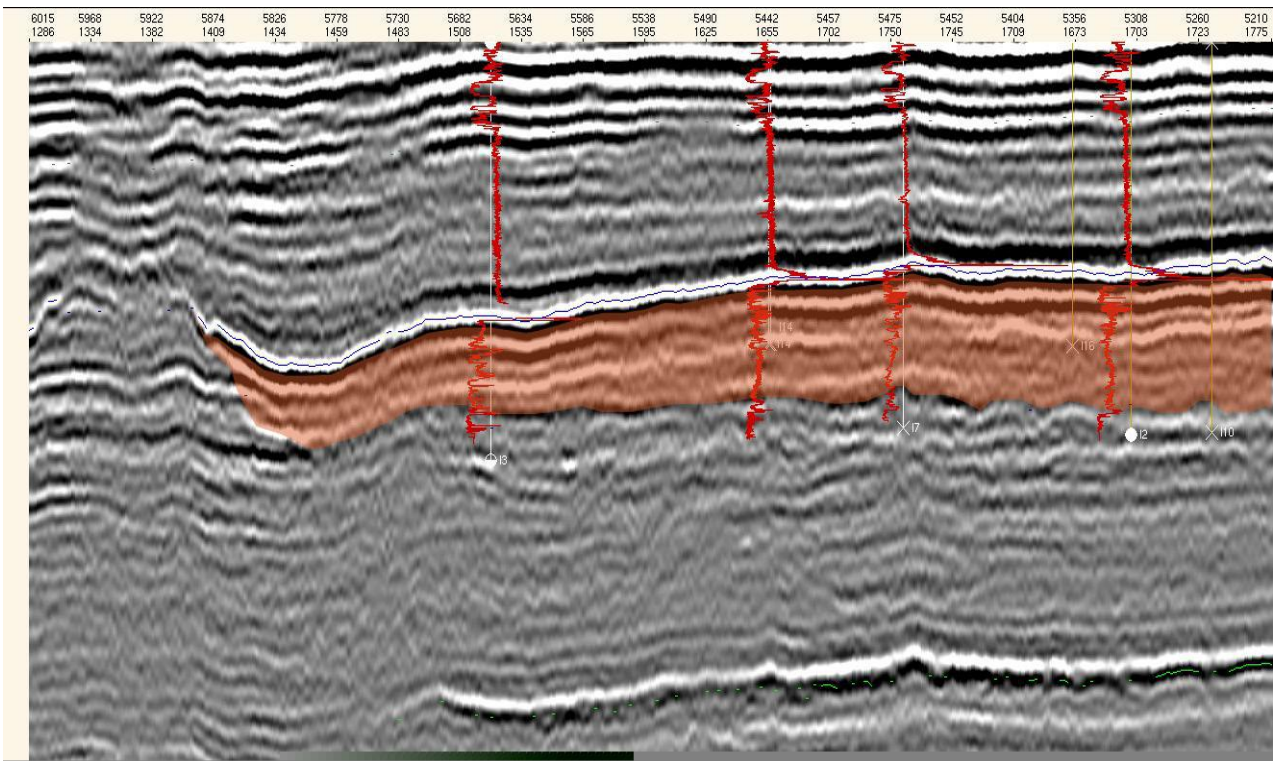


Figure 25 Seismic line "I3114I7116I2I10altgreyflatondembada" interpreted.

Area 2

In this area, we selected a series of screen-shots visible in Figure 21.

Seismic line “A168A268N1J3J5grey” (Figure 26) runs through wells A1-68, A2-68, N1, J3 and J5-NC186. This triangle shape well correlation gives an overview on the structural appearance of the area in a southwest-northeast cross-section.

The seismic line shows a U-shape incision marked by the reflector situated at the bottom of well N1-NC186. The incision is about 100m deep and about 3.5 km wide. In Figure 28, a zoomed view of the previous line, this reflector appears in red and it deepens towards the west (left) and shallows towards the east (right). The reflectors within the infilling material inside the u-shape incision can have parallel geometries but also complicated and hard to distinguish geometries towards the centre of the incision. This suggest several stages of infilling with incision of the previous deposits and lateral changes in facies. All reflectors seem to terminate against the bounding red reflector with onlap geometries at both sides, indicating one episode of deep incision and several stages of later infill.

Figure 27 shows the interpreted picture of seismic line “A168A268N1J3J5grey” by Neil McDougall. In this interpretation we can see how variable the thickness of the infilling material is, and how it thins and drapes over the palaeo-highs topography. Faults have also been interpreted at each side of the palaeo-highs, showing signs of structural control on the u-shape incision.

Finally, Figure 29 shows the transition from Area 2 to Area 3. Another U-shape incision occurs east of well J5-NC186, well B3-NC186 being situated at the flank of another palaeo-high.

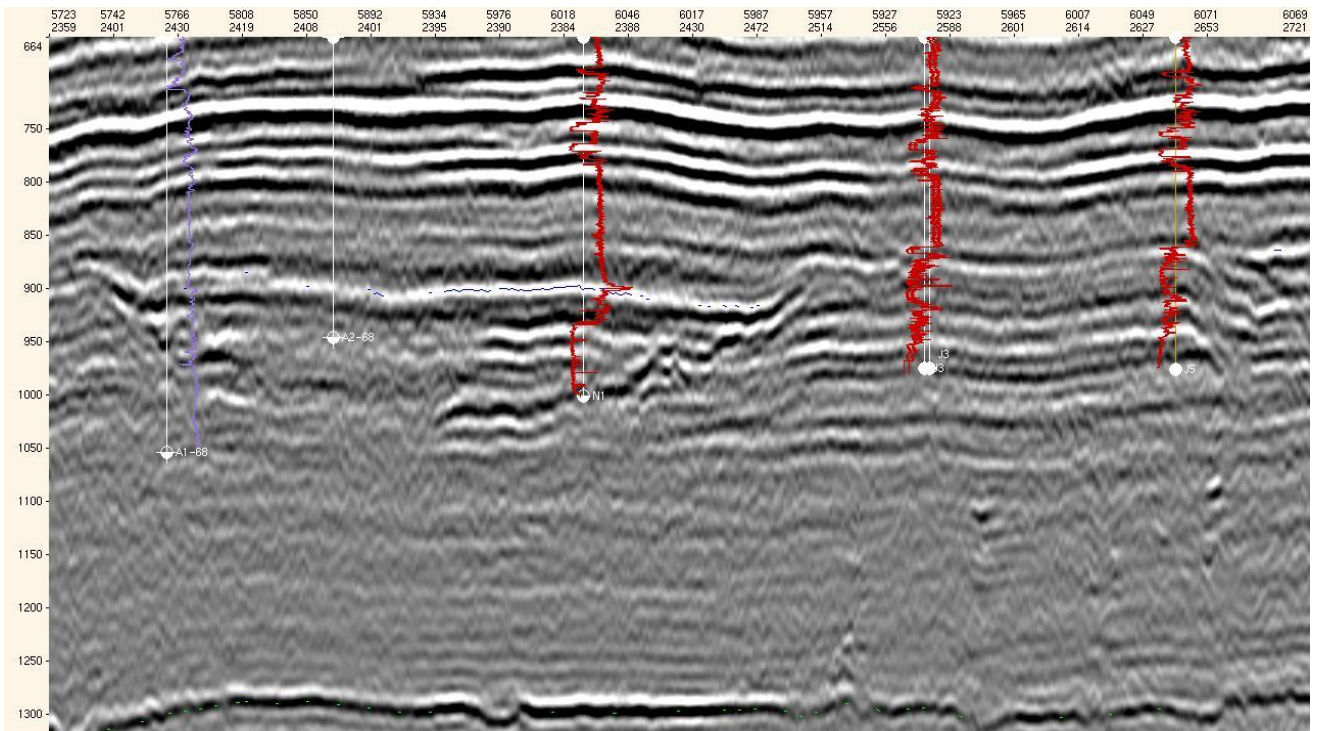


Figure 26 Seismic line "A168A268N1J3J5grey" running through wells A1-68, A2-68, N1-NC186, J3-NC186 and J5-NC186, SW-NE. Wells show gamma ray log in red and sonic log in purple. The Upper Ordovician deposits are mainly deposited in the incision between wells A1-68 and J3-NC186.

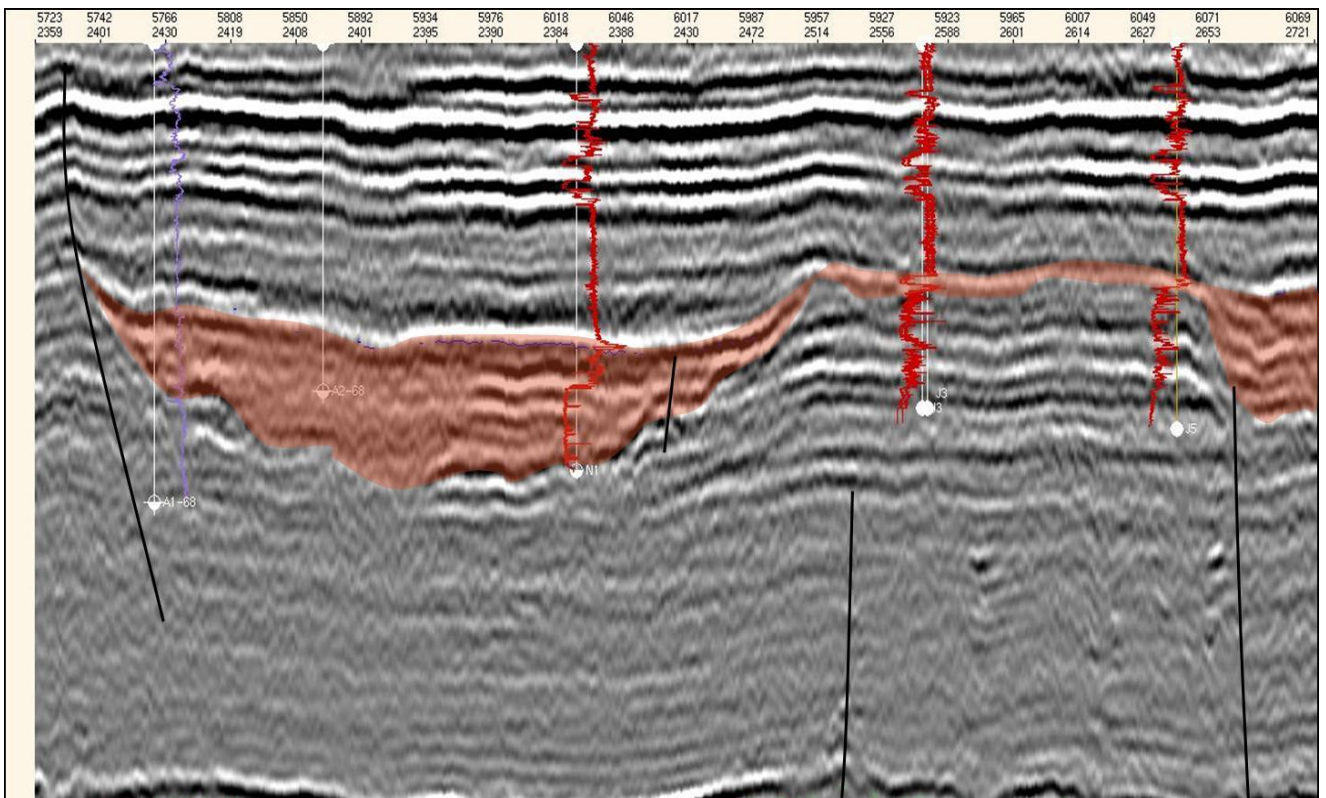


Figure 27 Interpretation of line "A168A268N1J3J5grey" by Neil McDougal. Orange colour shows the infilling Upper Ordovician deposits. Black lines are faults. From left to right, well A1-68 is situated in the flank of the incision, wells A2-68 and N1-NC186 are situated in the centre of the incision and finally, wells J3 and J5-NC186 are situated in the east bounding palaeo-high.

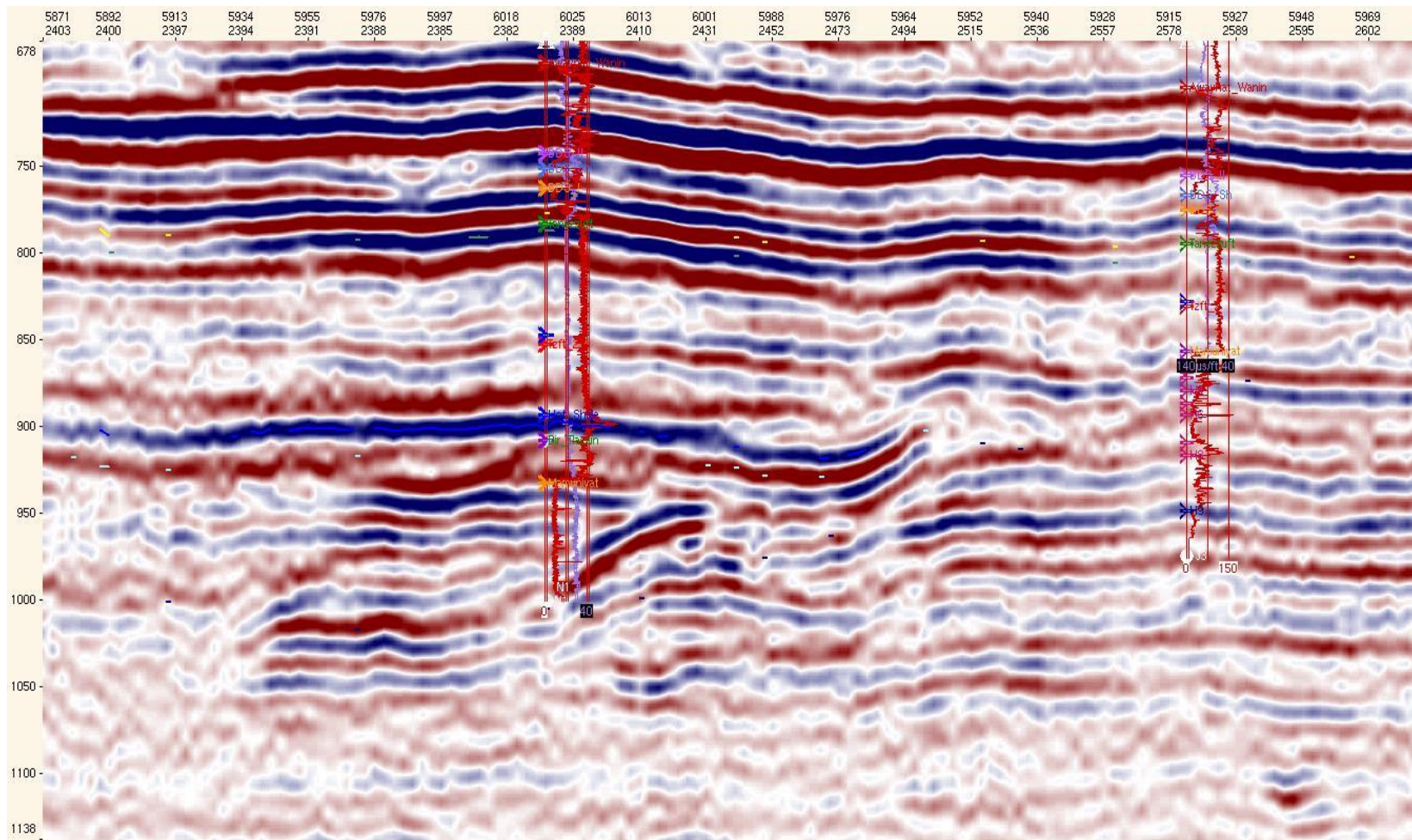


Figure 28 Seismic line "N1J3red" running through wells N1 and J3-NC186. This is a zoomed version on the previous seismic line showing more in detail the contacts between the pre-incision deposits and the infilling Upper Ordovician deposits, N1-NC186 being deposited in the incision and J3-NC186 in the palaeo-high.

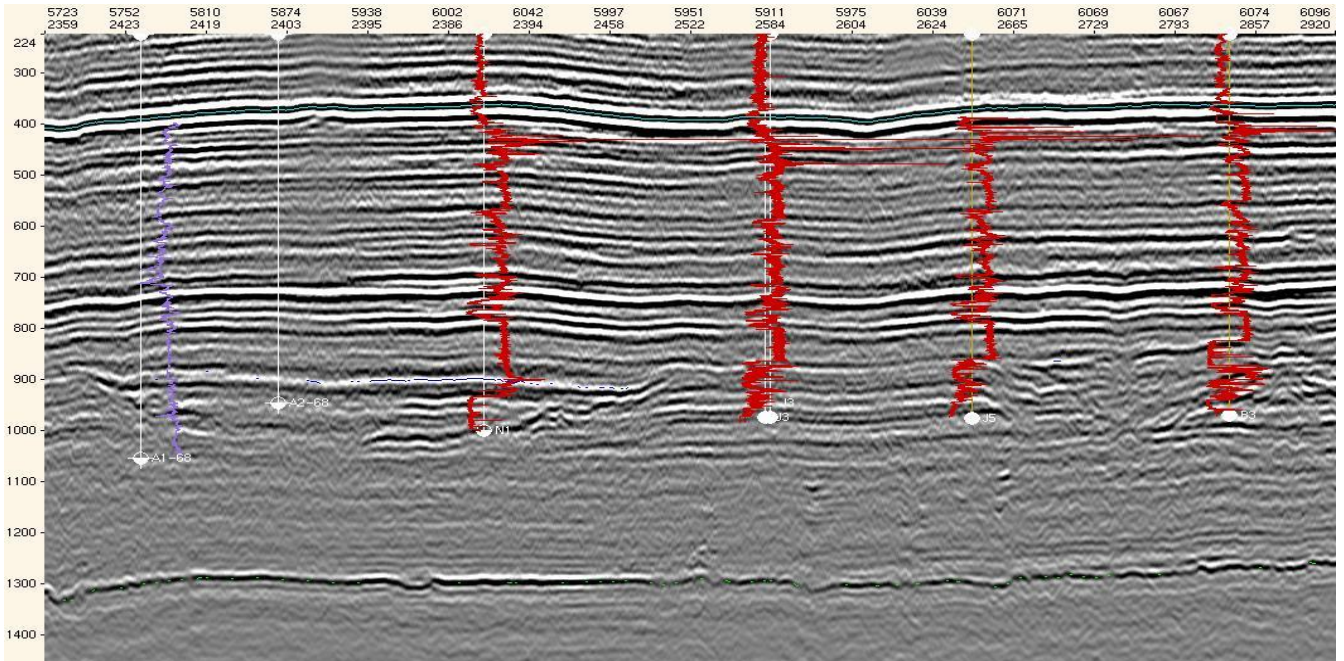


Figure 29 Seismic line "A168A268N1J3J5B3grey". This line shows the transition between Area 2 and Area 3, separated by a paleohigh where wells J3 and J5-NC186 are situated.

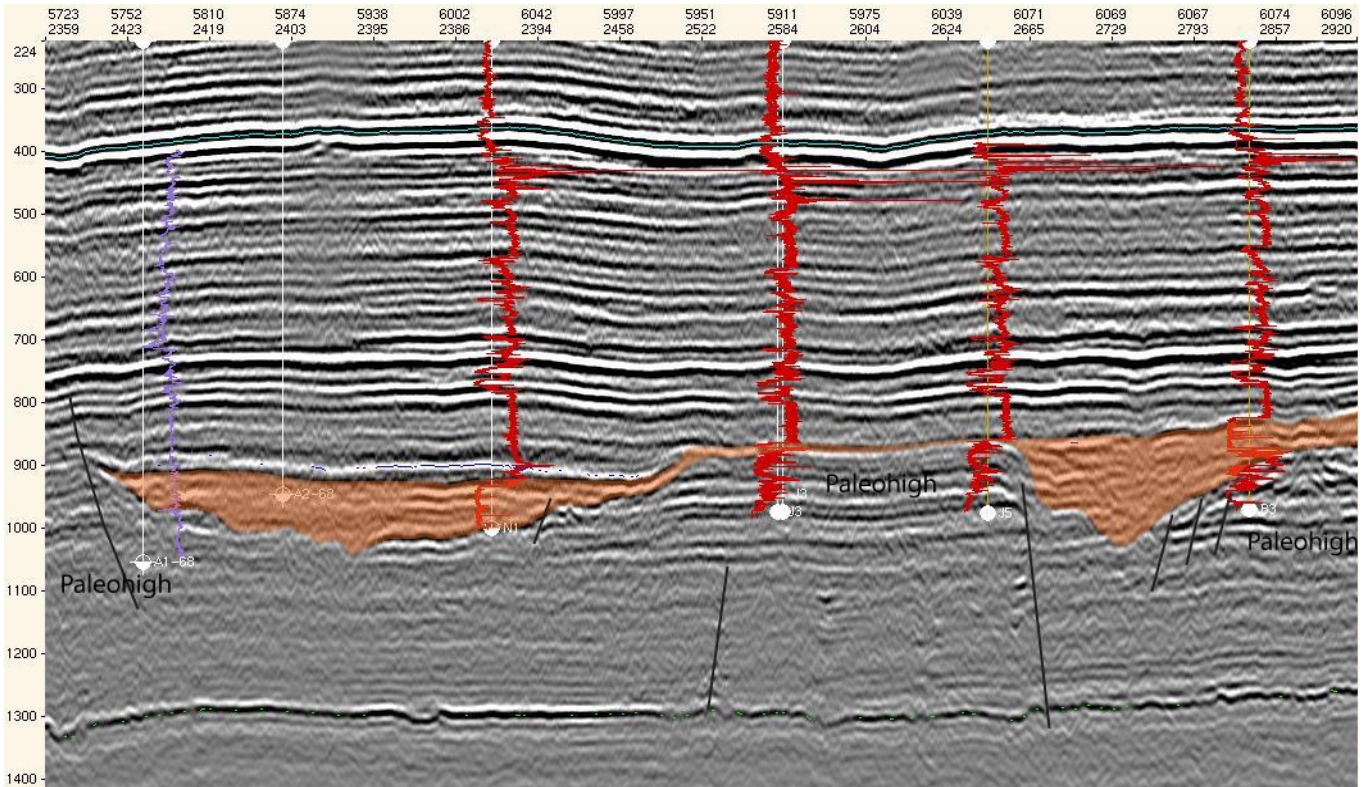


Figure 30 Seismic line "A168A268N1J3J5B3grey" interpreted. Orange colour shows the incision's infill by the Upper Ordovician glacial deposits.

Area 3

More examples of subglacial erosion and incision are visible in Area 3. The isopach map shows that Area 3 has two main SE-NW oriented incisions. The first incision, situated between wells J5 and B3-NC186 has similar dimensions to the incision seen in Area 2 and probably related to tunnel valley formations. The second incision situated between wells B1 and D30-NC186 is wider and might be associated with other type of erosion different from subglacial erosion.

For this Area, 3 lines have been selected and interpreted (see map Figure 21). Lines "J5B3B1greyflatondembada" (Figure 31 and Figure 32) and "B8B2B1B3B4grey" (Figure 33 and Figure 34) show a perpendicular cross-section (W-E) of the small and large-scale incision respectively. Finally, line "K2K1B8B2B1B3greyvcomp" (Figure 35 and Figure 36) gives an overview of how Area 3 looks in a SE-NW cross-section, crossing both incisions. These lines show how the infilling deposits (orange or red in the interpreted pictures) vary in thickness laterally. The thickness of the deposits varies according to the distance to the palaeo-highs and the direction: very thin or no deposition over the highs and towards the north-northwest part, and very thick deposits in the centre of the incision and south-southeast part. Palaeo-highs mark the boundaries of the incisions. A tectonic control seems also to influence the thickness of the deposits; palaeo-highs are often bounded by faults, probably creating preferential pathways for glacial erosion and creation of accommodation space.

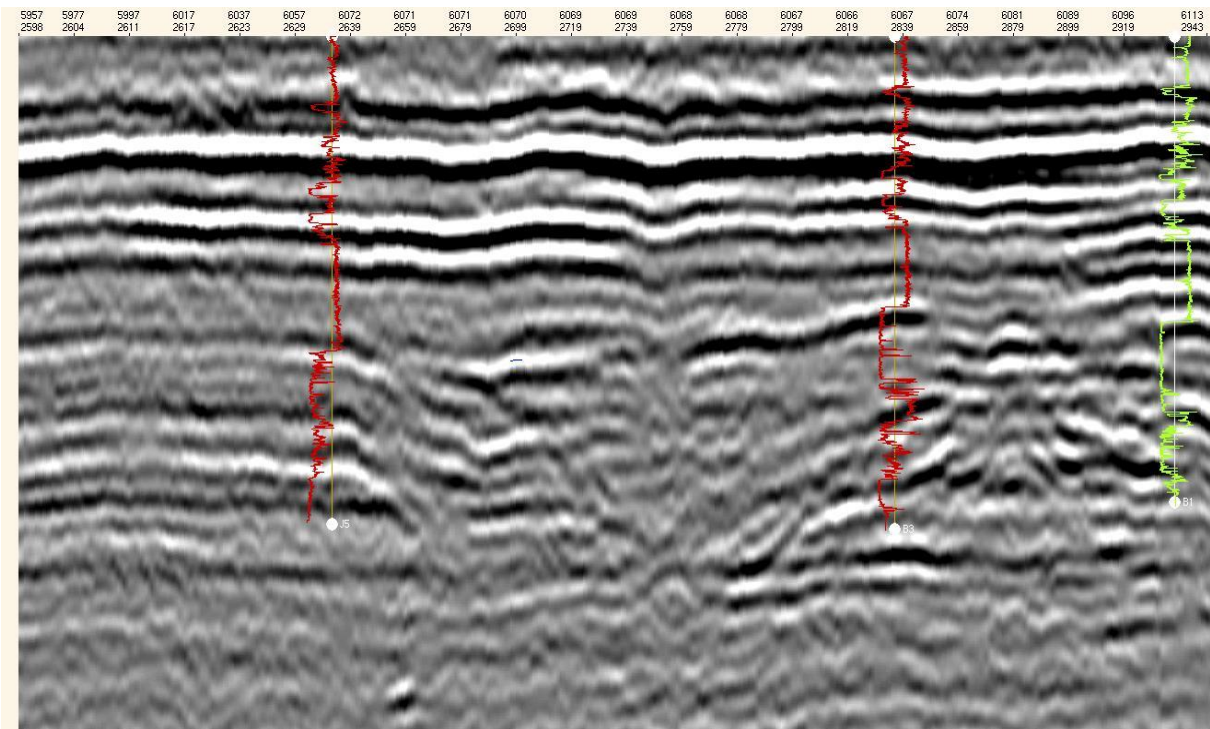


Figure 31 Seismic line "J5B3B1greyflatondembada".

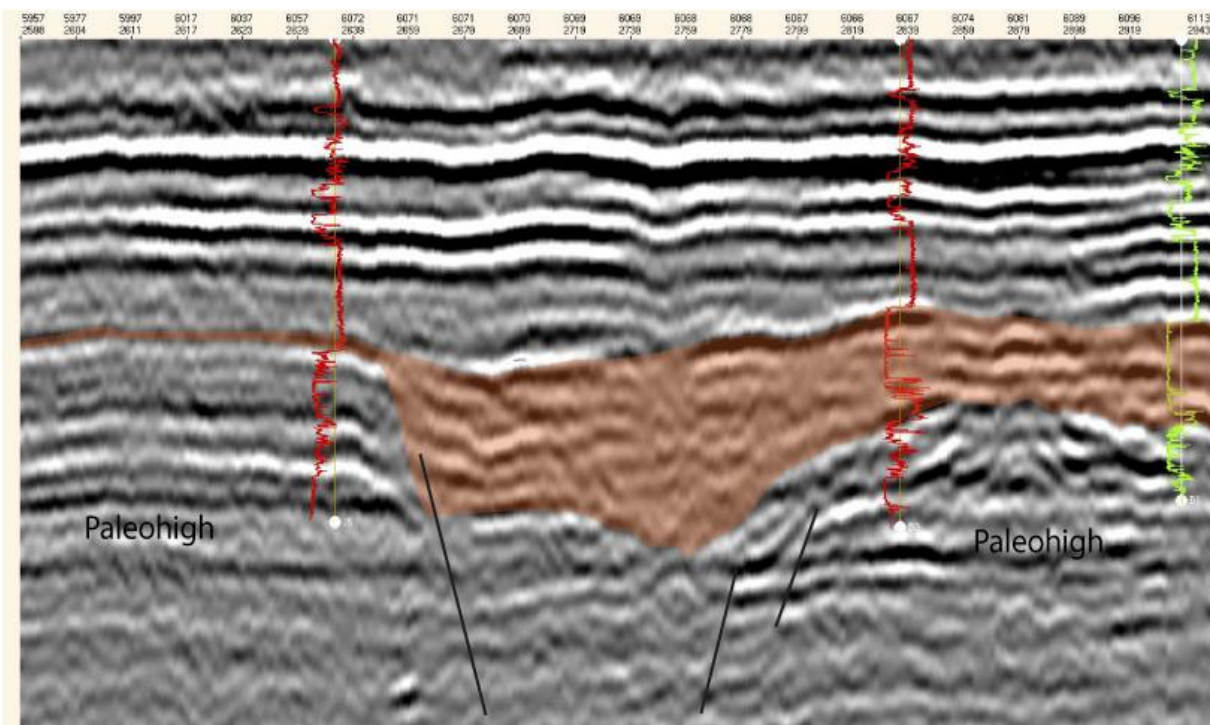


Figure 32 Seismic line "J5B3B1greyflatondembada" interpreted.

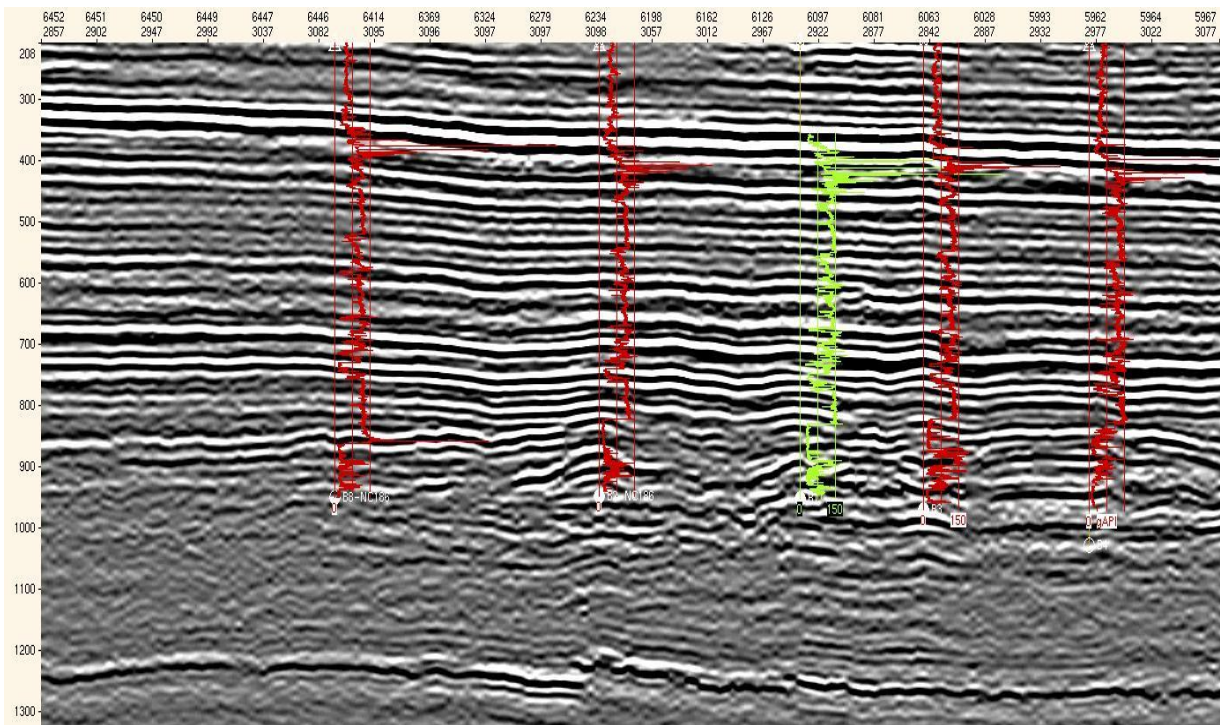


Figure 33 Seismic line B8B2B1B3B4grey

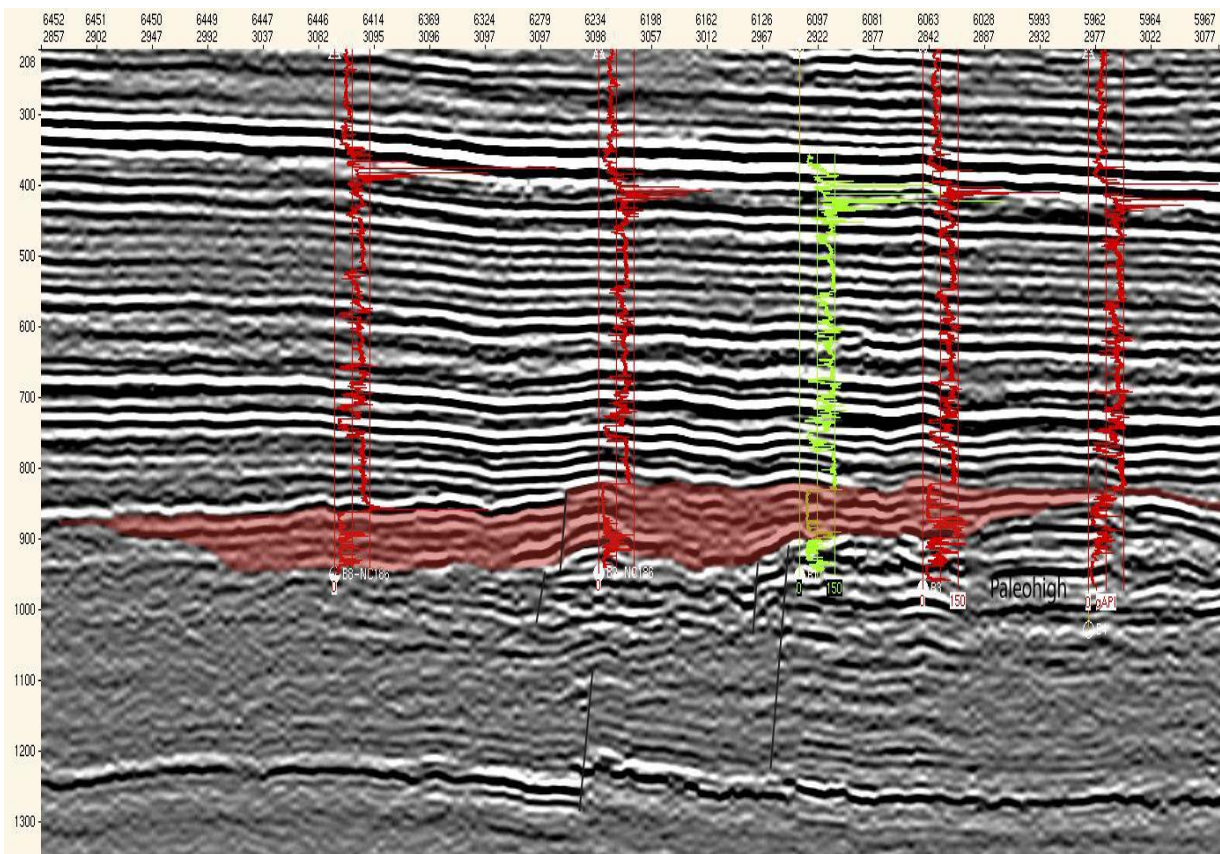


Figure 34 Seismic line :B8B2B1B3B4grey" interpreted.

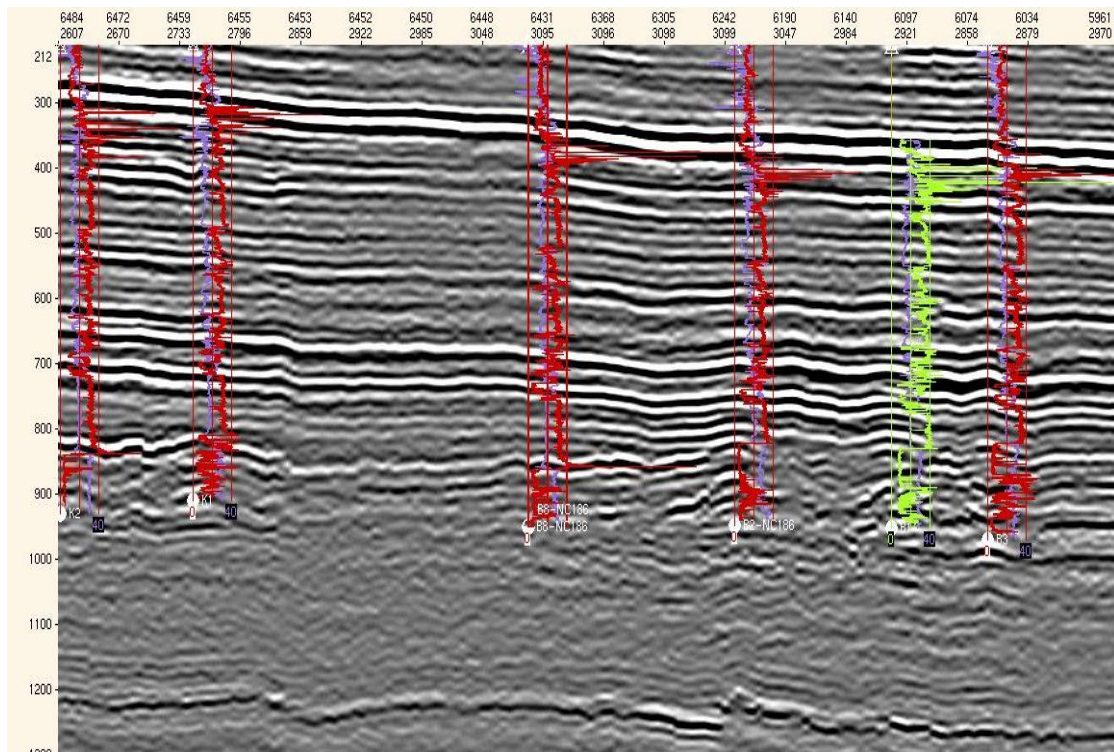


Figure 35 Seismic line K2K1B8B2B1B3greyvcomp.

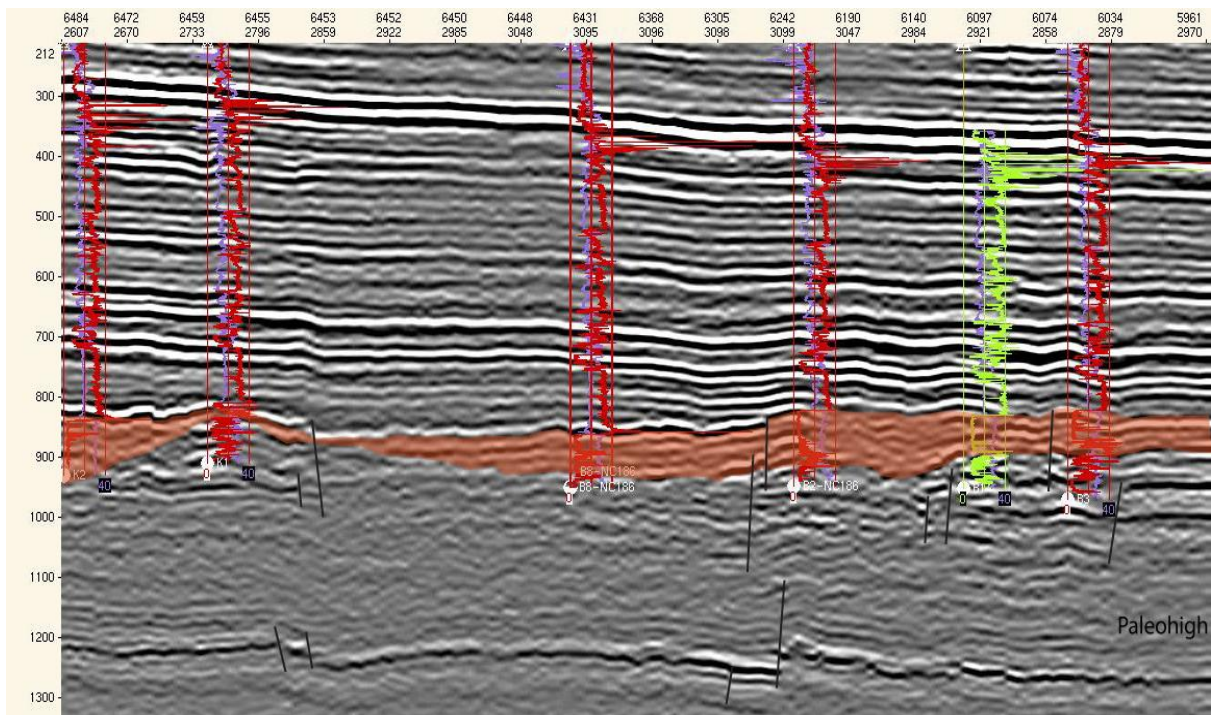


Figure 36 Seismic line K2K1B8B2B1B3greyvcomp interpreted.

9.2 Interpretation of the results

9.2.1 Chemostrat results

After describing the geochemical proxies chosen to compare the different units of the Upper Ordovician formations found in our study area, an attempt to interpret and correlate the units through chemical proxies is presented.

First, representatives' wells from Block-NC186, situated in the centre of incisions where Upper Ordovician deposits are present, will be compared in order to understand the Upper Ordovician environments in terms of provenance, weathering and depositional conditions.

After, a local correlation will be attempted in order to correlate sand units within the different Upper Ordovician formations in one of the three selected areas of Block-NC186.

Proxies signal comparison between wells I1, N1, K2 and B2-NC186

CIA, U/Th, Rb/K and Zr/Ti ratios were calculate for each sandstone sample along depth in four different wells (I1, N1, K2 and B2-NC186). The resulting curves were imported into the Petrel software and plotted against log measurements such as Gamma Ray, and later, the provided well tops were incorporated. Having the characteristic signal for each interval we compare certain conditions for the Upper Ordovician formations at different geographical positions.

The panel presented in Figure 37 shows the results used for this comparison. Interpretations are made from description of the overall shape of the curves within each interval and are not based on values. By looking at the overall shape, we exclude value changes related to measurements and most of all to the grain-size dependency of the chemostrat analyses. Colours applied to Figure 37 correspond to cut-off values based on literature. These values are explained in the "Proxies" paragraph in Chapter 9.1.1.

Melaz Shuqran Formation

The Melaz Shuqran is only present in two of the four wells; these are situated in the large-scale incisions found in Area 1 and Area 3.

The Melaz Shuqran is clearly differentiated from the overlying Mamuniyat formation in different logs due to its fine nature and more clayish content. Furthermore, a striking difference between the two formations is seen in the geochemical proxies: it has a very regular and monotonous geochemical signature compare to the highly variable Mamuniyat Formation.

Chemical index of Alteration

The Melaz Shuqran shows two main intervals in terms of CIA values. The first interval corresponds to the bottom of the formation until Top MS2, which is only found in the very large-scale incision of Area 1. This interval has values of CIA of 50 to 70, indicating intermediate weathering conditions from what has been characterise as cold/arid and warm/humid. The MS3 part of the Melaz Shuqran is found in both Areas 1 and 3, in these areas they present higher CIA values between 70 and 85 suggesting a change towards more humid and higher weathering conditions.

U/Th

This ratio does not show clear variations within the same formation and suggest poor weathering and rapid sediment deposition of the Melaz Shuqran in both areas where it's present.

Rb/K

As observed in the two previous ratios, the values for the salinity indicator proxy are also constant within this formation. Values suggest a transitional environment between a brackish to a marine environment.

Zr/Ti

The provenance proxy indicates a two main provenance source in the Melaz Shuqran Formation. From the bottom of the formations to the Top MS2, values under 0.13 indicate a more shaly sediment source. Close to the Top MS2 and within all the MS3 sub-unit, a more granitic or sedimentary clastic source of provenance is suggested.

To sum up, the proxy signals suggest that the Melaz Shuqran was rapidly deposited into a marine environment highly influenced by fresh meltwater probably coming from the glaciers. Weathering conditions changed from colder to relatively warmer conditions and eroding first the shaliest part of the Hawaz Formation and later introducing a more clastic component.

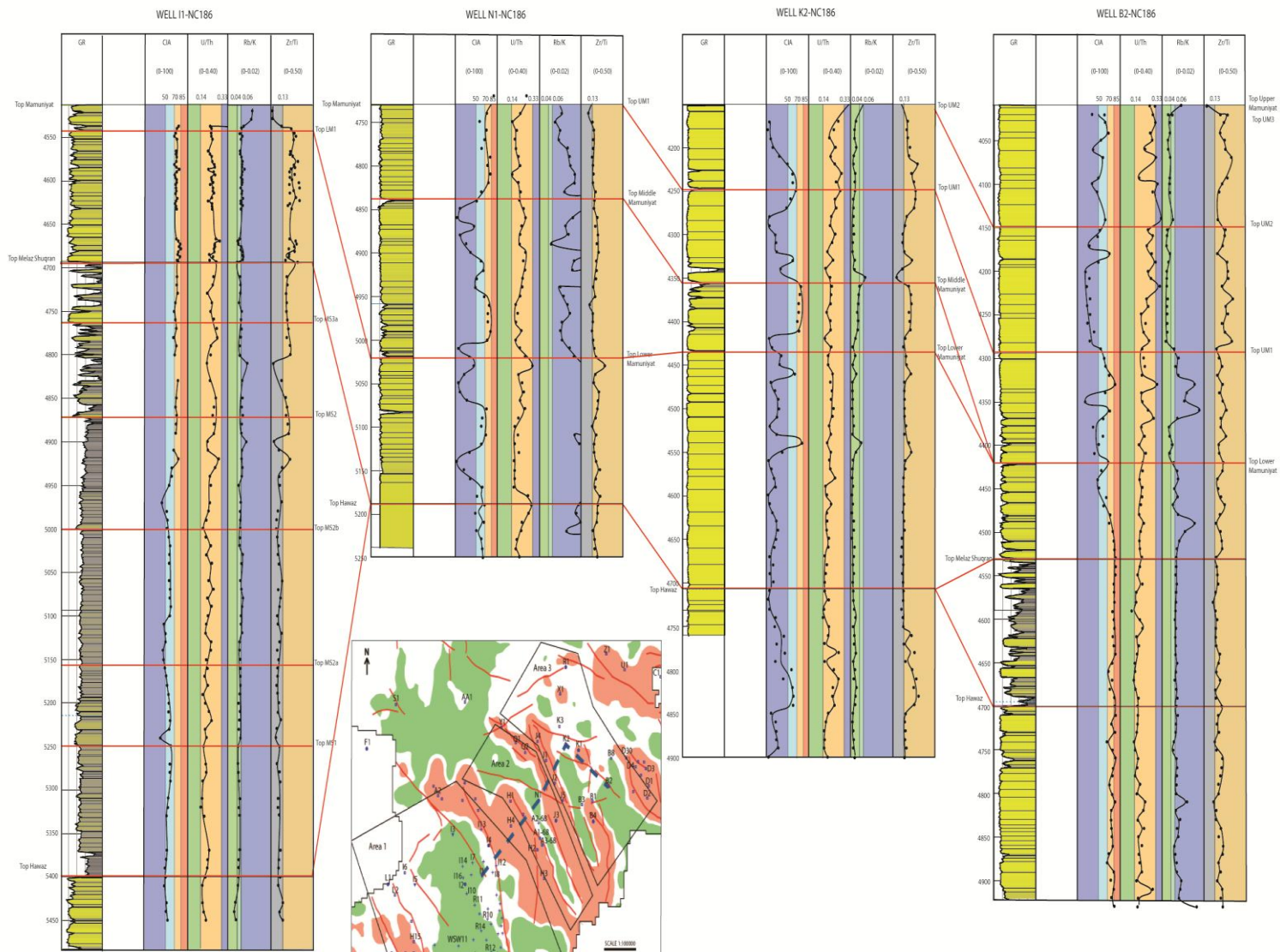


Figure 37 Panel showing selected wells from the centre of incisions in each are, showing Gamma Ray log, CIA, U/Th, Rb/K and Zr/Ti geochemical proxies. Red lines represent wells tops identify from wells, use here to differentiate the proxy signals in each well.

Lower Mamuniyat

The Lower Mamuniyat is present in all four wells and therefore in all areas and incision types.

The same formation shows different log curves, such as Gamma Ray, from well to well, suggesting changes in the sandstones types. We observe that in Areas 1 and Area 3, in wells I1 and B2-NC186 respectively, situated in larger incisions, the formation appears to be less homogeneous (serrated profile in GR log) and thin sand units can be distinguish. In the small incision (tunnel valley type), the formation appears to be very homogenous. These differences are reflected in the proxy signals presented below.

Chemical Index of alteration

CIA values are high where Gamma Ray log values indicates the presence of thinner and fine-grained sand units, with values around 70-85 in well I1 and bottom of the Lower Mamuniyat in well B2-NC186.

In wells N1, K2 and the top of the Lower Mamuniyat in well B2-NC186, values of CIA decrease and show a more sinuous curve type with values ranging from 10 to 70.

These extreme changes in CIA ratio indicate a change in conditions from the Melaz Shuqran Fm to the Mamuniyat Fm.

Furthermore, different types sandstones, fine in the big incision (wells I1 and B2-NC186) and clean and coarser sandstones in the tunnel valley type incisions (wells N1 and K2-NC186) suggest that different weathering condition prevail during their deposition. A lateral diachronous deposition could also be responsible for the lateral variability in the CIA values.

U/Th

The redox-proxy has a more constant signature within areas. It is characterise by values comprise with the “poor weathering and rapid deposition” interval (0.14 to 0.33) with slight increase of the ratio towards the top of the formation indicating a more distal environment.

Rb/K

The Rb/K ratio in the Lower Mamuniyat formation does not give clear indications of salinity conditions since each well presents relatively constant but very different values.

Zr/Ti

The provenance proxy indicates a “granitic or sedimentary clastic” provenance or the sediments composing the Lower Mamuniyat Fm although, a shalier provenance type seems to affect the deposits found in wells presents in the smaller incisions (N1 and K2-NC186) where values are closer to the cut-off value of 0.13.

In general, the proxy signals indicate two main types of depositional conditions depending on the palaeo-topography. Big incisions are characterised by finer-grained sandstones and smaller Lower Mamuniyat sequences (probably eroded by later Mamuniyat formations), whereas in tunnel valley type incisions, the

sandstones seem to be more sandy. The transition between Melaz Shuqran and Lower Mamuniyat formations is not observed in tunnel valley incision making a correlation in terms of depositional conditions between wells even harder to achieve.

Finally, we suggest that the processes responsible for the deposition of the Lower Mamuniyat were different depending on the area (type of incision) but the sediment source and redox conditions were the same.

Middle Mamuniyat

The Middle Mamuniyat is found in wells N1 and K2-NC186 situated in the tunnel valley shaped incisions, although the deposits are thicker in well N1-NC186.

Chemical Index of Alteration

Both wells present the same CIA signature for the same thickness interval corresponding to the bottom of the formation. The curve shows very low values (10) at the beginning with a sudden increase to higher values (70-85). The rest of the Middle Mamuniyat seems to be truncated in well K2-NC186; well N1-NC186 instead, contains a longer record of the CIA conditions showing a gradual decrease of the values.

The Middle Mamuniyat suggest fast changes in the weathering/climate conditions going from cold/arid to warm/humid and back to cold/arid in a short period of time.

We can further suggest that the Middle Mamuniyat was deposited under the same climatic conditions in both incisions and later truncated in a deeper extend in Area 3 than in Area 2.

U/Th

The redox proxy, with values situated between 0.14 and 0.33, falls again within the range of "poor weathering and rapid deposition".

Rb/K

The Rb/K ratio in the Middle Mamuniyat formation doesn't give clear indications of salinity conditions. Values obtained for well N1-NC186 don't always fall within the expected range and differ from the result found in well K2-NC186, without yielding any specific results.

Zr/Ti

The provenance ratio indicates values very close to the boundary between a shalier source and a granitic or sedimentary clastic source. The overall falling within the second type, a change in provenance rock from the Lower Mamuniyat to the Middle Mamuniyat is not considered.

According to these proxies, the Middle Mamuniyat should have been deposited in a short period of time under rapidly changing weathering condition from a clastic sedimentary source.

Upper Mamuniyat

The Upper Mamuniyat Fm is present in wells N1, K2 and B2-NC186. It presents the thickest section in well B2-NC186, situated in the big incision of Area 3 where all sub-units UM1, UM2 and UM3 are found. In well K2-NC186, situated the small incision east of Area 3, sub-units UM1 and UM2 are presents. In well N1-NC186, situated in the centre of the tunnel valley shape incision of Area 2, only UM1 is found. These observations suggest that the Upper Mamuniyat Fm had more influence in the eastern par of Block NC186, where it incise deeper into previous Mamuniyat deposits depositing thick package of sands.

Chemical Index of Alteration

As seen in the rest of the Mamuniyat Fm, CIA values are very variable along this interval.

No clear pattern is found within the UM1 formation. This sub-unit has high CIA values (50 to 85) in well N1-NC186, low values in well K2-NC186 (<50) and variable values (<50 to >85) in well B2-NC186.

Sub-unit UM2 shows, in both wells where it is present, a decrease from CIA values above 50 to lower values (<50) suggesting an onset of colder and more arid conditions.

Finally, sub-unit UM3, present only in well B2-NC186, shows again a very variable CIA signature with values varying from 40 to 70, suggesting intermediate weathering conditions.

U/Th

Values for this redox-proxy show a tendency to increase from sub-units UM1 and UM2 to UM3, going from the interval “poor weathering and rapid deposition” to “extraction of U from the sea”. This increase of U will then indicate more distal and marine conditions, which could be an indicator of a transition towards the transgressive and shaly Tannezuft Fm.

Rb/K

As for the other examples, this proxy is not very indicative of the salinity conditions during the deposition of the Upper Mamuniyat since abnormal values are found at some depths. However, wells K2 and B2-NC186 show values under 0.04, indicating low salinity and more fresh water conditions.

Zr/Ti

The provenance proxy shows mainly two things in the 3 wells where the Upper Mamuniyat Fm is present. The first is an increase in Ti towards the east (see well position) and the second in an increase of the ratio from units UM1 to UM3. These two observations indicate a transition towards a more sedimentary clastic source with time, and that this source was more eroded and transported close to Area 3 where it fed the UM3 deposits.

To sum up, the Upper Mamuniyat show very variable weathering conditions and the decrease in influence of the glacial period, with redox conditions closer to “sea” conditions. The influence of meltwater is visible in the salinity proxy. Furthermore, the pronance proxy shows that preferential areas for the

deposition of the Upper Mamuniyat were found towards the east of Block-NC186.

Well correlation using chemostrat data: example of Area 3

Here, an attempt of well correlation using chemostrat data in wells from Area 3 is presented.

Area 2 was disregarded due to the fact that only one well (N1-NC186) presented enough measurements in the Upper Ordovician infill.

Area 1 presents very thin sequences of Mamuniyat Formation. The main infill corresponds to the Melaz Shuqran Formation. Due to the small thicknesses of Mamuniyat Formation and low variations of the proxies selected within it, this area will not be presented in the results.

Results, in Figure 38 and Figure 39, show that correlation between glaciogenic rock units remains very uncertain due to the fast lateral and vertical changes in facies.

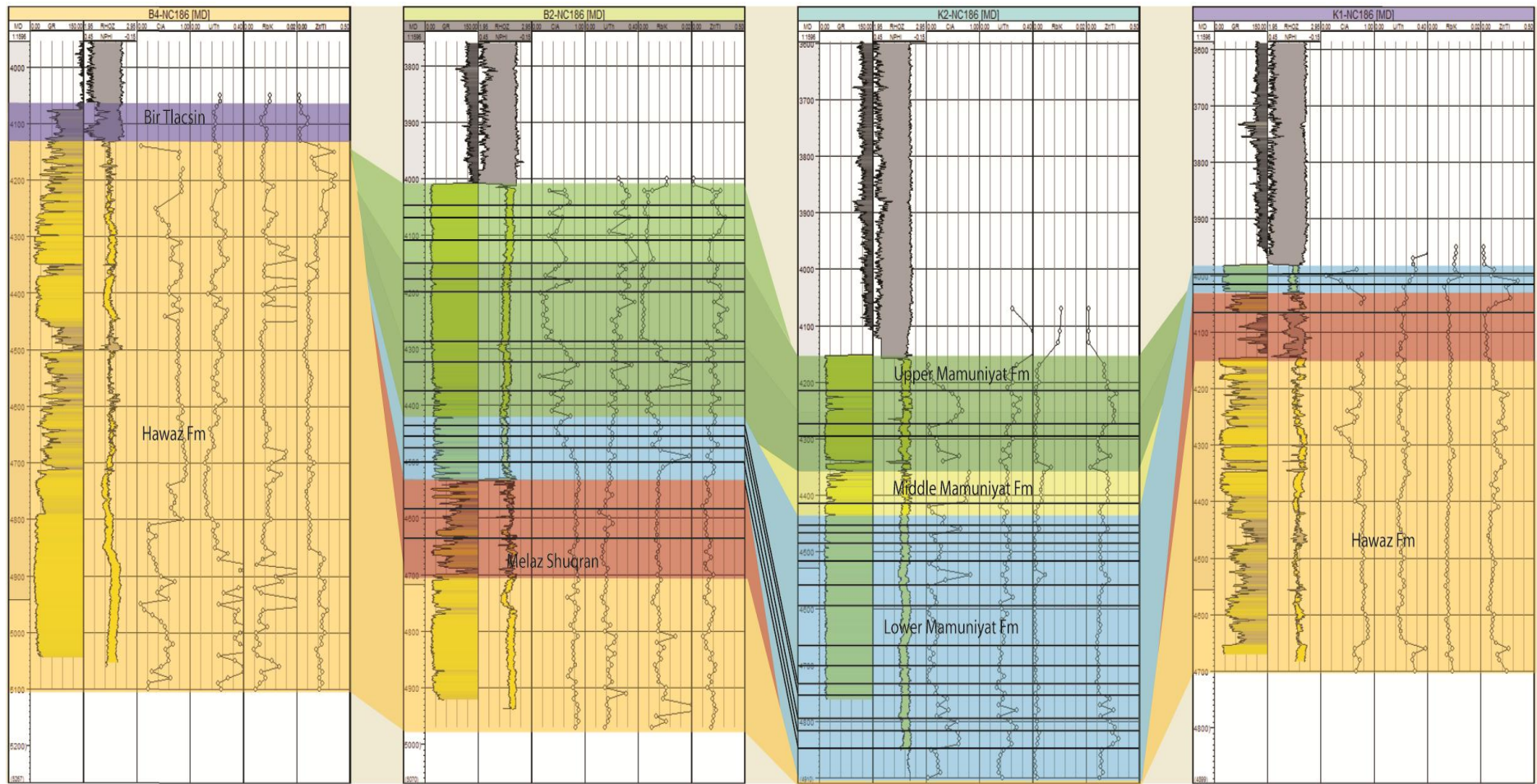


Figure 38 Well correlation in Area 3 between wells B4-B2-K2-K1-NC186. This correlation uses the assigned Repsol well tops in order to establish boundaries between the formations. Black lines correspond to sand units with a characteristic geochemical signature which can be in some cases correlated laterally.

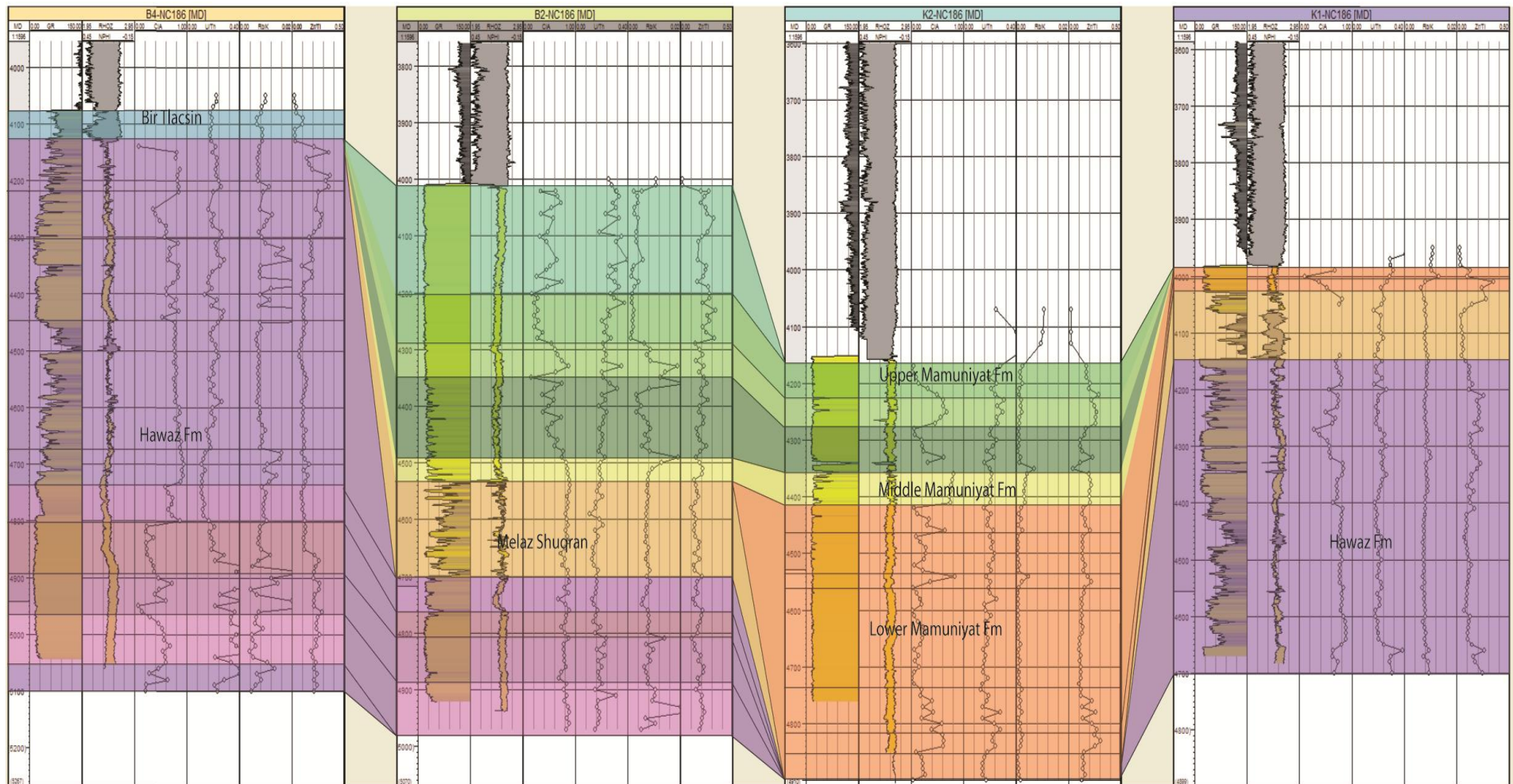


Figure 39 Same well correlation panel as above between wells B4-B2-K2-K1-NC186. This well correlation does not use well tops provided by Repsol, showing slight changes that lead to different correlations between sand units.

9.2.2 Interpretation of the formations and depositional environments

Combining the previous results concerning depositional conditions in the Upper Ordovician deposits, a series of bloc diagrams depicting the depositional environments of Area 3 have been created. Only this area was selected for this purpose since core data was only available in four wells, all situated in Area 3 and acting as control points.

Figure 40 shows the area and surface used for the creation of the depositional environment presented below.

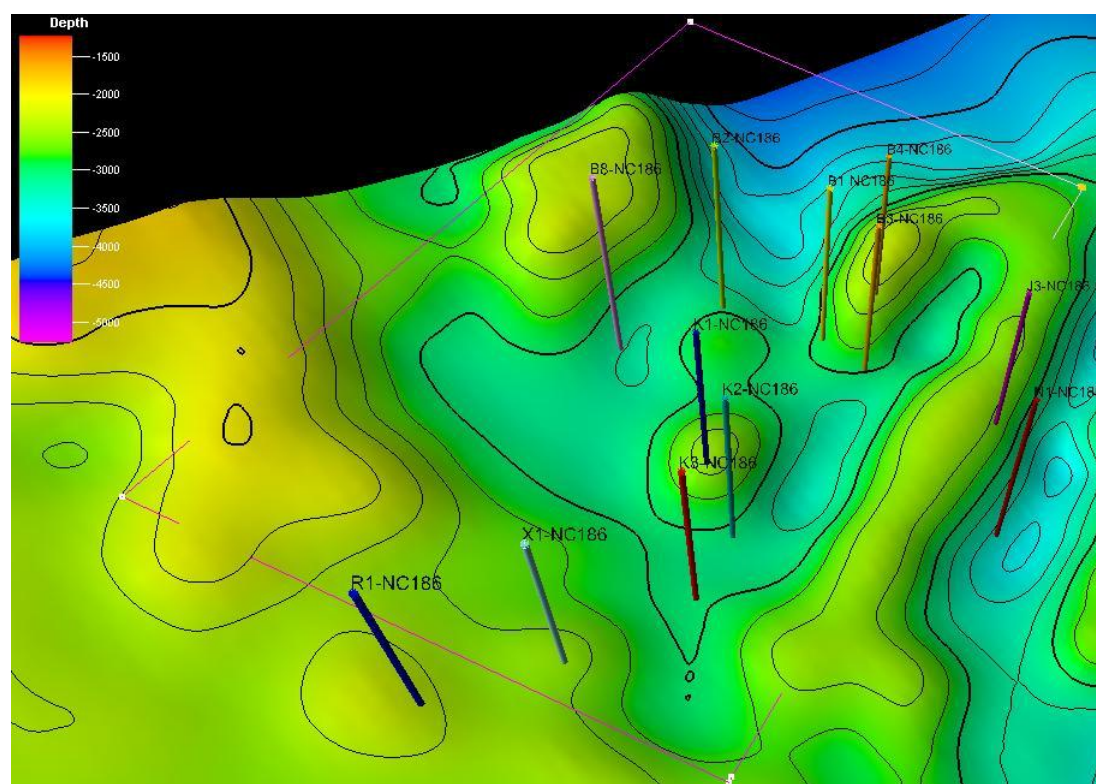


Figure 40 Area selected for recreation of the depositional environment shown in this chapter. The surface corresponds to the Top Hawaz. Wells used as control points are also represented. The red rectangle represents the limits of the study area.

Lower Mamuniyat

The fining upwards sandstones sequences with interclast intervals can be interpreted as ice-contact deposits described by Powell & Cooper (2002) and Sutcliffe et al. (2000). Signs of localised bioturbation and coarsening upward sequences towards the top of the sequence could correspond to the described post-glacial deposits. Both types of deposits will belong to the described glacial retreat system tract (GRST).

Furthermore, in Area 3, three main types of facies were interpreted in the core analyses with from south to north:

- Low gradient braid delta plains with sandflats, distributary and tidal channels,
- Storm influenced shallow marine setting with wave dominated upper shoreface and proximal mouth bars,

- Shelf deposits in the form of submarine sediment flows and sandy slope deposits.

The lithological description and the facies association suggest that the Lower Mamuniyat was deposited in a proglacial and periglacial setting during a retreat of the ice-sheet to the south (Figure 41).

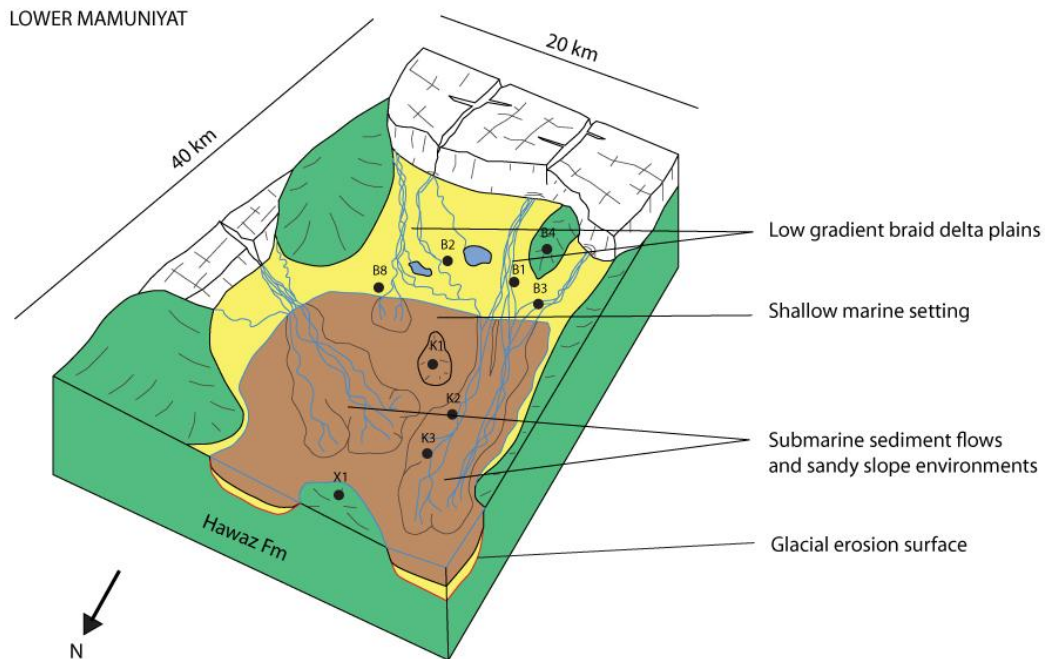


Figure 41 Schematic Lower Mamuniyat depositional environment. Depositional environments range from low gradient braid delta plains to shallow marine setting, ending with deeper turbidite lobes deposits. The presence of ice in the area is not clear, glaciers have been drawn to illustrate glacial conditions and the zones of preferential erosion of the Hawaz Fm.

Middle Mamuniyat

The presence of more argillaceous sandstones in the described cores suggests a more distal environment than the one found during the Lower Mamuniyat. In fact, the described Middle Mamuniyat sequences could correspond to the “glacial marine shelf” elements described by Sutcliffe et al. (2000). These should have been deposited during a GRST (of Powell & Cooper, 2002) after a pulse of ice-advance that would have eroded part of the Lower Mamuniyat. The ice position, when depositing the Middle Mamuniyat in our area, should have then been situated further south.

Furthermore, in Area 3, similar depositional environments to the ones found in the Lower Mamuniyat have been interpreted (Figure 42).

Following this description we suggest that the Middle Mamuniyat was deposited after a short ice-advance and that the glacial influence still prevailed in the area. The end of the deposition of the Middle Mamuniyat is marked by a post-glacial small flooding event in the area.

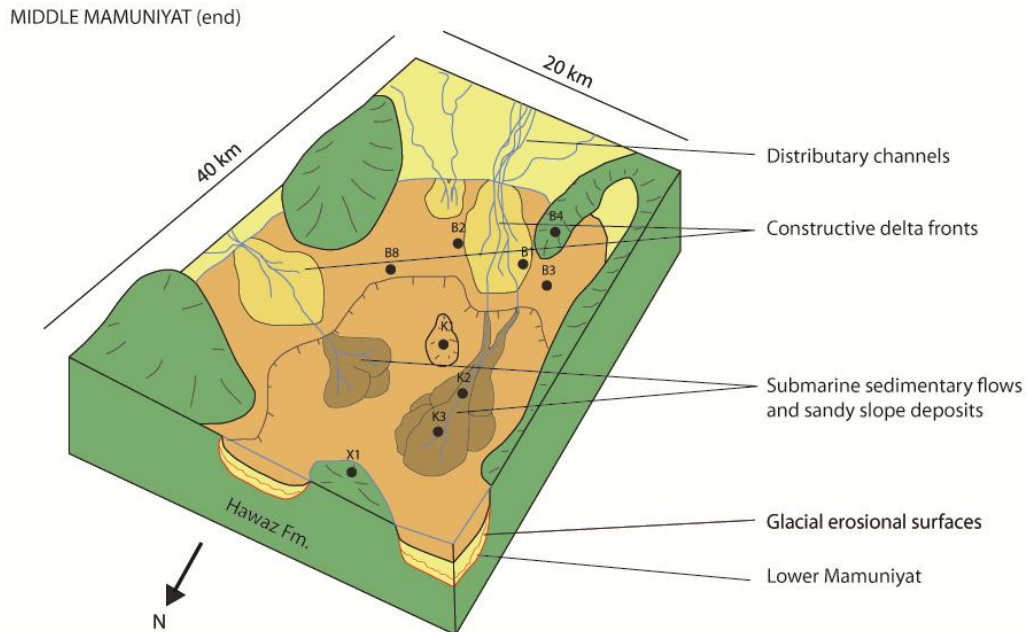


Figure 42 Schematic representation of the Middle Mamuniyat depositional environment. A higher relative sea-level is considered for this period. Ice-sheets have not been represented in order to show an important ice-sheet retreat to the south.

Upper Mamuniyat

The Upper Mamuniyat, although subdivided into three sub-units UM1, UM2 and UM3, presents similar facies associations at each control point (wells):

Towards the north of Area 3, thick and often clean sandstones with dewatered and slumped structures with some mudclast interclast are described. Deformation is not believed to be associated with an ice-advance and loading. The presence of mudclast intervals and the clean and thick sandstones will rather indicate that we are in glacial-shelf conditions with ice-rafted debris introducing mudclast in fans deposited by submarine sediment flows.

Further south, the presence of sequences showing a general fining upward sequence and topped by thinner coarsening upward sequence (found in UM2 and UM3) would correspond to the ice-contact and post-glacial elements described by Sutcliffe et al. (2000).

Furthermore, more continentally influenced facies are found showing retrogradational parasequences close to the palaeo-highs. The parasequences contain traces of incision and infilling by fluvio-glacial channels succeeded by shoreface and later upper marine shelf deposits (Figure 43).

These features will suggest that these sub-units were deposited during a GRST (Powell & Cooper, 2002). Each of the sub-units will suggest small pulse of ice-advance and retreat. According to this interpretation, glacial-advance elements would have been eroded in our area of study during each ice-retreat. The retrogradational sequences also suggest that an increase in relative sea-level followed the ice-retreat, with accommodation space outpacing the sediment supply, indicating a probable end of the glacial episodes.

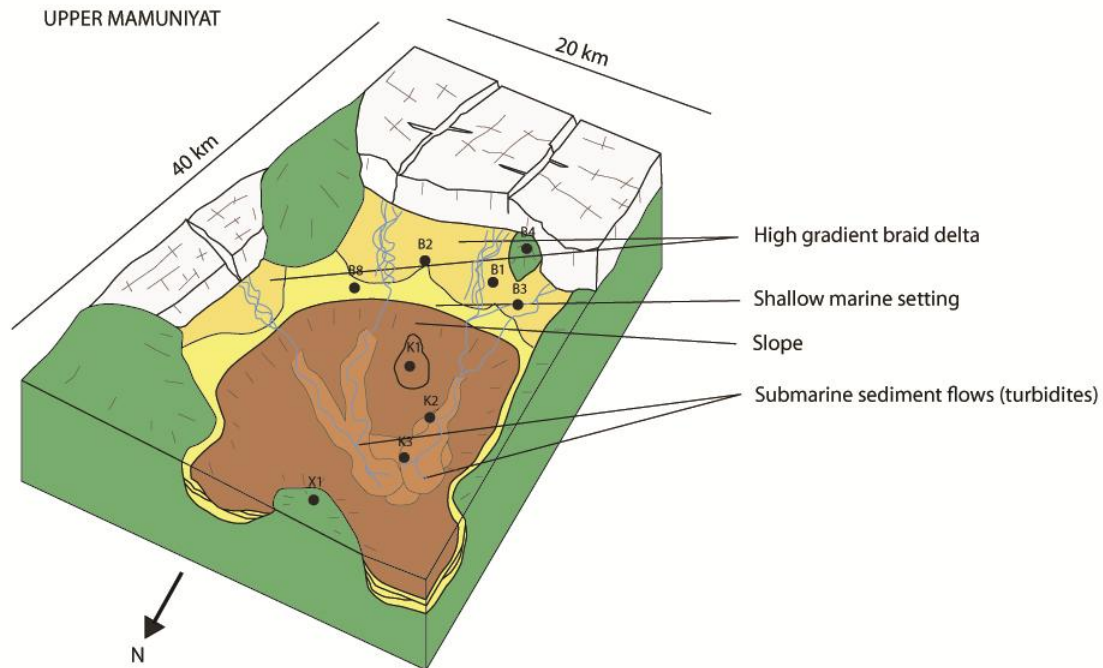


Figure 43 Schematic representation of the Upper Mamuniyat depositional environment. Higher energy conditions occurred during deposition. Ice-sheet position has been represented further north than in the other Mamuniyat formation in order to represent the last ice-advance with associated erosion in the region.

9.2.3 Cross-sections

Here we present two well correlations/cross-sections create using seismic data, well tops and log data.

Cross section in Figure 44 shows a SSE-NNW longitudinal cross-section of Area 3 running through wells B4, B3, K2, K3 and X1-NC186. The cross-section illustrates the complexity of the formation distribution due to the fact that their boundaries correspond to erosional surfaces and are barely visible on seismic. Furthermore the section shows the distribution of the formations near palaeo-high flanks, tunnel-valley axis, the proglacial area and how it ends in another bounding palaeo-high.

Cross section (Figure 45) shows a pseudo WSW-ENE cross-section in Area 3. The cross-section intersects wells B3, B4, B1, B2 and B8-NC186 and shows the lateral distribution of the Upper Ordovician formations.

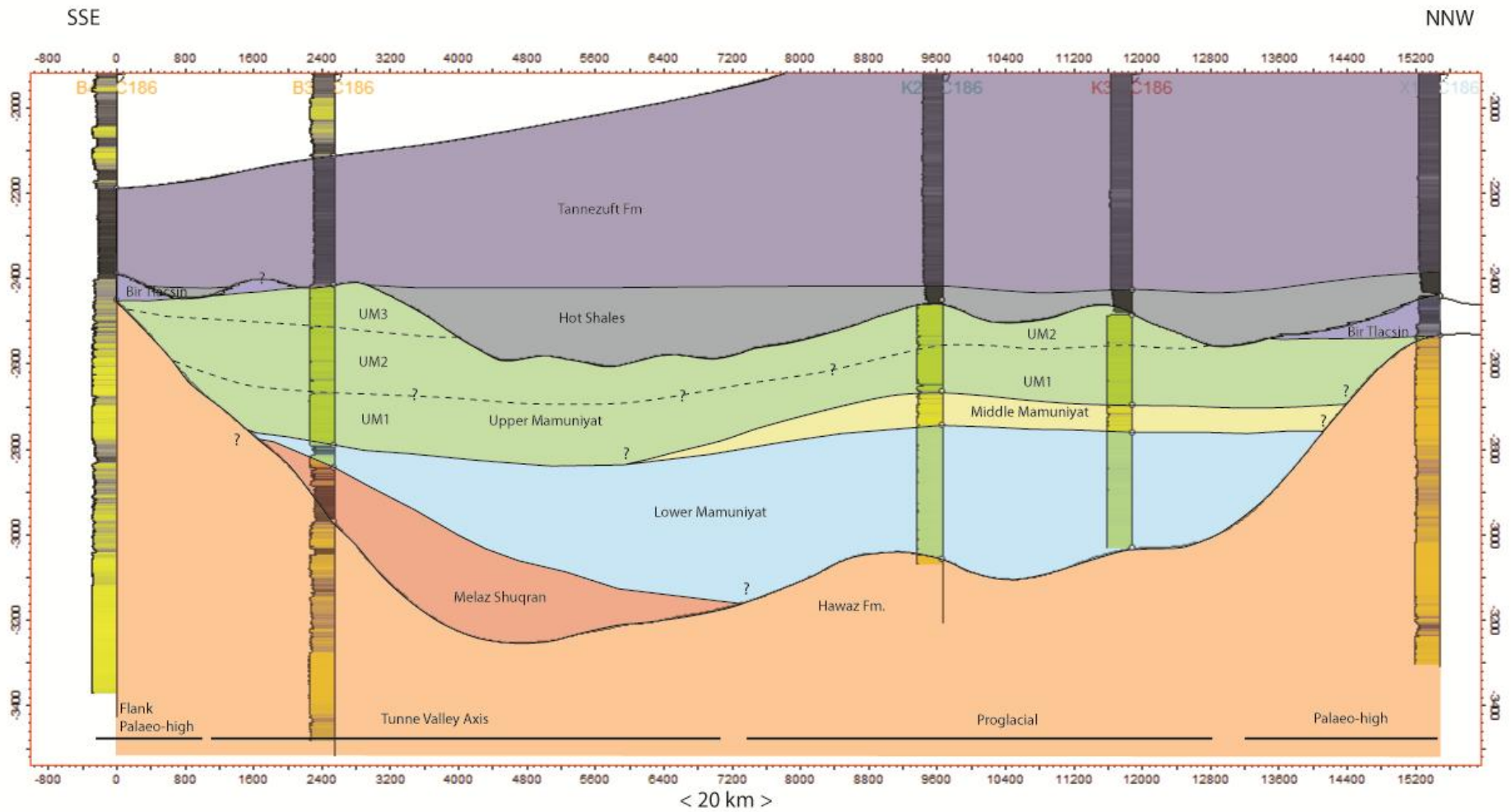


Figure 44 SSE-NNW cross-section created using seismic data and well tops in Area 3. Question marks (“?”) at the contact between formations show the high uncertainty in the lateral variability in a longitudinal view across a tunnel valley axis. Each contact between formations corresponds to an erosional contact. Vertical scale in [ft] and horizontal scale in [m].

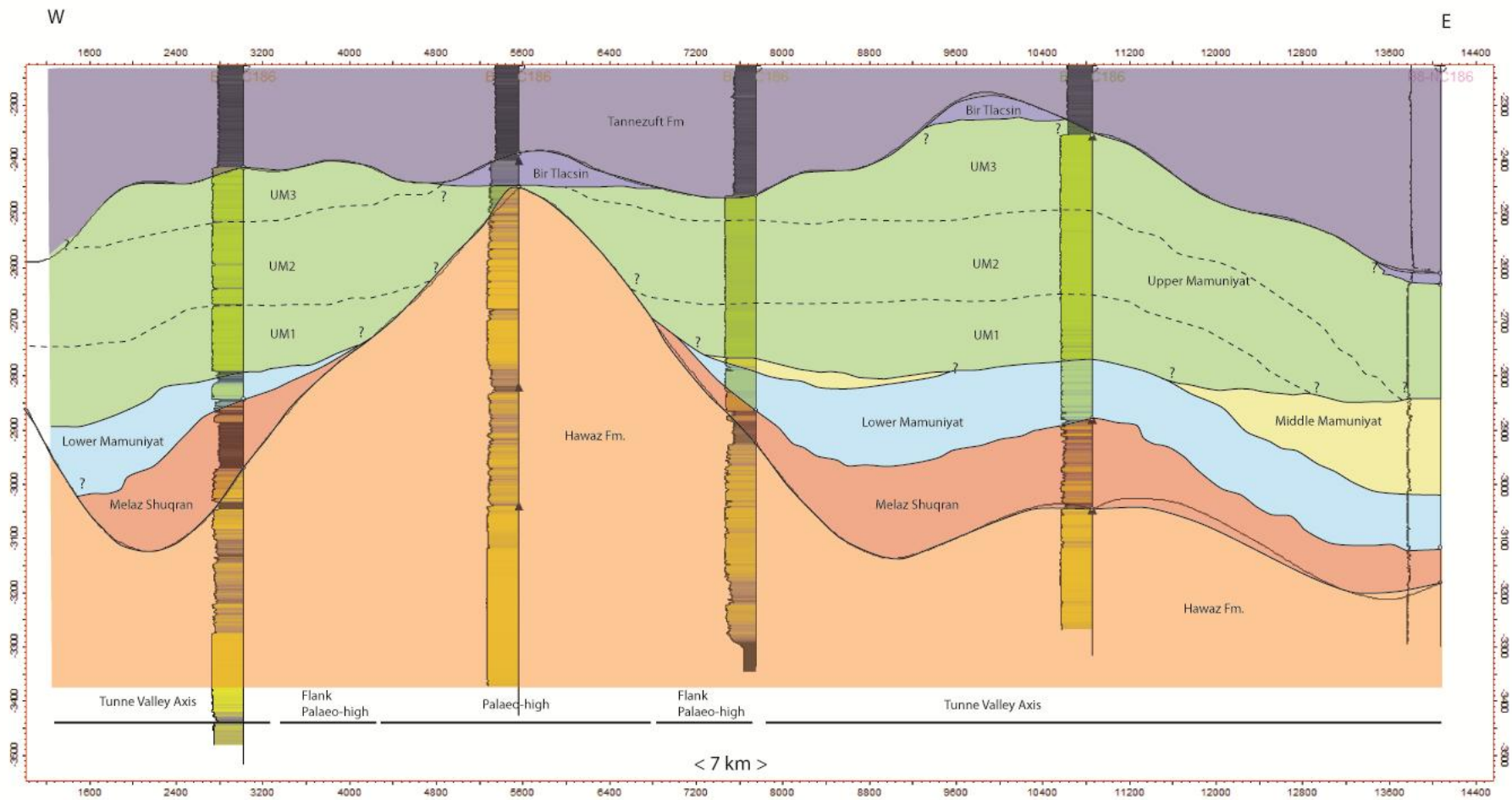


Figure 45 Pseudo W-E cross-section in Area 3. The cross-section shows the lateral variability of each unit perpendicular to a paleo-valley incision. Erosional contact between units has been represented by sinuous black lines.

9.2.4 Infilling history

The previous results allow us to propose the infilling history based on chemical proxies indications, facies association found in cores and the distribution of the Upper Ordovician units within Block-NC186.

In general terms, the sedimentary architecture found in the area, suggest that the deposition was controlled by a series of ice-advance and retreat that formed the former palaeo-topography and deposited the Upper Ordovician formations.

In more detail we can divide the Upper Ordovician glacial period in a series of events. The first event would correspond to the creation of the remnant palaeo-topography found in the area. This is composed of series of elongated incision and small basins bounded by palaeo-highs. Moreover, Ghienne et al. (2003) suggest that the ice-sheet erosion was guided by the pre-existing NW-SE oriented fault system.

The topography was then mainly created by erosion of the pre-glacial Hawaz Formation and extended further north in the region. Therefore, the first event associated with the creation of most of the palaeo-topography would correspond to a large episode of ice-sheet advance that could have covered and eroded the basin area.

After this large episode of ice-sheet advance, a rapid retreat and flooding event deposited the Melaz Shuqran formation. The combination of these two factors could explain the fine-grained nature of this formation and the fact that it is mainly present in the large and wide incisions in Block-NC186.

Following the large ice advance/retreat episode, another glacial episode should have taken place. This new episode is characterised by the presence of the ice-sheet front close to the centre of our study area. This would be indicated by a series of smaller-scale elongated incisions, with glacial tunnel valleys morphologies, that terminate in the centre of Block-NC186. The presence of the ice-front in the area would have induced the subglacial erosion by highly concentrated and pressurized flows responsible for creating the tunnel valleys incisions.

The creation of these new incisions should have been followed by the deposition of the Mamuniyat Formation. Each of the 3 units that compose the Mamuniyat Formation would then correspond to small fluctuations of the ice-sheet position with ice-sheet advances and retreats. The sediment sequences studied from each unit in the wells situated in our area have mainly been interpreted as glacial retreat sequences. Final ice-sheet retreat would have started during the deposition of the Upper Mamuniyat.

The retreat of the ice-sheet further south would have left behind areas topographically depressed where accommodation space was available. In combination with the ice-sheet retreat, large amount of melt water would have contributed to the increasing relative sea-level rise. During the transitional period, the Bir Tlacin Formation would have been deposited, but the sediment supply was probably not enough to fill the accommodation space available.

The transgression, marked by the deposition of the Tannezuft (Silurian) Shales, would mark the end of the glacial events.

Part 2: Lake Simcoe, Ontario

10 Introduction

In order to have a better understanding of the spatial variability of the sedimentary architecture and lithologies found in glacial tunnel valleys settings, the Lake Simcoe in Ontario (Canada) has been studied.

Lake Simcoe was formed during the last glacial period and therefore contains sedimentary records from the late-glacial (14-12 ka) and post-glacial Holocene period. Moreover, Cook's Bay, in the southwest part of the lake presents all features of a glacial tunnel valley (SW-NE oriented deep incision), necessities for the study.

The Canadian Geological Survey has carried out several geophysical surveys in the area. The main focus of their research was to map neotectonic features recorded in the lake sediments. Shilts and Clague (1992) describe the lake deposits as being composed mainly by clay or organic material with high water content. These sediments are therefore highly deformable and susceptible to disturbance during earthquakes (Shilts and Clague, 1992). Such tectonic events should then be preserved in the sedimentary record.

However, in this chapter, we focus on the interpreting and understanding selected parts (the Cook's Bay area) of the seismic lines, acquired in the Lake Simcoe for reservoir geology purposes. The aim of this interpretation is to transpose Quaternary glacial features seen in the subsurface to the Ordovician reservoirs deposits of the Mamuniyat Formation in the Murzuq Basin, Libya.

11 Location

The Lake Simcoe is a lake in Southern Ontario, Canada. It is the fourth largest lake in the province. Simcoe County, Durham Region and York Region border the Simcoe Lake. (Figure 46)

The lake is situated 40 km southeast of Georgian Bay and 70 km north of the Lake Ontario. Finally, the lake has an extension of 45km from north to south and from east to west.

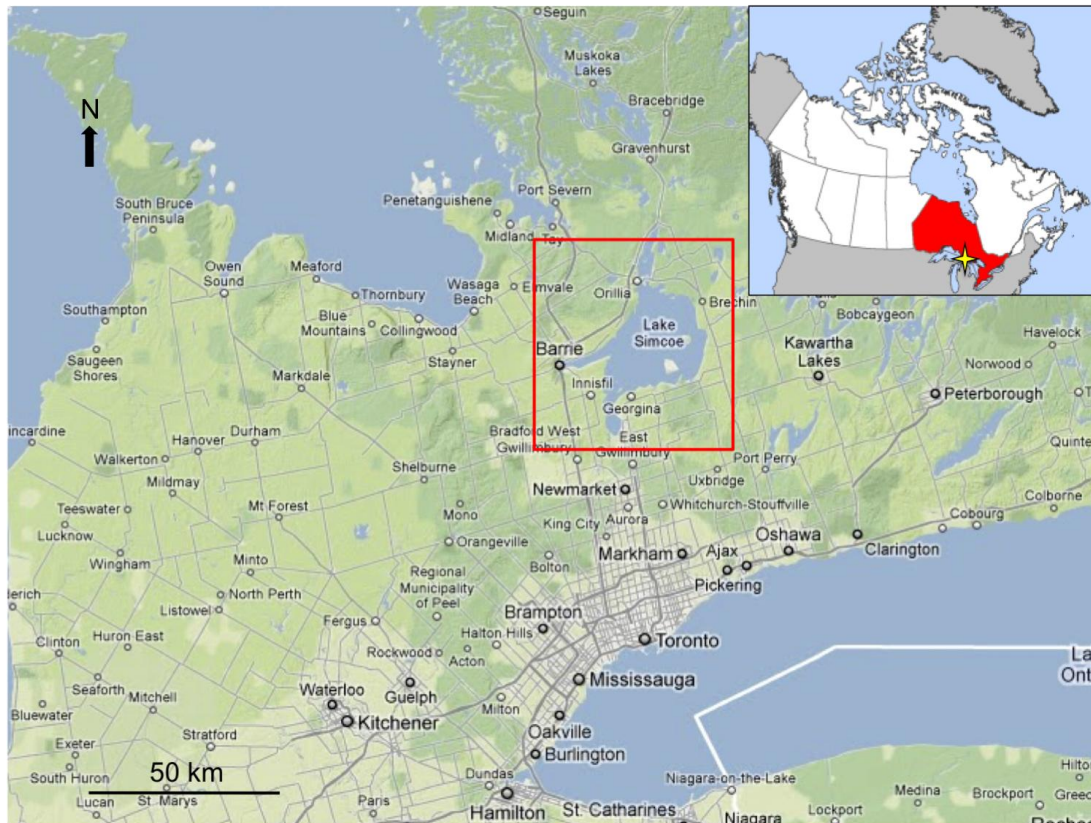


Figure 46 Location of Lake Simcoe, Ontario Canada.
 Source: Google Maps

12 Geological setting

Lake Simcoe is formed over the Middle Ordovician limestone, south of the Greenville's Precambrian metasedimentary and gneissic rocks. Bedrock surface is described as being highly irregular over the Precambrian rocks and planar when in presence of the Ordovician carbonate rocks. According to Todd et al. (2003), dips of the proglacial substrate in the region are very gentle although they are known to be greater when the Palaeozoic rocks drape the Precambrian relief.

Todd et al. (2003) explain that the Lake Simcoe area was glaciated during the advance of the Laurentide Ice Sheet (Figure 47). The ice-sheet had a south to southwest ice-flow direction. Exposed glaciogenic deposits have been given a Wisconsinan age. The deposits have been described as undifferentiated tills, glacio-fluvial ice contact and outwash deposits and glaciolacustrine deposits (Dean, 1950; Gravenor, 1957; Barnett et al., 1991).

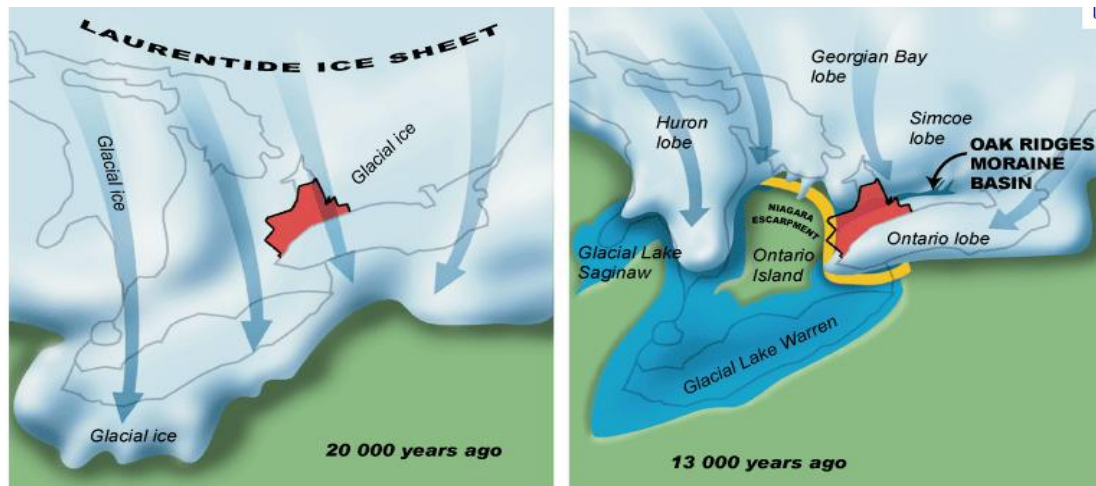


Figure 47 Schematic map view of the evolution of the Laurentide Ice Sheet during the last glaciations. The red polygon shows the position of the city of Toronto, the Lake Simcoe being situated few kilometres north. (Reference unknown from the www)

In our area of study, in the southwest of the Lake Simcoe and more precisely in Cook's Bay, the Oak Ridges Moraine complex represents most of the sedimentary infill in the lake.

The Oak Ridges Moraine is well described by Pugin et al. (1999). They describe the Oak Ridges Moraine (ORM) as a sandy, glaciofluvial-glaciolacustrine landform complex deposited near the margin of the Laurentide Ice Sheet towards the end of the last glacial advance (Late Wisconsinan, -20.000 kybp). The ORM has been classified by several authors (Sharpe and Cowan 1990; Barnett et al. 1998; Pugin et al. 1999) as a moraine dominated by meltwater processes due to its sandy character.

A paper written by Russel et al. (2004) describes the depositional history of the Oak Ridges Moraine. Different stages of deposition are described, starting by the widespread deposition of the Newmarket Till during the last ice advance (Figure 48).

The upper part of the Newmarket Till is marked by the presence of northeast-southwest oriented drumlins. The beginning of the ORM deposition is characterized by a sheet-flood erosional event that covered the drumlinized surface of the Newmarket Till. Erosion during the deposition of the ORM was also related to episodic outbreaks floods. The episodic outbreak floods imply more catastrophic and localized events, which are responsible for tunnel channel erosion features. Subglacial erosion by meltwater flows incised into older sediments and locally reached the Palaeozoic shales and carbonates.

Later stages of formation of the ORM imply the infilling of the incised features and filling the space available created by erosion under the ice retreat regime. A first stage of deposition (Stage I from Russel et al. 2004) corresponds to an active channel fill that is followed by rhythmites deposition (Stage II), which drapes the subglacial flooded tunnel channel deposits by seasonal meltwater discharges. Later described stages of infilling (Stage III) correspond to an ice-contact basin model and subaqueous fan sedimentation of flood discharge from subglacial conduits.

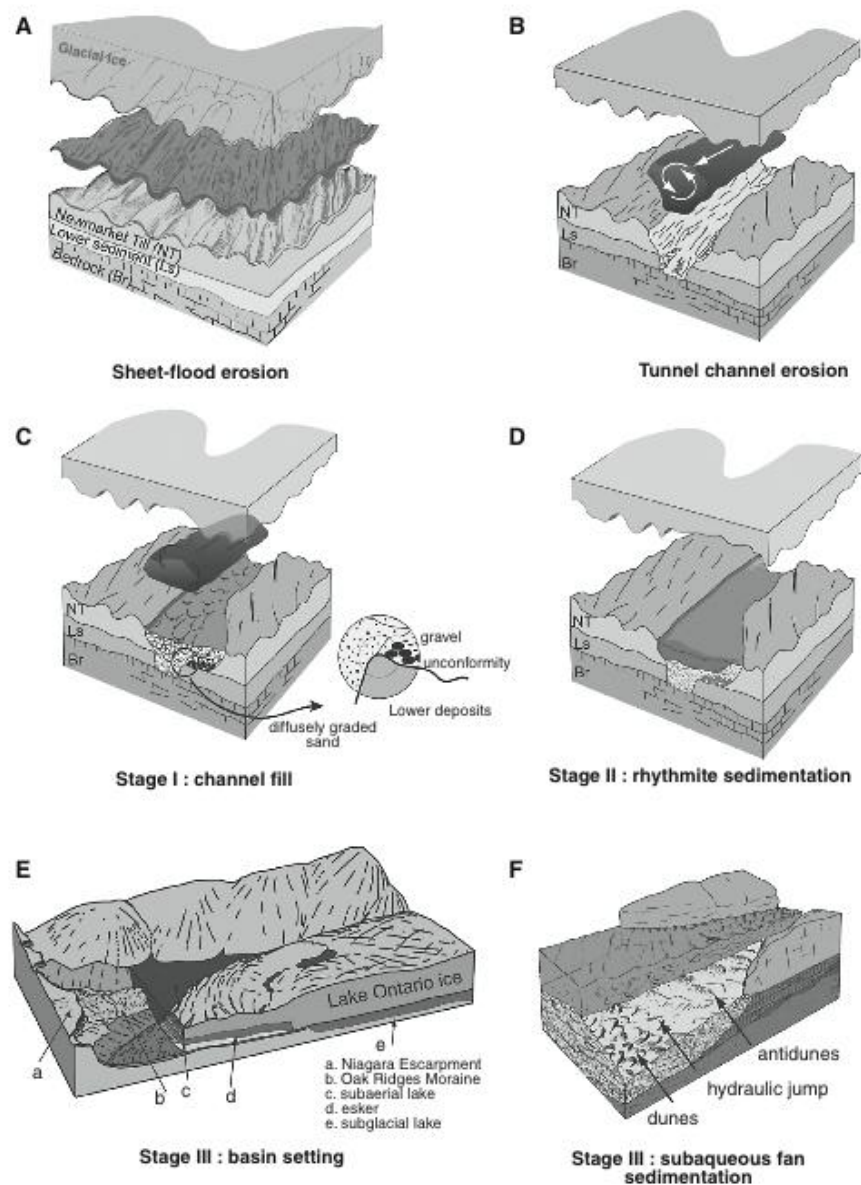


Figure 48 Depositional history of the Oak Ridges Moraine according to Russel et al. (2004).

Now, that the Lake Simcoe geological context has been described, we will give an overview of the material available for the reservoir architecture analysis of the glacial tunnel valleys in Cook's Bay and the methods for interpretation.

13 Data set

The material available for the study of Lake Simcoe is a seismic survey acquired in mid 90s by the Geological Survey of Canada.

The data comprises 53 seismic lines, 8 of which are oriented north south, 44 in the east-west direction and one line is oriented southwest northeast (Figure 49). The total survey covers an area of about 30 km², which extends almost 9 km from north to south and 4 km from east to west.

Average seismic velocity for the shallow glacial tunnel valley infill in this region is assumed to be 1500 m/s (Pugin et al. 1999). Therefore in this work the conversion $10\text{m/s} \approx 15\text{ m}$ is used for sediment thickness interpretation.

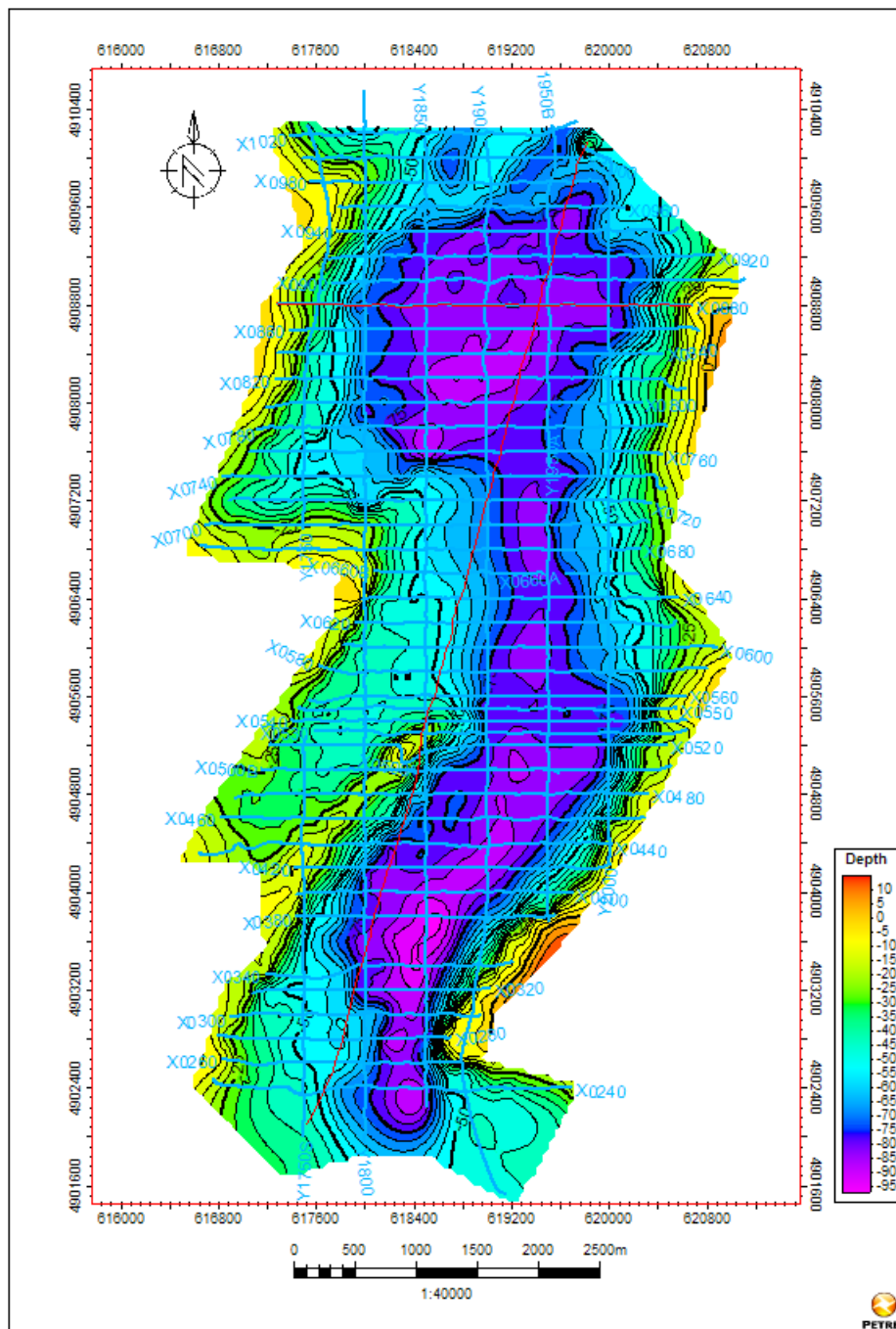


Figure 49 Map view of the Cook's Bay, southwest of the Lake Simcoe. The blue lines represent the acquired seismic lines and the 2 red lines, the selected study lines. The plotted surface corresponds to the "Major Erosion Surface" interpreted from this survey showing the direction and depth of the incision.

Three north to south and 2 east to west seismic lines were selected and interpreted in Petrel. Once the main geological formation were identified (coloured sequences), the seismic lines (or part of them) were imported into Adobe Illustrator in order to interpret the main features visible within each of

the formation (erosional surfaces, downlaps and onlaps reflectors, channelized features, etc.)

From these five seismic lines, two seismic sections (Figure 50) corresponding to part of section SWNE and the entire section X0880 were used for detailed interpretation and reconstruction of tunnel valley sedimentary infill processes.

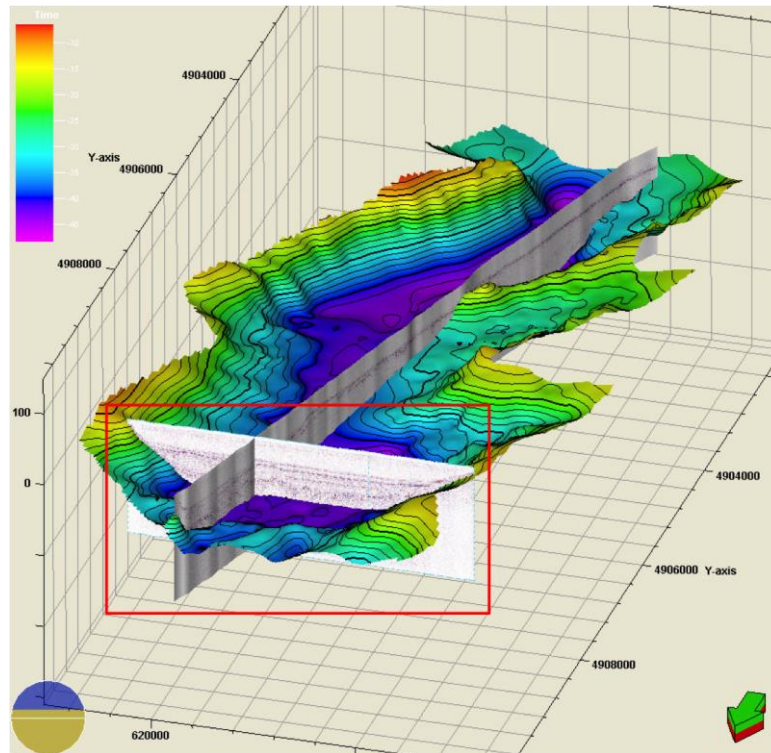


Figure 50 3D view of the Cook's Bay study area showing the two studied seismic lines. The red rectangle indicates the area of study (northern part).

These two lines were selected as they display good seismic features and can be used reliably for the purpose of this study.

13.1 Study Approach

The detailed interpretation of the selected seismic lines in this study was based on previous work carried out by the Geological Survey of Canada (Todd et al. 2003; and Pugin et al. 1999). These works represent key references in this region and have been used to guide us to interpret stratigraphy, the lithologies and depositional environments recorded in the Lake Simcoe tunnel valley infill.

13.1.1 Lake Simcoe : seismostratigraphic sequences

The seismostratigraphic units used in this study are based on the work by Todd et al. (2003).

This work describes the acquisition of seismic data in the Lake Simcoe and contains detailed description and the interpretation of seismostratigraphic sequences. These descriptions are used here in order to identify the main sequence present in the studied seismic lines.

The authors describe four main sequences: the Red and Brown Sequences, the Purple Sequence, the Green Sequence and the Blue Sequence (Figure 51).

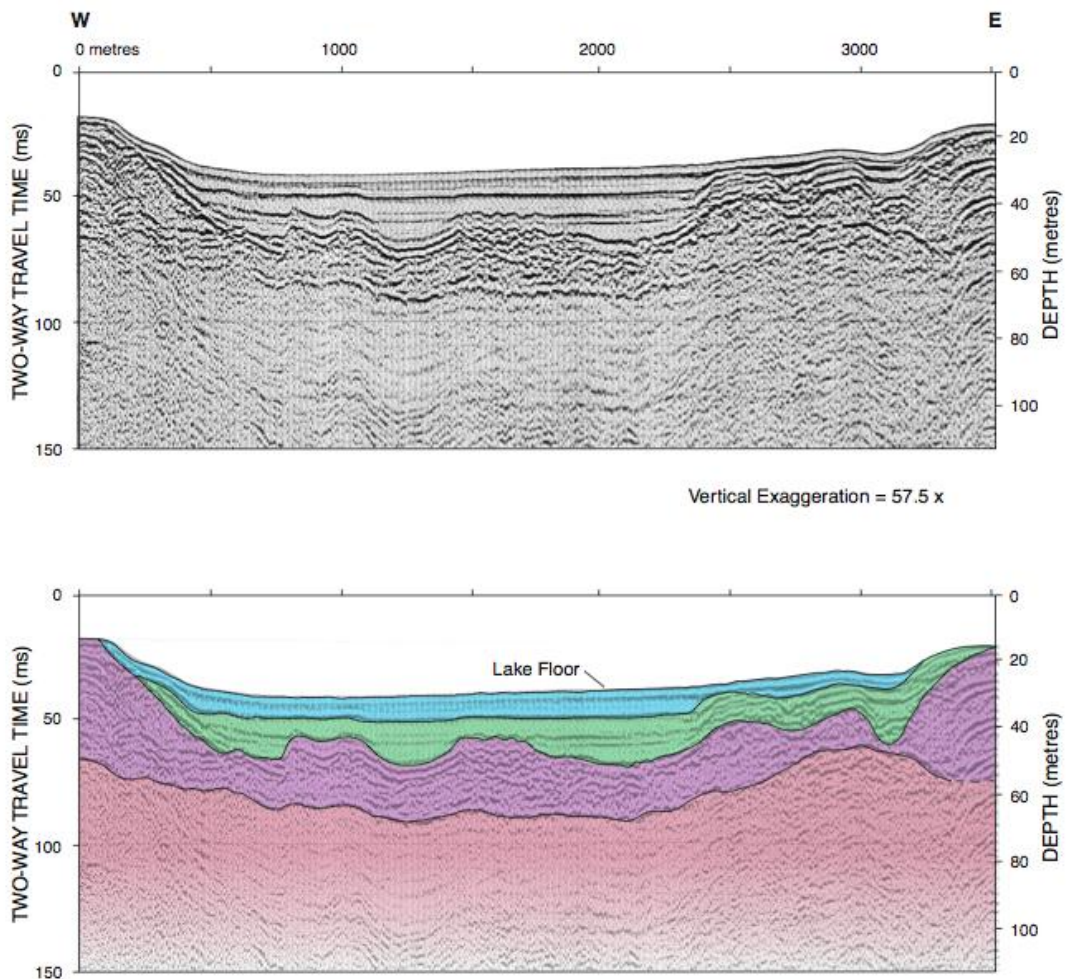


Figure 51 Airgun single-channel seismic reflection profile (upper) and interpretive cross-section showing the seismostratigraphic units in the northern part of Cook's Bay in southern Lake Simcoe. *Picture taken from Todd et al. (2003).*

The Red and Brown sequences are present only locally under the lake and are not found in our area of study (Cook's Bay). The sediments that compose these sequences are assumed to be the oldest till deposits within the Lake Simcoe.

The Purple Sequence is found all across Lake Simcoe and even outcrops in some area on the lake's floor. The authors describe this sequence as mounds having steep cross-sectional shapes and associate these features to the northeast-southwest oriented drumlins. According to their distribution, their reflectors configuration and their unconformable surface, the authors correlate this sequence with the Newmarket Till deposits.

The Green Sequence is found almost everywhere in the Lake Simcoe. In our area of study, Cook's Bay, thickness can reach up to 60 m. The sequence is characterized by parallel reflections configuration with relative strong amplitude and often truncated (indicating erosion and non deposition). The sequence has also been interpreted as post-glacial (Late Wisconsinan) glaciolacustrine fine sand, silt and clay deposited in a sheet drape manner.

The Blue Sequence is the youngest of all four. This sequence is not very thick and only reaches a maximum thickness of 12 m in the western part of the lake. It is characterised by acoustic simplicity and transparency in seismic and is interpreted as post-glacial (Holocene) mud deposits, which drape the lake floor.

13.1.2 Seismic facies

Pugin et al. (1999) created a detailed description of seismic facies found on the acquired data in Lake Simcoe. Here we summarize the main described facies in order to detect and interpret the internal geometries and architectures found in the selected seismic lines.

All seismic facies are found in the Oaks Ridge Moraine area. Pugin et al. (1999) have recognized four major facies depending on amplitude differences. The seismic facies were further divided into 10 subfacies depending on the configuration or continuity of the reflections. The authors also remarked that several sedimentary lithologies could result in similar seismic facies since they are a function of the contrast with the surroundings units (surface reflectivity). A table taken from Pugin et al. (1999) summarize the list of seismic facies: see Figure 52.

Facies I is the most reflective facies. It caps units tens of metres thick and because of the high contrast on seismic velocities within sedimentary units it is characterised by large-amplitude reflections observed regionally and in different stratigraphic settings. This highly reflective seismic facies is interpreted in terms of lithology as coarse-grained sediments, diamicton or bedrock. In order to distinguish between such lithologies different subfacies have been identified based on internal reflection characteristics and on the stratigraphic position. Subfacies Ia have an irregular nature (hummocky) and its interpreted to be occasional gravel lag surfaces. Subfacies Ib presents internal diffractions, which are interpreted as dense till sheet surfaces. Finally, subfacies Ic presents planar geometries and is associated to the bedrock surface or thin till surfaces deposited over the bedrock.

Facies II is medium to highly reflective. The authors associate this facies to two different settings in the ORM: channels or planar strata. The later can be tens of meters thick and laterally extensive. Facies II is associated with medium to coarse-grained lithologies. In more detail, gravels and sands in channels or lenticular shapes have been assigned to subfacies IIa. Layering of contrasting

lithologies (sands, silts and diamictons) with continuous reflectors corresponds to subfacies IIb. Finally, sands and gravels in cross-beds found in dipping reflectors are associated to subfacies IIc.

Facies III is more transparent and has low reflectivity. It is associated to massive sediment packages (10 to 40 m thick and several kilometres across) with low signal strength. Reflectors are often tabular in shape.

Subfacies IIIa corresponds to low-amplitudes (semi-) continuous reflections that drape underlying elements or fill depressions. Subfacies IIIa has been associated to silt and sands deposited by suspension. Subfacies IIIb has better defined planar reflections and it is associated to beds of glaciolacustrine sequences. Finally, Facies IIIc is used when lower signal strength and lower continuity is found. Facies IIIc is associated with sands, silts and diamictons lithologies.

Finally, Facies IV corresponds to the incoherent and chaotic facies, which comprises disorganized, discontinuous reflections reaching tens of meters in thickness and kilometres in width. Only the lower boundary seems to be well defined. Lithologies have not correctly been associated with this seismic facies due to the lack of core data is available. Nevertheless, the author assigns this facies to high-energy deposits and syn-sedimentary deformations along channel margins responsible for the loss of internal geometries.



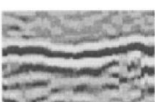







Facies	Description	Subfacies	Example	Interpreted Lithology
I	Highly reflective	a) hummocky, irregular		gravel, sand
		b) reflective surface, internal diffractions		diamicton
		c) planar, continuous surface, little penetration to deeper horizons		bedrock, thin till over bedrock
II	Medium to high reflectivity	a) channel, lenticular		sand, gravel
		b) continuous		interbedded silts, sands, diamictons
		c) dipping reflectors		cross-bedded sand and gravel
III	Transparent, low reflectivity	a) low amplitude, (semi-)continuous		silt, sand, bedded
		b) planar, weak reflectivity changes		distinct sand, silt bed sets
		c) poor signal strength and continuity		shale-till
IV	Incoherent, chaotic	a) angular		variable, disturbed

Figure 52 Table summarizing the seismic facies found in the ORM area by Pugin et al. (1999)

14 Results

14.1 Description

Section SWNE was partially interpreted over 2 km out of the 8.5 km covered by the seismic line. The interest of this profile is to show a longitudinal cross-section of the Cook's Bay area and be able to observe features oriented parallel in the axis of the ice flow (NE-SW) within the Oaks Ridges Moraine deposits. The northern part of the line was selected due to the variability of the signals found within a single sequence.

Section X0880 was interpreted in its full extent (3 km) and gives an overview of the sedimentary architecture perpendicular to the flow regime.

In the interpreted sections, three main types of reflections were observed (see Figure 53), (1) an acoustically transparent signal corresponding to the bedrock, (2) an overlying highly reflective group of reflectors with different geometries, and finally, overlying this two types, (3) a low amplitude tabular section with continuous to semi continuous reflections.

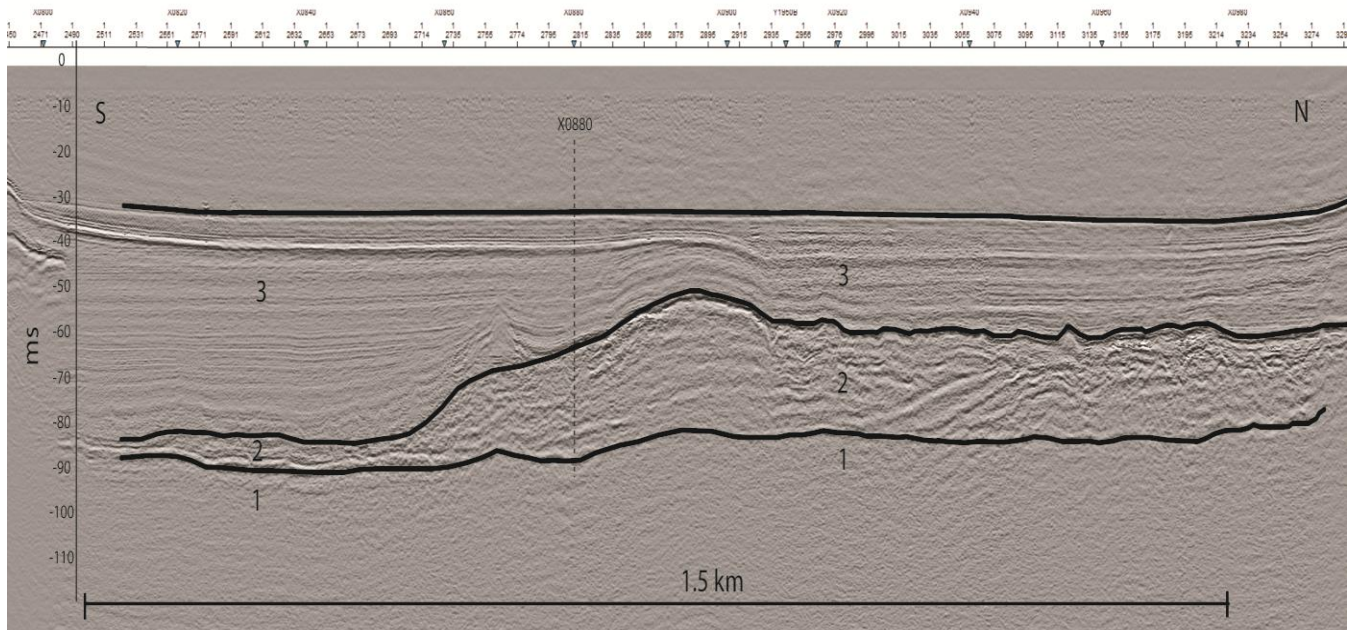


Figure 53 Part of interpreted cross-section SWNE (northern side) showing the three main seismic signals found in the section. Numbers 1 to 3 (bottom to top) correspond to the each of the described signals.

As explained in Chapter 13.1, the first task that was achieved was to determine the formations present in the seismic profile.

Using the description of the seismostratigraphic sequences by Todd et al. (2003) we identified two of the sequences, the Blue and the Green Sequence.

14.1.1 Seismic stratigraphy

The Blue Sequence was identified under the lake's floor. Its upper boundary was interpreted at the top of the last coherent and low amplitude reflector visible on the seismic section. The lower boundary was interpreted in a highly reflective reflector, which probably corresponds to an erosion or non-deposition surface marking a change in the flow regime visible when observing the interpreted internal reflectors, going from north to south to south to north. This change in flow regime is attributed by many authors to the post-glacial isostatic rebound that uplifts presently the southernmost most part of the Oak Ridge Moraine region. Further evidence is given when reflectors are observed in detailed: a SW to NE progradation of extensive draping reflectors can be observed (see the

internal geometries description for further information). The average thickness of the Blue Sequence in our selected area is 8 ms or about 12m.

The Green Sequence was identified under the Blue Sequence and represents the rest of the sedimentary infill visible in seismic in this area. The bottom boundary was identified at the end of the last high amplitude and coherent reflector visible before the bedrock (noisy signal).

The particularity of our study area is the clear thickness changes in seismic facies visible within the Green Sequence. When looking to the complete SWNE section (and all other seismic lines oriented NS), a clear feature is visible: the Green Sequence becomes thinner towards the south. Not only the Green sequence becomes thinner towards the south but also the seismic signature in the south is more homogeneous. Towards the northern parts of the seismic line, the Green Sequence becomes thicker and present at least two very different seismic facies.

After identifying the sequences present in the selected area (Figure 54 and Figure 55), the internal geometries were studied, first by analyzing the internal reflectors and later by associating the seismic facies proposed by Pugin et al. (1999).

Figure 56 (A) and Figure 57 (A) show the interpreted version of the selected area in section SWNE and section X0880 (complete). Figure 56 (B) and Figure 57 (B) show the same section interpreted in terms of seismic facies following the nomenclature of Pugin et al. (1999).

NOTE: No faults were observed during the interpretation of these lines

The description and interpretation of the results will be focus in the Green Sequence since this sequence is geologically correlated to the Oak Ridges Moraine's glacial lake infill and the tunnel valley deposition in the Cook's Bay area.

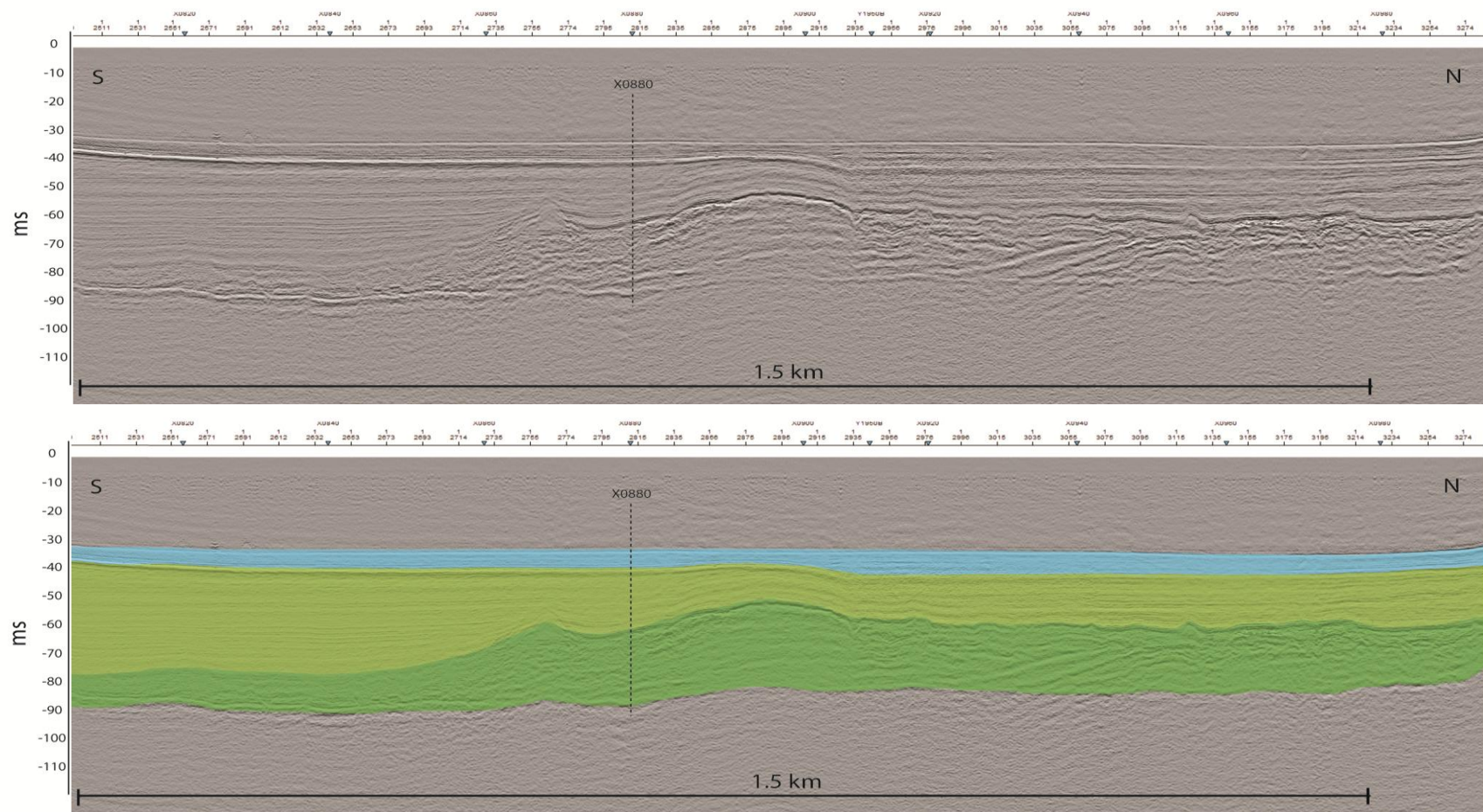


Figure 54 Above, part of seismic section SWNE (northernmost part), below, interpreted seismic section with all the sequences found in the area: Green and Blue Sequence according to Todd et al. (2003). In this study the Green Sequence has been divided into Lower and Upper Green Sequences due to the difference in seismic facies.

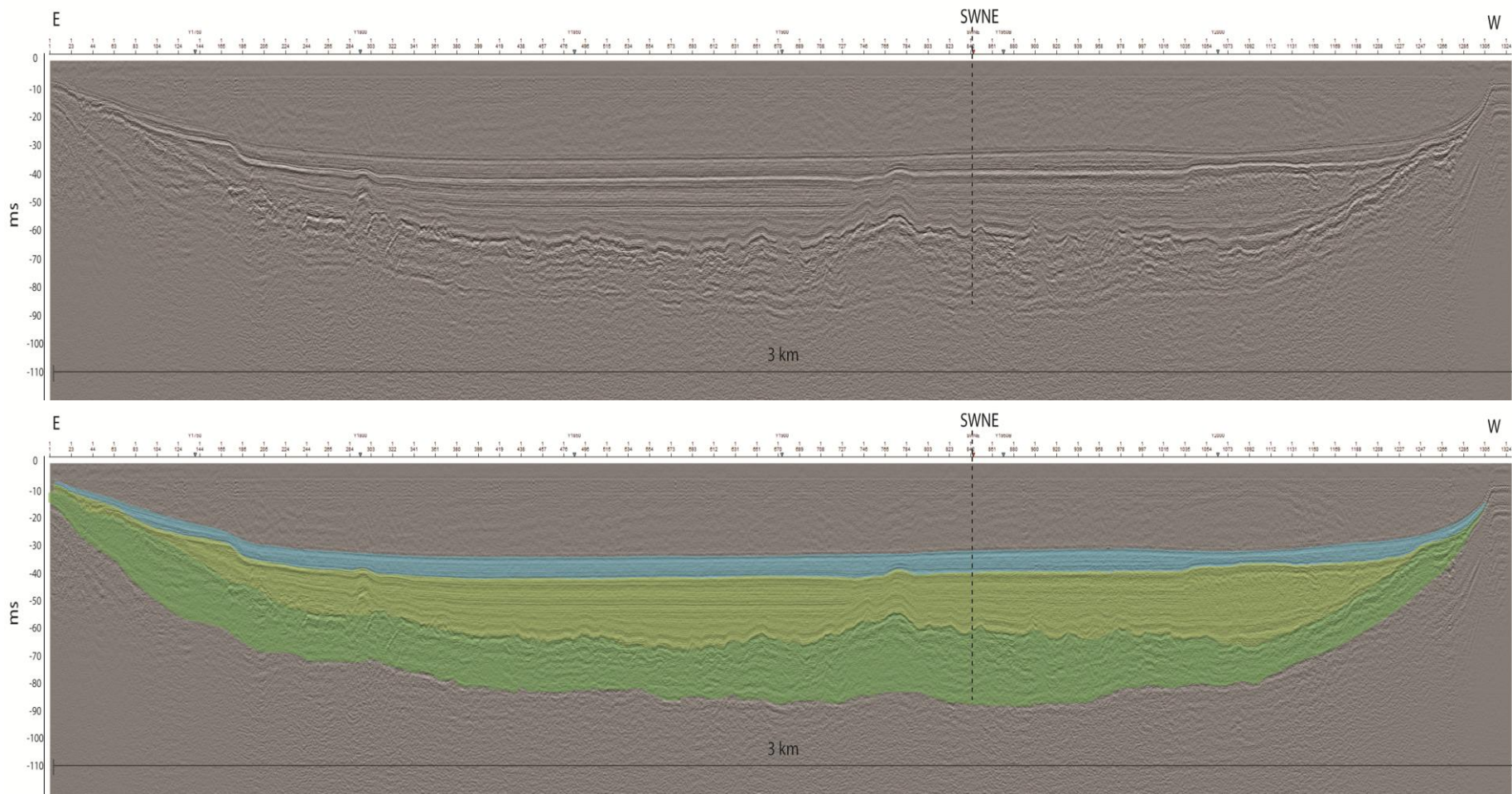


Figure 55 Above, seismic section X080, below, interpreted seismic section with the correspondent coloured sequences described in the chapter above.

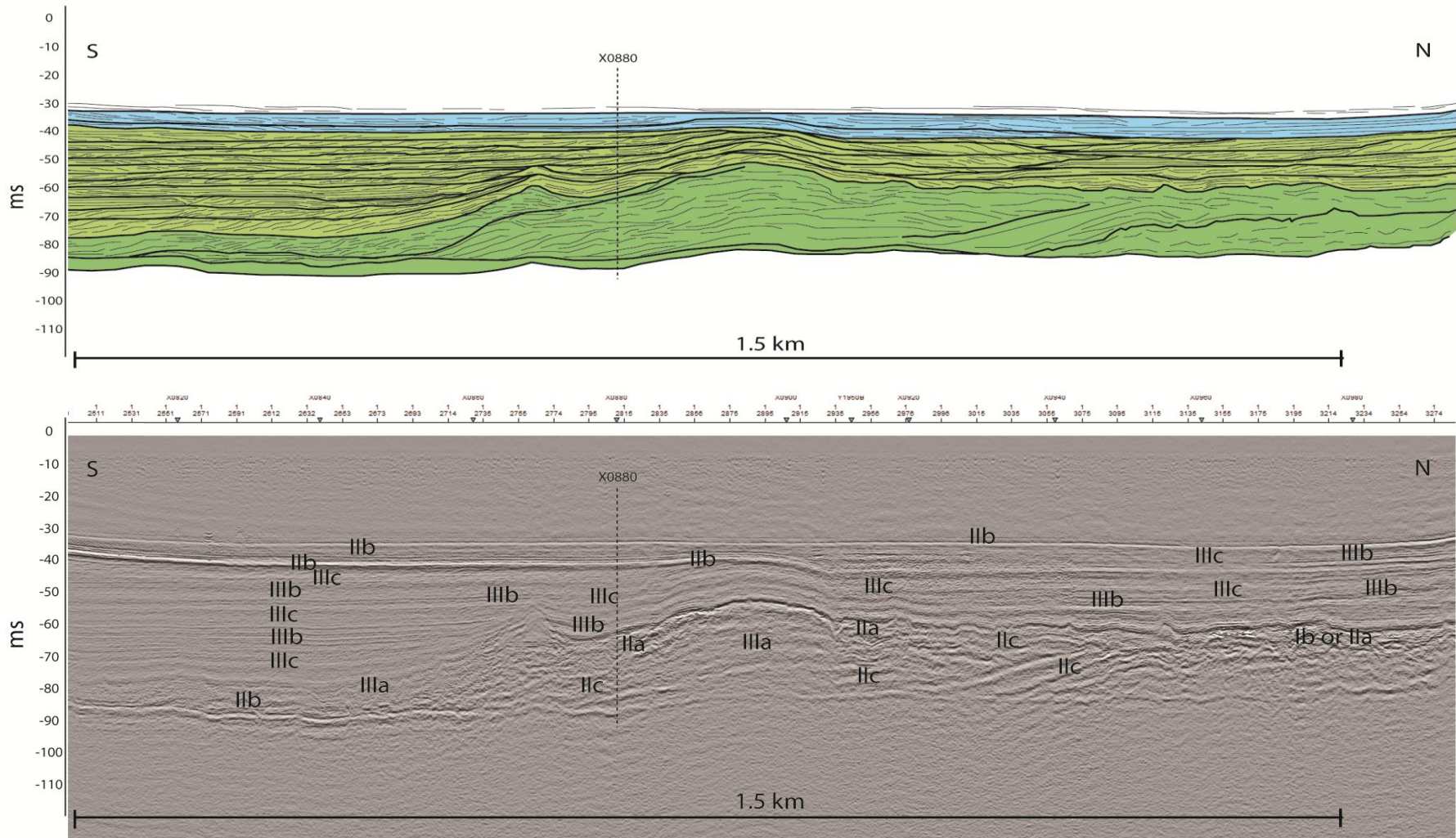


Figure 56 Above (A), final outcome showing interpreted reflectors geometry and seismic sedimentary sequences in seismic section SWNE (northernmost part), below (B), assigned seismic facies in the same seismic section.

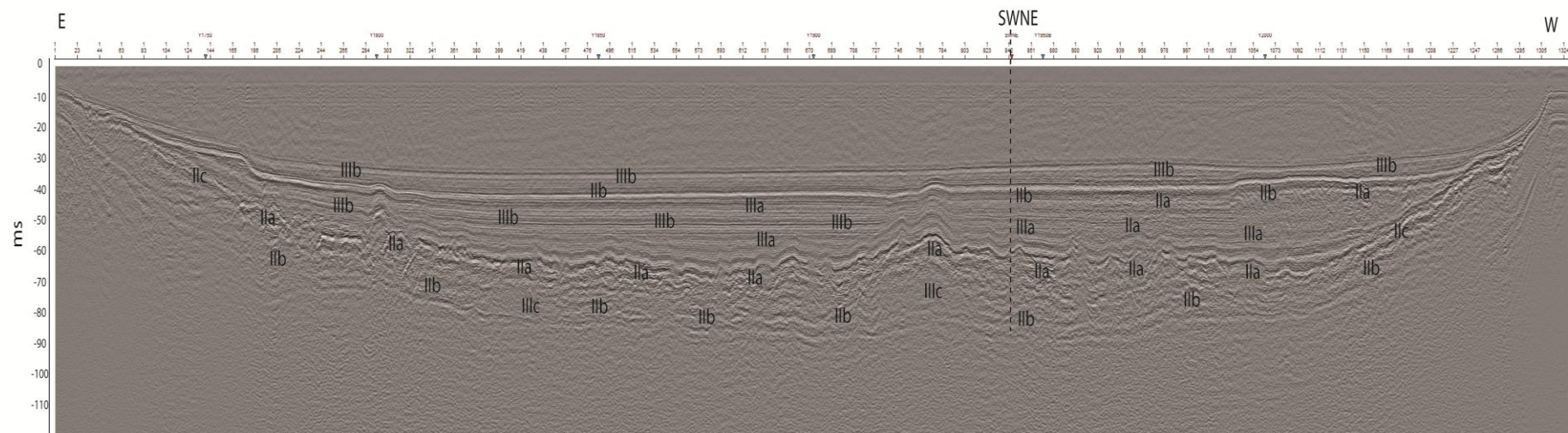
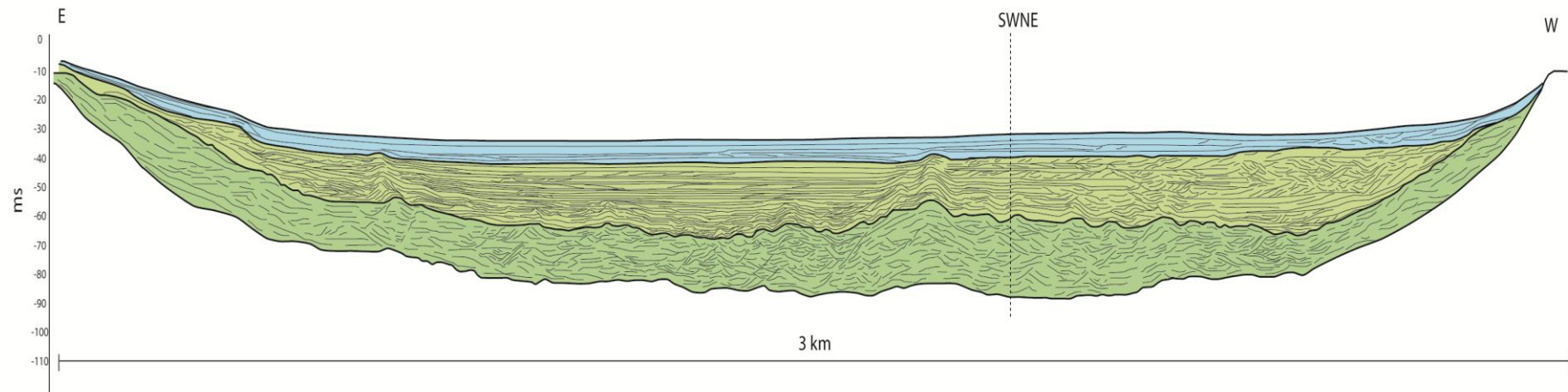


Figure 57 Above (A) final outcome showing interpreted reflectors geometry and seismic sedimentary sequences in seismic section X0880. Below (B), seismic facies associated to this seismic line.

14.1.2 Internal reflection characteristics

Section SWNE

As depicted before, the Green Sequence present in this area has two very different seismic signatures, and will be divided into Lower and Upper Green Sequence.

From the north end towards the south of the section, over a distance of about 1.4 km and with a thickness of approximately 20ms (35m) diminishing to the south, tangential oblique progradational reflections are observed. Clear downlaps terminations are visible towards the southern part of the section. Most of the dipping reflectors, prograding south, offlap or onlap into older dipping sequences towards the north. At least three of these prograding sequences are observed. Another observation that can be made is that the last of these prograding sequences presents an antiform shape. The high reflectivity of these reflectors indicates high-energy deposits with a southward progradational tendency. Facies IIa, IIb and IIc from Pugin et al. (1999) have been assigned to them. This would indicate the presence of mainly sand and gravel with occasional silt interbedded lithologies in a channelized depositional setting.

A very reflective and continuous reflector, that marks the transition with upper part of the Green Sequence, caps this thick sequence. The Upper Green Sequence drapes the underlying topography with parallel to subparallel reflections. Reflections here seem to lose strength towards the south indicating a loss in transport energy and probably a gradual change in grain size towards the south, indicated by the changes in seismic facies from IIIb to IIIc. These seismic facies indicate that most of the Upper Green Sequence is composed of sand and silts bed sets with occasional shale or till.

The layers present a compensational stacking, filling up the space available left by the previous draping sediment sheets and by the lower Green Sequence (onlap terminations over the oblique progradational reflections).

After, when observing the seismic reflections in detail, progradational features are also observed within the thin layers that compose the Upper Green Sequence. Most of these reflections indicate a southward progradation tendency although progradation in the other direction can also occur.

Section X0880

This section crosscuts section SWNE in its middle part. This perpendicular view gives us an insight on the Lower Green Sequence and Upper Green Sequence.

The previously described Lower Green Sequence is clearly differentiated from the bedrock by the high amplitude of its reflections. Reflectors in this case appear to be incoherent with occasional hints of a sub-parallel but discontinuous organization. The high amplitude of the signal indicates high-energy deposits, but the lack of continuity indicates an important lateral variability. Seismic facies IIa and IIb have been assigned to this interval as shown in Figure 57 (B) that matches the seismic facies signature of the perpendicular section. As stated before this seismic facies correspond to coarse-grained lithologies (sand and gravel) and its internal geometries (occasional concave shapes or channelized

features) suggest that these sediments have been deposited in a channelized environment.

As in the perpendicular section, this interval ends with a highly reflective reflector. Above, the Upper Green Sequence drapes the remnant topography and rapidly acquires its characteristic parallel geometry (seismic facies IIIb). As seen in section SWNE, the Upper Green Sequence is composed of several draping layers. These layers onlap the lower deposits on the east and west sides of the section (valley flanks). In the central part, geometries appear to be more parallel and no clear signs of reflector termination are visible. Another important observation is that the Upper Green Sequence does not show many signs of progradation in any direction within its internal layers, giving us information about what was the main flow direction.

14.2 Interpretation and infilling history

The reflectors signal and geometries combined with the associated seismic facies found in the Green Sequence all indicate a change from a high energy environment to a posterior low energy environment within a same geological formation: the Oak Ridge Moraine.

Reflectors found in the lower sequence have a stronger signal than the ones found above and their dipping directions clearly indicate progradation towards the south. Various stages of progradation are visible since the southern most reflectors from the Lower Green Sequence onlap dipping reflectors of previous sequences towards the north. Furthermore seismic facies with medium to high reflectivity (facies II) indicate the presence of coarse-grained lithologies common in channels.

The presence of the Lower Green Sequence only in the northern most part of the seismic section indicates that the depositional conditions were localized and only found close to the sediment source. This source must have been subjected to intensive erosional conditions.

Internal geometries suggesting a channelized context and the existing glacial geological context suggest that a glacier retreat and strong meltwater flows must be responsible for the formation of this sequence. The different progradational sequences within the Lower Green Sequence can then be ice-front indicators. This will explain why the northern most sequence appears to have a flatter top and the last sequence was not eroded and remained with its antiform shape.

We can then interpret this sequence as a channelized southward prograding system of limited extension building the equivalent of a frontal moraine morphology (see Lønne, 2001). This moraine morphology would have been formed in front of a glacier during at least three pulses of ice-advance during a global ice-sheet retreat episode.

The transition towards a calmer environment (probably lacustrine) (Upper Green Sequence) is rather abrupt and a strong bounding reflector, which would indicate non-deposition, by-pass or erosional conditions of the Lower Green Sequence, characterizes the transition. The transition would also indicate changes in the sediment source area and in subglacial flow dynamics.

Three scenarios for this transition are proposed in Figure 58.

Scenario 1 corresponds to an ice-sheet retreat that eroded the upper part of the Lower Green Sequence while retreating with a sediment by-pass over the Lower Green Sequence and deposition further south where accommodation space is available.

Scenario 2 implies that the ice-sheet is still present over the Lower Green Sequence but changes in the sediment source area (change in the transport direction or in rock type) would have stop the input of coarser sediment to the system.

Finally, Scenario 3 suggests the presence of a grounding ice-sheet over the Lower Green Sequence and the presence of floating ice over the rest of incised tunnel valley. This scenario would suggest a stop or a change in the sediment input from subglacial flows and sedimentation by suspension and precipitation of debris attached to the floating ice-sheet.

Later stages of infill still imply that the sediment source was then located further north, and the accommodation space available was filled with fine-grained sediments deposited mainly from suspension. The depositional model would explain how the Upper Green Sequence draped and mimicked the previous topography. The lacustrine type environment must have had occasional northward prograding sediment flows of medium to fine grained sediments indicating no more influence of ice-sheet in the north. The direction of this prograding sediment sheets indicates that the flows was still directed towards the south.

We conclude that the Upper Green Sequence was deposited in low energy conditions during a late post-glacial era.

The above Blue Sequence presents signs of slow progradation (almost flat and parallel reflectors) towards the north. This change in direction would mark the end of the glacial period and the glacio-isostatic rebound related to the unloading of the glacier, uplifting the terrains from south to north. In a map by Walcott (1973) the isostatic rebound in the area can be given an approximated height of about 20 meters.

Figure 58 shows the evolution model of the area in terms of sediment fill and ice-movements.

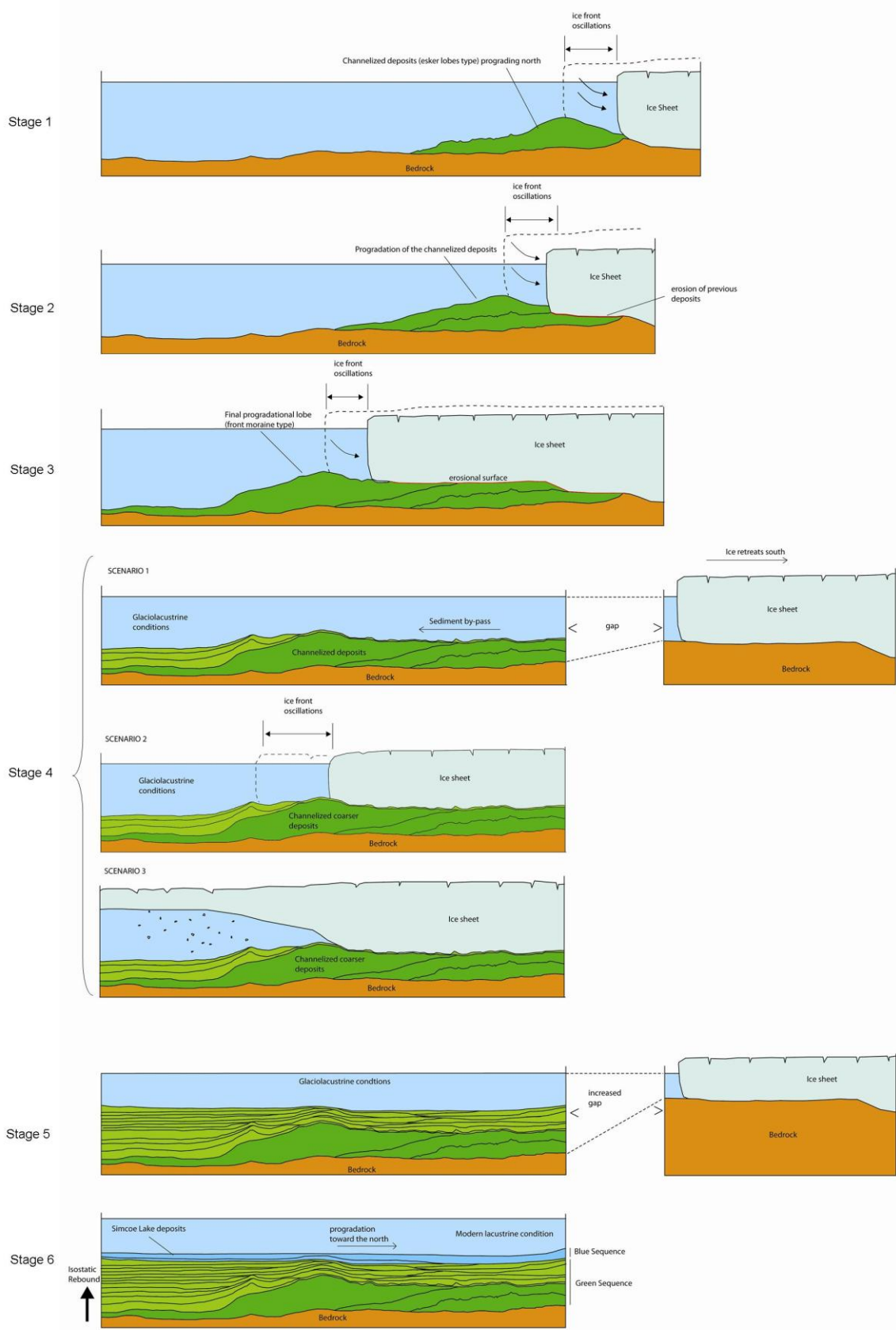


Figure 58 schematic depositional models of the Oak Ridge Moraine deposits found in the studies area in the northern part of Cook's Bay, Lake Simcoe (Canada).

15 Discussion

The study of two large glacially influenced incisions of different age and size, the Upper Ordovician from Block-NC186 in Libya and the Pleistocene from Lake Simcoe, Canada, highlighted the existence of several factors controlling the sedimentary processes and architecture of the resulting valley infills.

The two heterogeneous glacial systems infills seem to be influenced by a series of parameters such as the sizes of the glacial incisions, the bedrock type and the geographical setting (marine and lacustrine).

Previous studies by Le Heron et al. (2004) have interpreted the sedimentary architecture of Upper Ordovician tunnel valleys in the Murzuq Basin, and more precisely in the Gargaf Arch, located ca. 100 km north of our study area (Block-NC186).

In our study area, the Upper Ordovician Melaz Shuqran and Mamuniyat formations are found in a series of NW-SE elongated palaeo-valleys of different sizes forming a complex subsurface topography.

The creation of such complex topography is directly related to glacial erosion over the pre-glacial semi-lithified Hawaz Formation. Observations made from seismic sections and the isopach map of the Upper Ordovician deposits in Block-NC186 show that the incisions are mainly fault bounded suggesting an important structural control in the result subsurface morphology. Further studies in the Gargaf area by Ghienne et al. (2003) described the palaeo-valleys and fault-controlled depocenter of the Upper Ordovician successions and describe the main glacial valleys as partly controlled by inherited Panafrican structural trends. These fault trends are also observed in Block-NC186 and therefore suggest a similar origin to the incisions.

The spacing of these faults can be an important factor determining the type of incision and the later infill. A larger spacing will induce more unconfined incision types with wider erosional shapes. McDougall and the technical team working in the Block-NC186 (Remsa) suggest that these larger erosions are related to ice stream incisions (Area 1). In the other hand, a smaller spacing between faults will probably favour subglacial erosion associated with the incision of narrower glacial tunnel valley types (seen in Areas 2 and 3).

The type of bedrock could also influence the type of erosion and the palaeo-topography. In Block-NC186, the pre-glacial deposits correspond to the Hawaz Formation, an estuarine to shallow marine formation of Middle Ordovician age. The rock type and the close age of the later glacial episode (Upper Ordovician) suggest that the bedrock may have been poorly consolidated and therefore easily erodible.

Infilling differences within incision types also support two different types of depositional environments. Larger incisions present thicker Melaz Shuqran and thinner Mamuniyat sections (only part of the Lower Mamuniyat is present in Area 1) and thus containing therefore a lower sandy content. On the other hand, wells situated in narrower incisions (e.g. tunnel valleys such as in Areas 2 and 3) show very sandy sequences of Mamuniyat Fm. with the Melaz Suqran Fm. commonly absent in the centre of the incision and with some thin clayish

sections observed in the flanks.

The sedimentary architecture of the infill deposits in Block-NC186 is characterised by a series of vertically and laterally unconformity-bounded and very heterogeneous units, each of them corresponding to multiples incisions and depositional episodes. At least four main episodes of glacial advance, retreat and possible glacio-isostatic rebound have been determined through the sedimentological study and indicate large fluctuations of the ice-sheet front (>10km). Moreover, the type of infill corresponds to sediments deposited in glacio-fluvial and glacio-marine conditions in an open marine setting.

Comparing the previously described Upper Ordovician system to the Oak Ridges Moraine (Pleistocene) in Canada, we can observe some similarities.

The morphology of the incision observed in seismic sections in the Cook's Bay area, show one single tunnel valley few kilometres wide and tens of kilometres long, similarly to the examples observed in Libya (Areas 2 and 3), although no faults were identify on seismic.

Fewer parallel incisions are found in the region and most of the parallel tunnel valley networks appear further north of Lake Simcoe area. However, in this case, no apparent fault system seems to influence or control the location of these incisions.

The bedrock type could then explain the lack of abundance of tunnel valleys in this area. Here, the tunnel valleys are cut into the Newmarket Till until locally reaching the hard Ordovician limestone bedrock. In contrast to the Hawaz Formation in the Murzuq Basin (Libya), the limestone bedrock is hardly erodible, and the extension of the Newmarket till will be responsible for the development of a tunnel valley network in the Lake Simcoe area. The development of such network is more visible further north where the Cambrian shales bedrock is present.

In agreement with previous work in the area (e.g. , Russel et al., 2004; Todd and Lewis 2008) the study of the sedimentary sequences found in Lake Simcoe shows that a single episode of incision occurred. The infilling sediments were deposited during a single ice-sheet retreat characterised by small pulses of ice-advance over short distances (<1km). Deposits are characterised by channelised deposits changing towards the south into a lacustrine environment indicating fast changes in energy conditions.

Nevertheless, discrepancies between our infilling model of Lake Simcoe and the one proposed by Russel et al. (2004) can be highlighted. The seismic characteristics observed in this study indicate that infilling of the continental lake implies deposition occurred at the ice-contact front in a moraine like morphology similar to the ones observed in Norway and described by Ida Lønne (2001), instead of a subglacial infilling system (Russel et al., 2004).

In summary, glacial erosion and formation of tunnel valleys seem to be formed over softer bedrock formation (Hawaz and Newmarket Till Fm). The size and morphology of the incisions are likely influenced by the pre-existing structural grain (e.g. lineaments and faults). Size and morphology will also influence the type of sediment infilling such incisions. Sedimentary architecture will vary according to the extension of the glaciations and the fluctuations of the ice-sheet in time. Furthermore, the geographic setting also plays an important role in the

facies types found in glacial setting, with higher energy environments found in marine shelf settings and low energy facies found in continental lake settings.

16 Conclusions

The study of glacial tunnel valley reservoirs from the Upper Ordovician from North Africa and the Pleistocene from Canada show the development of these glacial incisions in different geographical and geological settings.

The Upper Ordovician deposits from Block-NC186 show a series of unconformity-bounded units infilling a palaeo-topography formed by several episodes of glacial erosion. The different types of incisions present in the area influence the conditions and therefore the depositional environments in which each of these units are accumulated, leading to important changes in reservoir architecture and possibly reservoir properties. In the other hand, the Pleistocene from Lake Simcoe shows a single phase of infill of a tunnel valleys incision with different facies associated to small fluctuations stages of a single episode of ice-sheet retreat.

The reliability of the sedimentary models proposed in this work depends on the amount and quality of data available. The large complexity, intrinsic of glacial systems further increases the level of uncertainty of the outcomes of this type of studies.

However, the use of an integrated approach can play a key role in reducing uncertainties. Like in this study the use of large-scale data such as block-scale seismic and isopach maps can help determining a structural framework, whereas punctual data from wells can provide the information needed to determine the sedimentology and depositional mechanisms associated with the sedimentary infill.

Furthermore, the use of Quaternary analogues has proven its importance not only in improving the understanding, at a smaller scale but at higher resolution, of single events occurred during glacial events, but also in showing the influence of other factors such as bedrock type and depositional setting (lacustrine) responsible for variations in observed features in the same kind of environments.

From this study, we conclude that when modelling glacial tunnel valley, we have to take into account a series of factors such as the influence of a pre-existing structural trends, the bedrock type, the magnitude of the glaciations (and associated eustatic-levels variations) and the (palaeo-)geographical setting (marine or continental).

Improving modelling parameters in such systems can improve prediction in such heterogeneous depositional systems and determine a better understanding of good reservoir quality facies and possible magnitude and distribution intraformational seals/non reservoir facies.

17 References

- Bahlburg H., Dobrzinski N. (2009). A review of the Chemical Index of Alteration (CIA) and its applications to the study of Neoproterozoic glacial deposits and climate transitions. In: Arnaud E., Halverson G.P., Shields G. A. (eds.), *The Geological record of Neoproterozoic Glaciations*. Geological Society, London, Memoir 36.
- El-ghali M.A.K. (2005). Depositional environments and sequence stratigraphy of paralic glacial, paraglacial and postglacial Upper Ordovician siliciclastic deposits in the Murzuq Basin, SW Libya. *Sedimentary Geology* 177, pp. 145-173.
- Ghienne J-F., Deynoux M., Manatschal G., Rubino J-L. (2003). Palaeo-valleys and fault-controlled depocenters in the Late-Ordovician glacial record of the Murzuq Basin (central Libya). *C. R. Geosciences* 335, pp. 1091-1100.
- Hambrey M. J. (1985). The Late Ordovician-Early Silurian Glacial Period. *Palaeogeogr., Palaeoclimatol., Palaeoecol.*, 51, pp. 273-289.
- Le Heron D., Sutcliffe O., Bourgig K., Craig J., Visentin C., Whittington R. (2004). Sedimentary architecture of Upper Ordovician tunnel valleys, Gargaf, Lybia: Implications for the genesis of a hydrocarbon reservoir. *GeoArabia*, Vol. 9, No. 2, pp. 137-160.
- Lønne I. (2001). Dynamics of marine glacier termini read from moraine architecture. *Geology*, vol. 29; no.3; pp. 199-202.
- McDougall N., Adballah H., Tawengi K. (2008). Late Ordovician Palaeo-valleys in the Sahara. *AAPG-ER Newsletter*, pp. 11-14.
- Ó Cofaigh, C. (1996). Tunnel valley genesis. *Progress in Physical Geography*. 20, 1-19.
- Powell R.D. & Cooper J.M. (2002). A glacial sequence stratigraphic model for temperate, glaciated continental shelves. In: Dowdeswell, J.A. & O Cofaigh, C (eds) 2002. *Glacier Influenced Sedimentation on High-Latitude Continental Margins*. Geological Society, London, Special Publications, 203, 215-244.
- Pugin A., Pullan S. E., Sharpe D. R. (1999). Seismic facies and regional architecture of the Oak Ridges Moraines area, southern Ontario. *Can. J. Earth Sci.* 36, pp. 409-432.
- Ramos E., Marzo M., de Gibert J. M., Tawengi K. S., Khoja A. A., Bolatti N. D. (2006). Stratigraphy and sedimentology of the Middle Ordovician Hawaz Formation (Murzuq Basin, Libya). *AAPG Bulletin*, Vol. 90, No. 9, pp. 1309-1336.

Russell H. A. J., Arnott R. W. C., Sharpe D. R. (2004). Stratigraphic Architecture and Sediment Facies of the Western Oak Ridges Moraine, Humber River Watershed, Southern Ontario. *Géographie physique et Quaternaire*, vol. 58, n° 2-3, pp. 241-267.

Scheffler K., Buehmann D., Schwark L. (2006). Analysis of Late Palaeozoic glacial to postglacial sedimentary successions in South Africa by geochemical proxies – Response to climate evolution and sedimentary environment. *Palaeogeogr., Palaeoclimatol., Palaeoecol.* 240, pp. 184-203.

Shilts, W.W. and Clague, J.J. (1992). Documentation of earthquake-induced disturbance of lake sediments using subbottom acoustic profiling. *Canadian Journal of Earth Sciences*, 28: pp. 1018-1042.

Sola M. A., Echikh K. (2000). Geology and Hydrocarbons occurrences in the Murzuq Basin, SW Libya. In: *Geological Exploration of the Murzuq Basin*, Chapter 9.

Todd B. J., Lewis C. F. M. (1993). A Reconnaissance Geophysical Survey of the Kawartha Lakes and Lake Simcoe, Ontario. *Géographie physique et Quaternaire*, vol. 47, n° 3, pp. 313-323.

Todd B. J., Lewis C. F. M. (2008). Quaternary features beneath Lake Simcoe, Ontario, Canada: drumlins, tunnel channels, and records of proglacial to postglacial closed and overflowing lakes. *J Paleolimnol*, pp. 361–380.

Walcott R. I. (1973). Structure of the earth from glacio-isostatic rebound. *Annual Review Earth Planet. Sci.*, pp. 15-37.

18 Appendixes

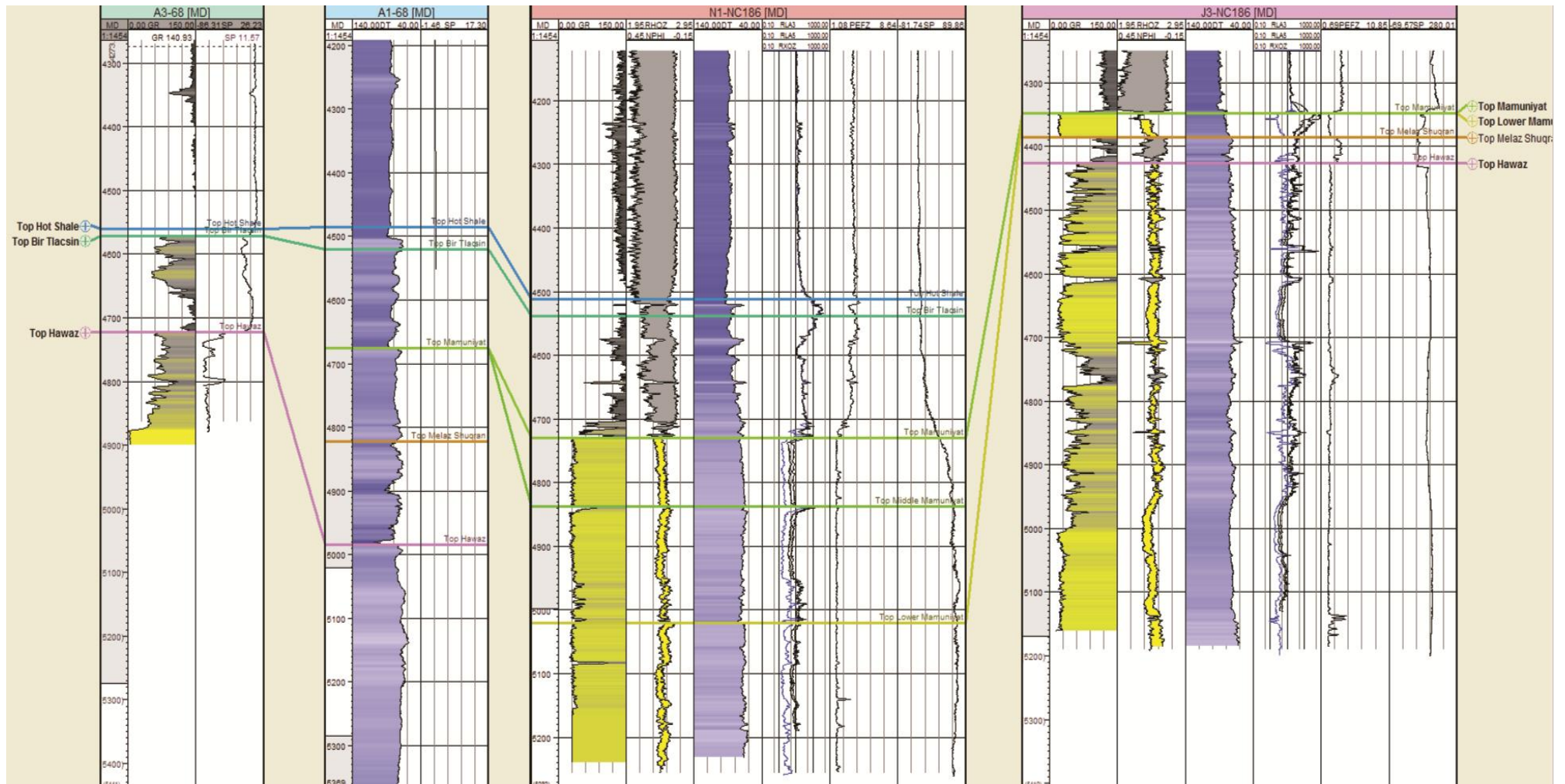


Figure 60 Area 2: Example of well correlation and well logs available for the study, flattened on top Tannezuft.

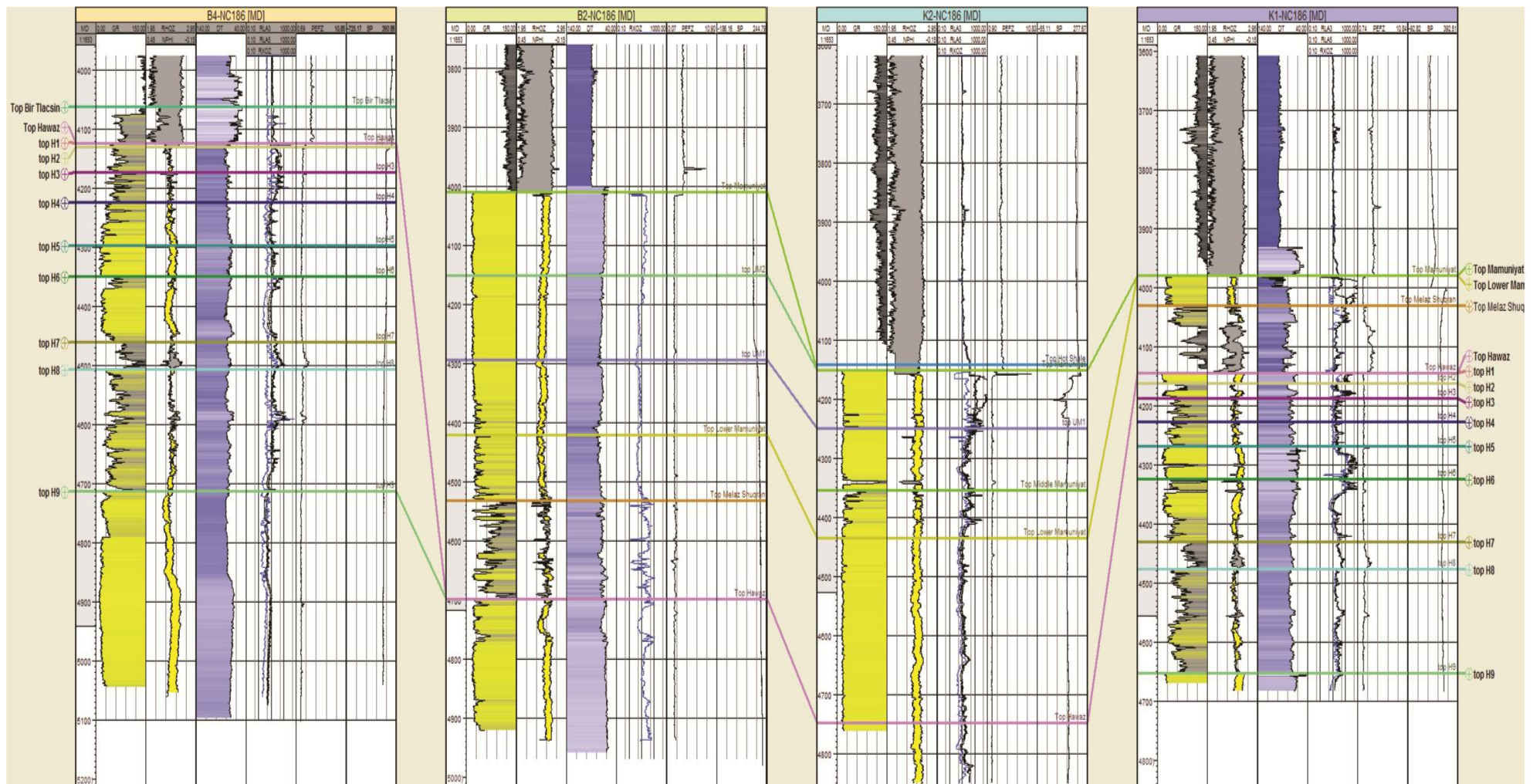


Figure 61 Area 3: Example of well correlation and well logs available, flattened on Top Tannezuft.

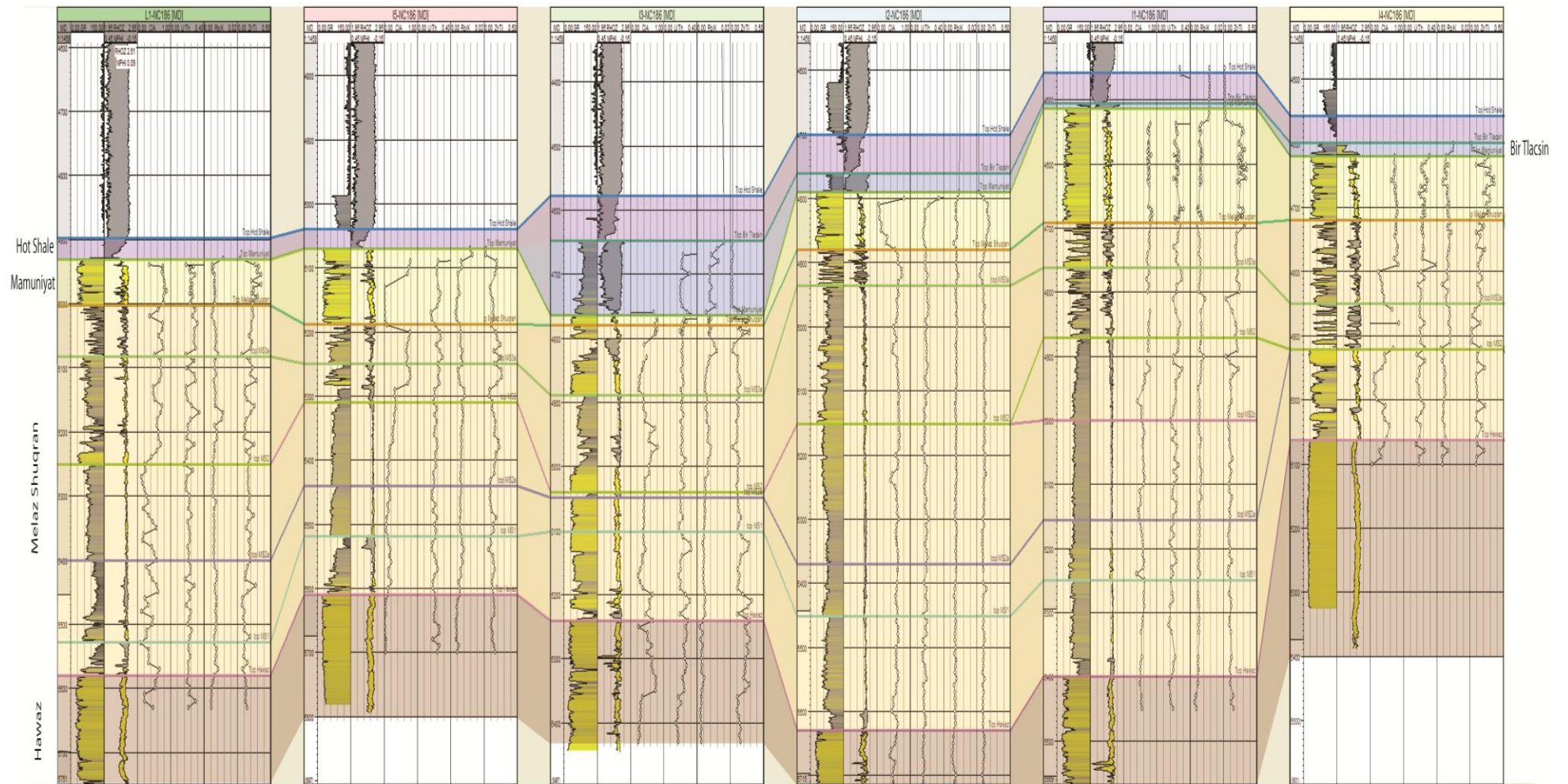


Figure 62 Area 1: Well logs and Chemostrat data available for correlation.

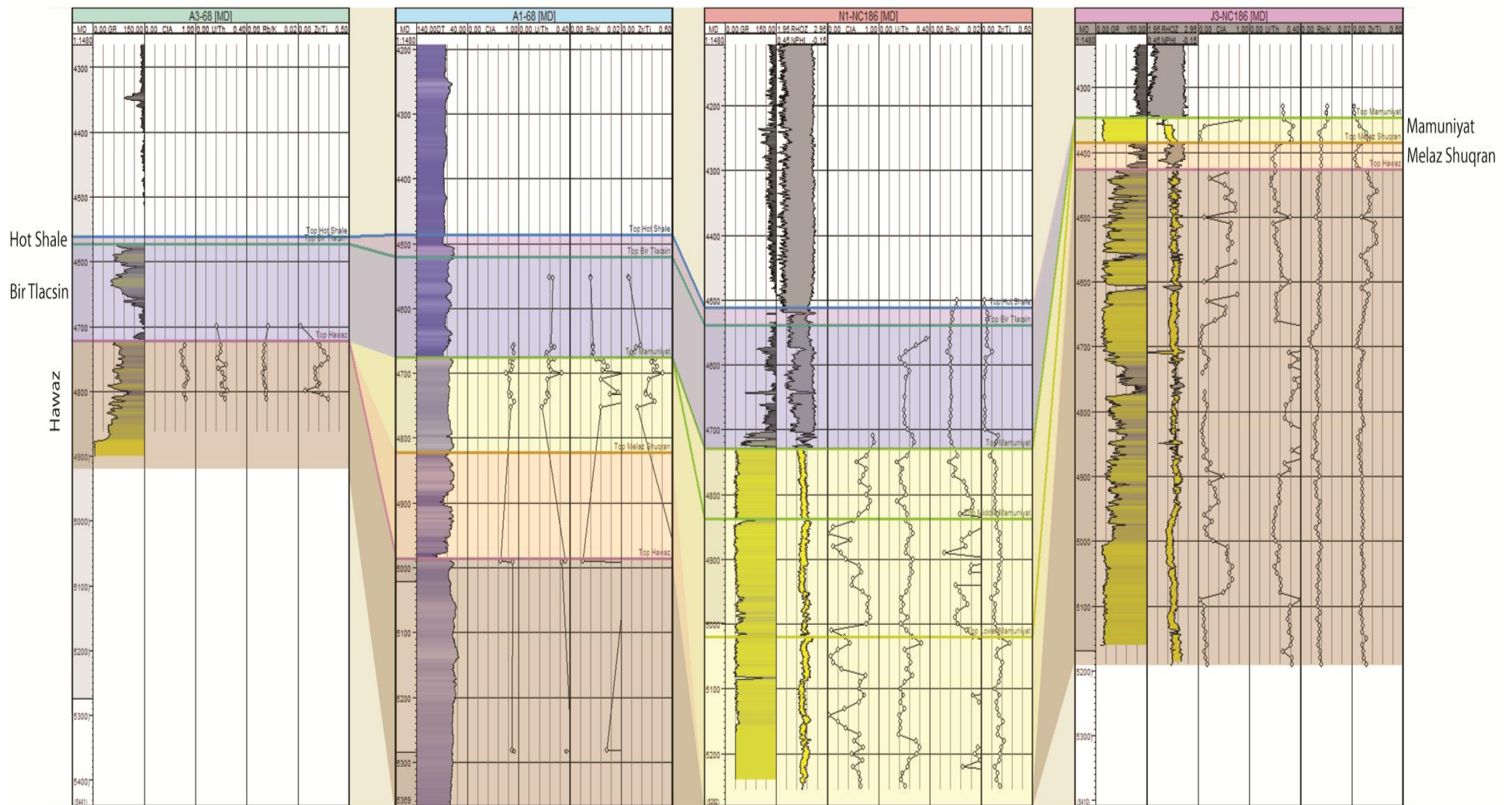
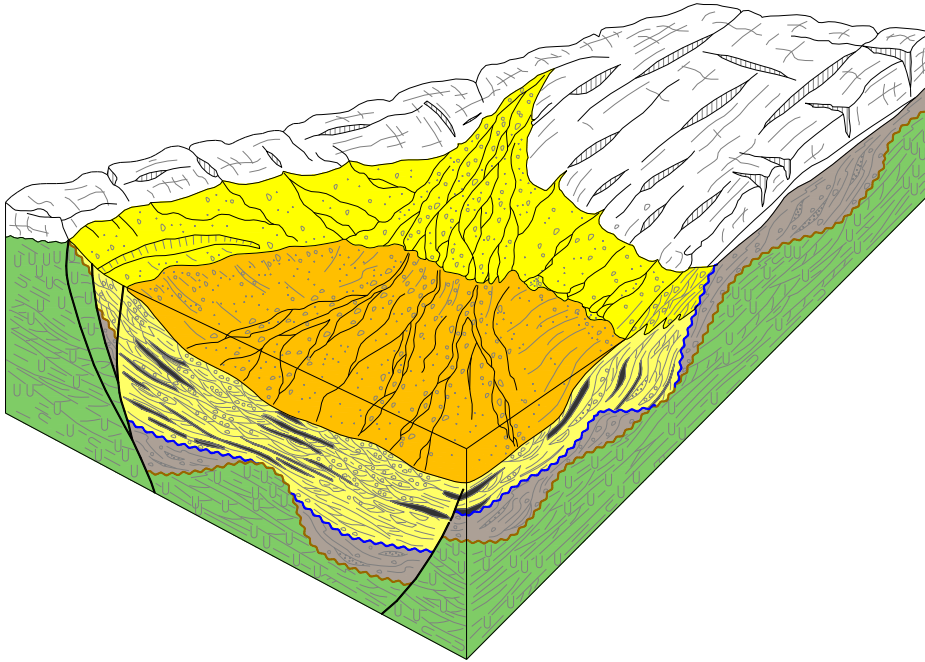


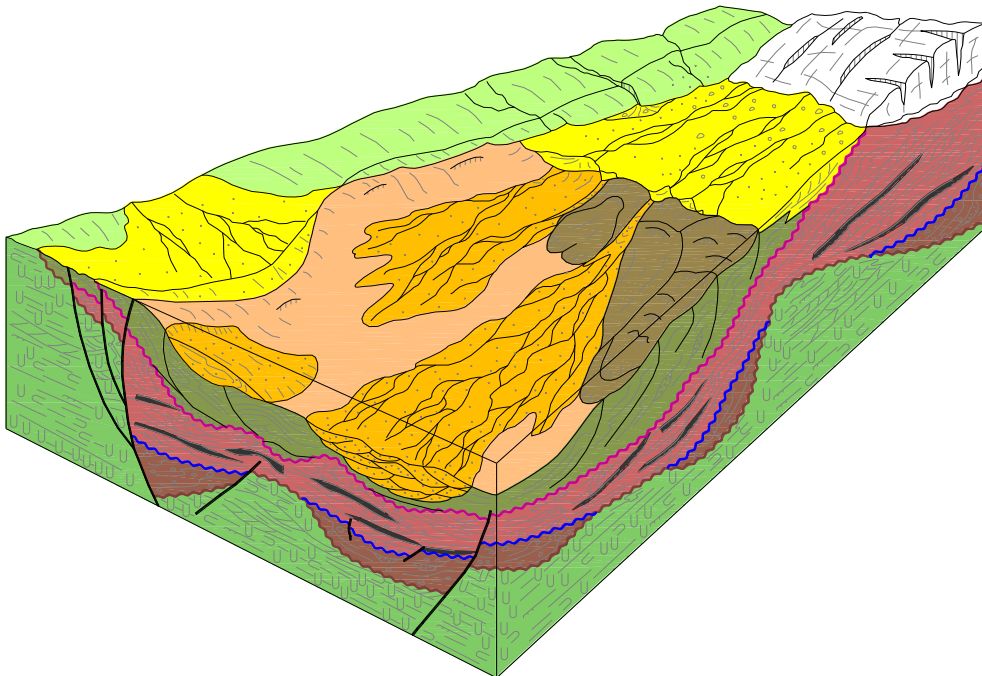
Figure 63 Area 2: Wells logs and Chemostrat data available for correlation

Examples of depositional environments from Neil McDougall for the Upper Ordovician formations

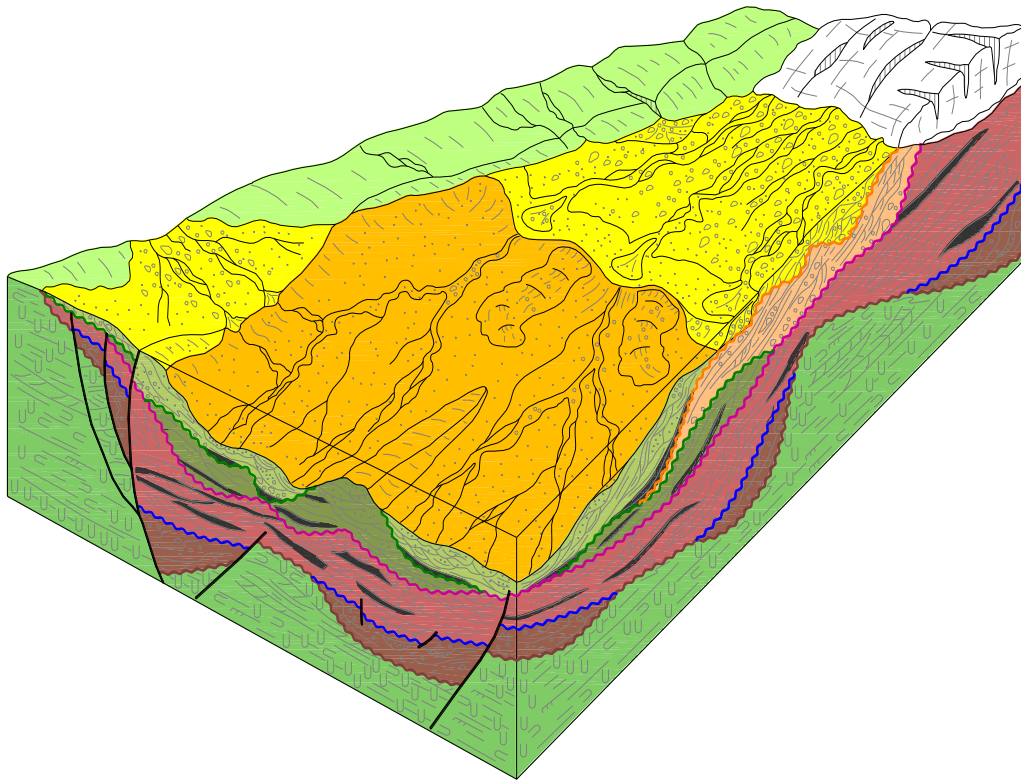
Lower Mamuniyat



Middle Mamuniyat

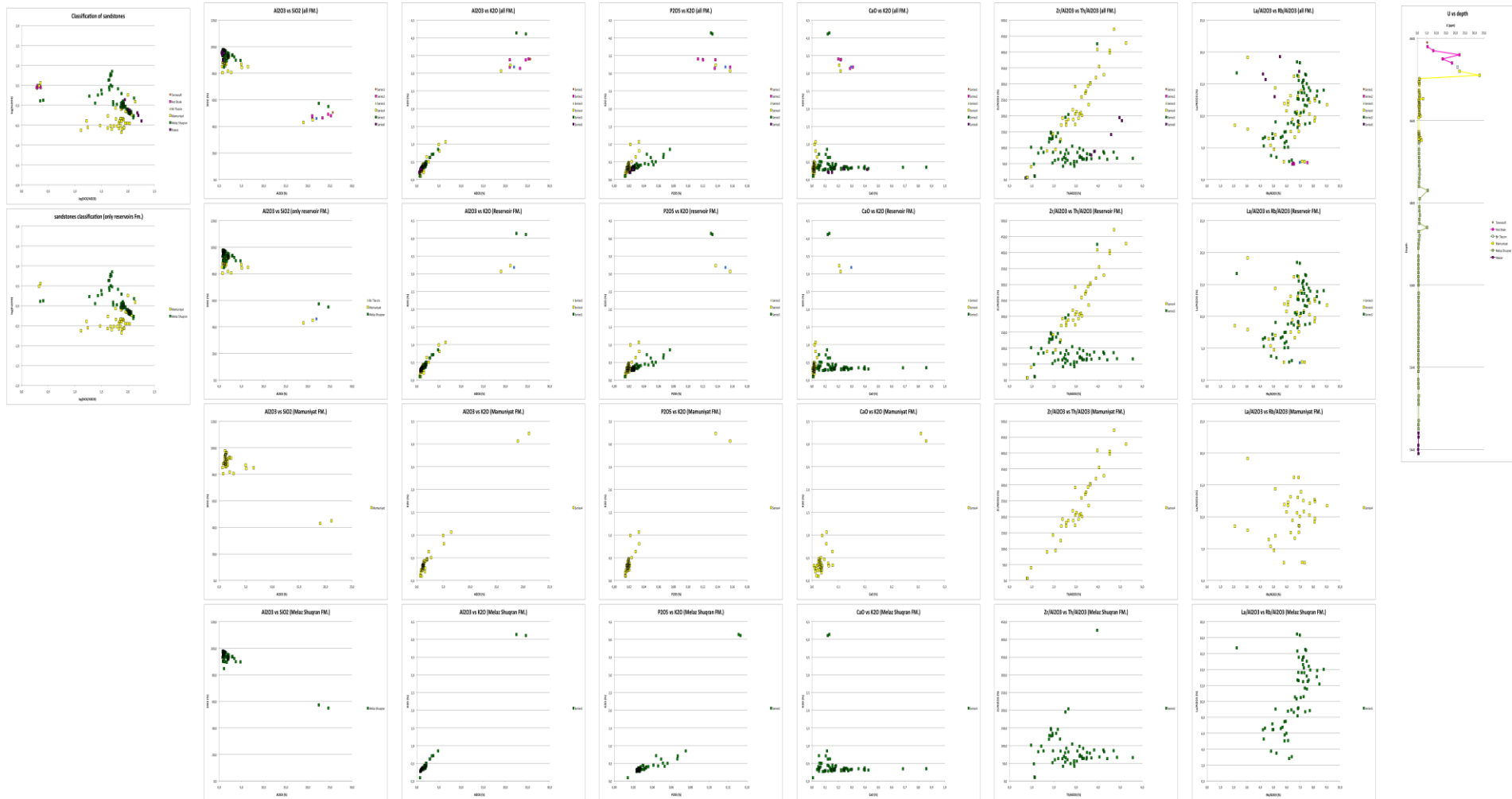


Upper Mamuniyat

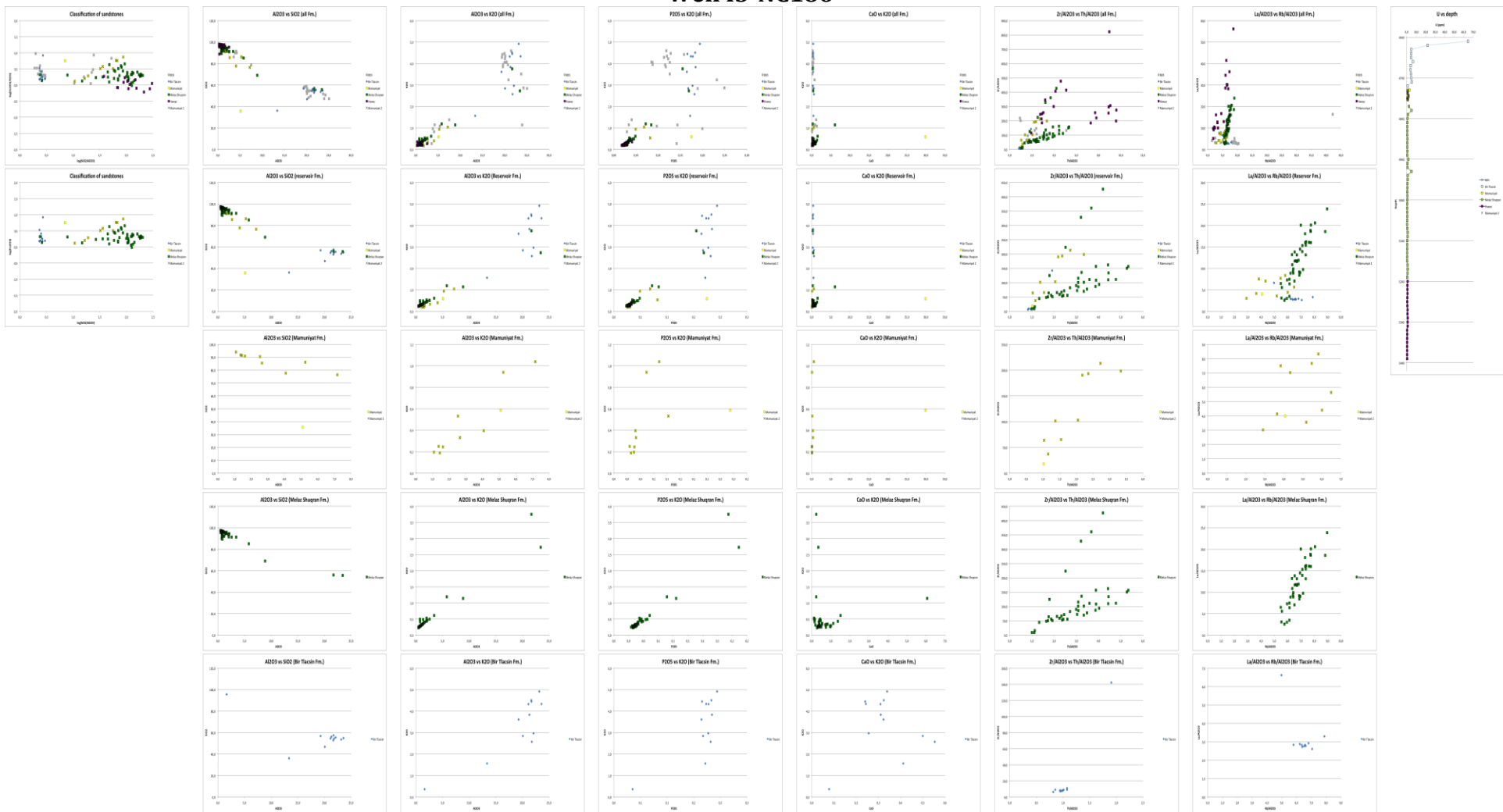


Examples of Chemostrat analysis: chemical ratios plotted for all formation and later by each formation individually:

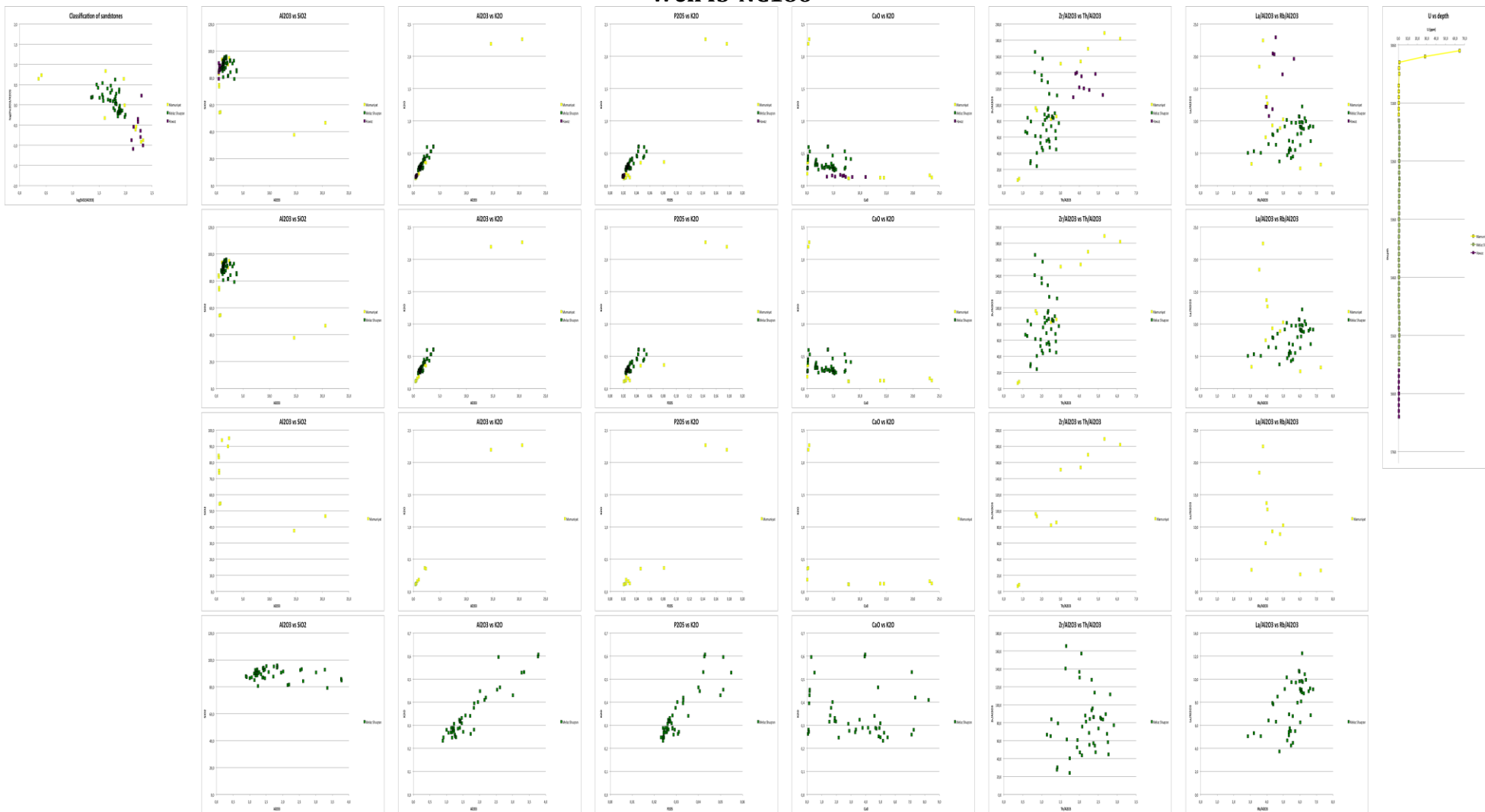
Well I1-NC186



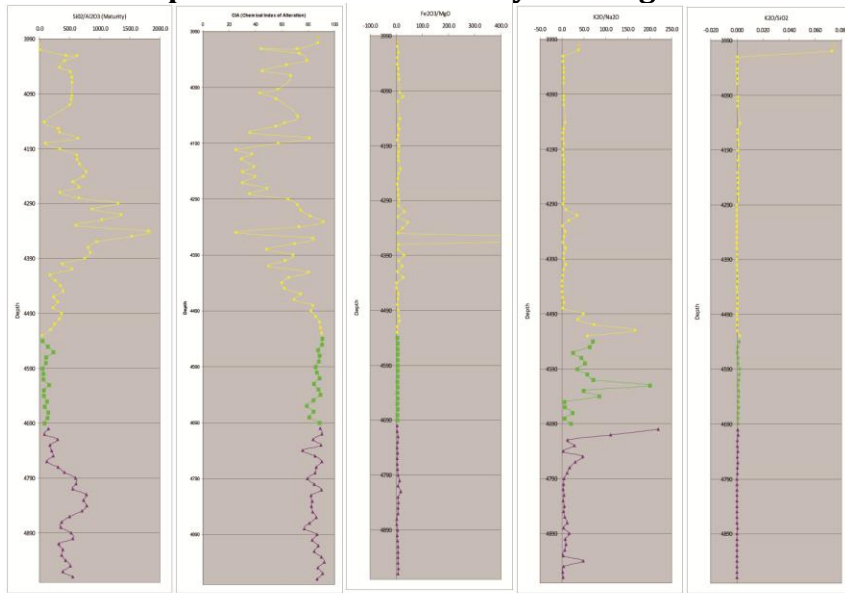
Well I3-NC186



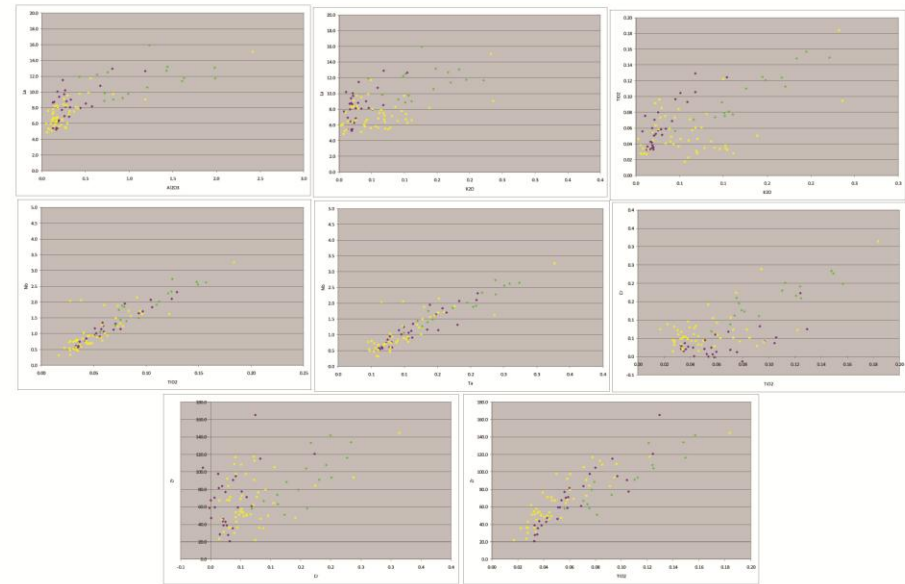
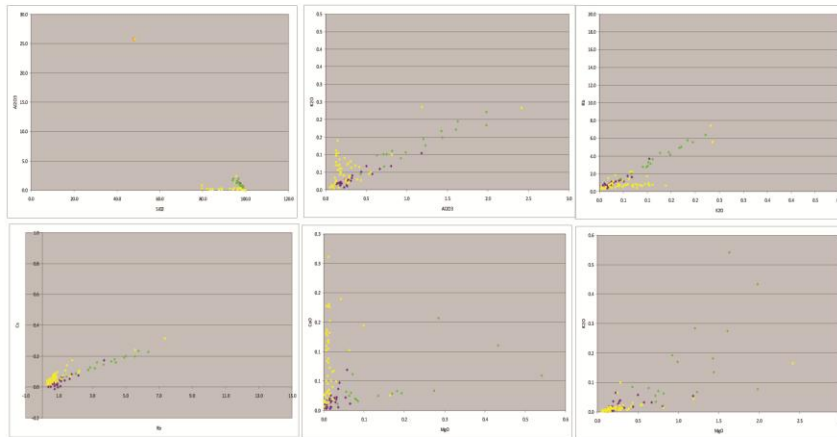
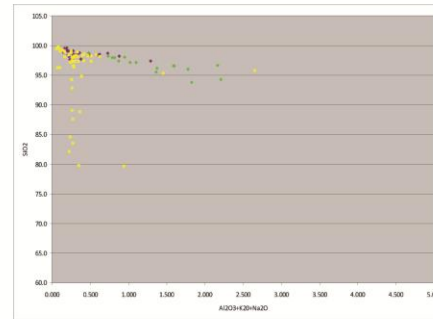
Well I5-NC186

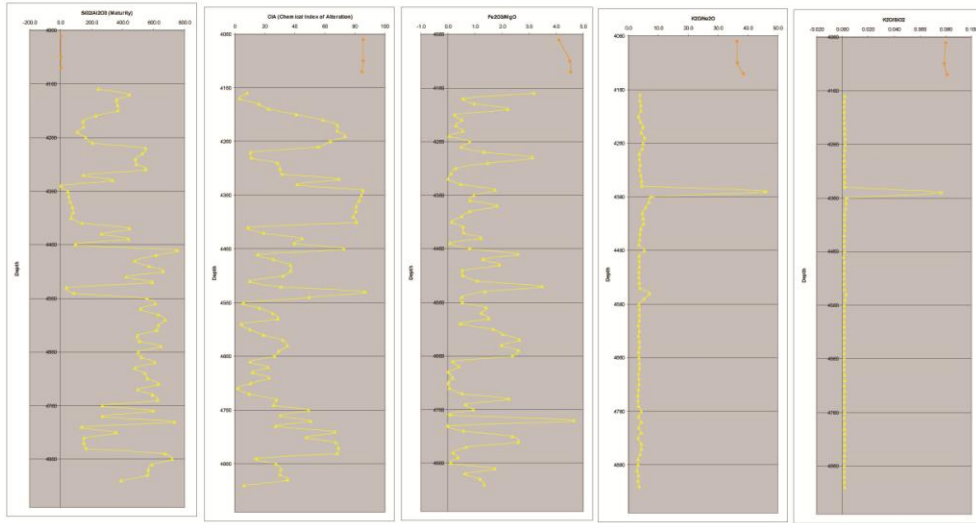


More examples of Chemostrat analysis using different wells and different geochemical ratios

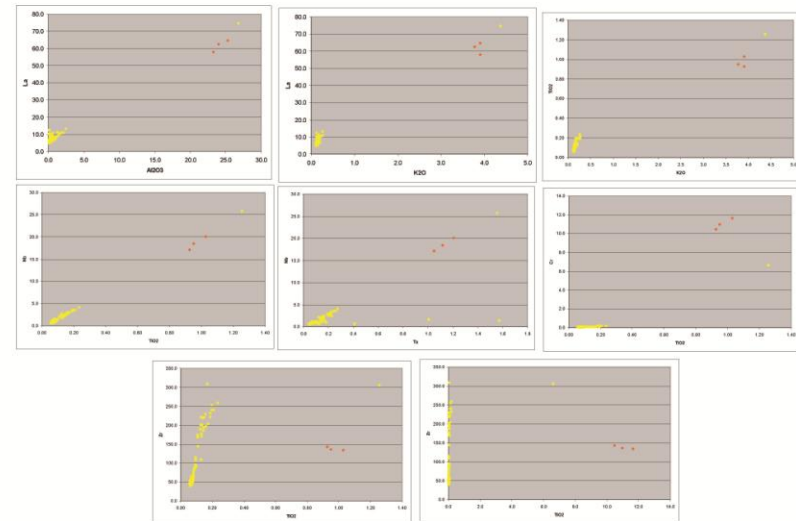
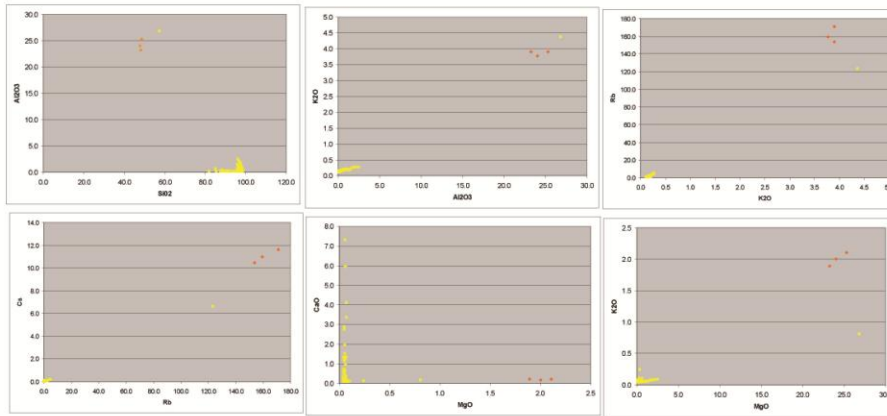
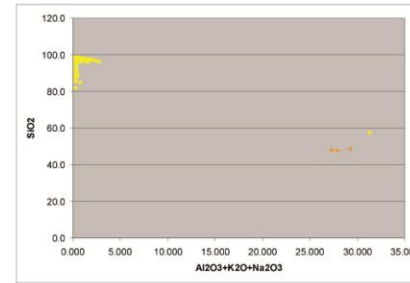


B2-NC186

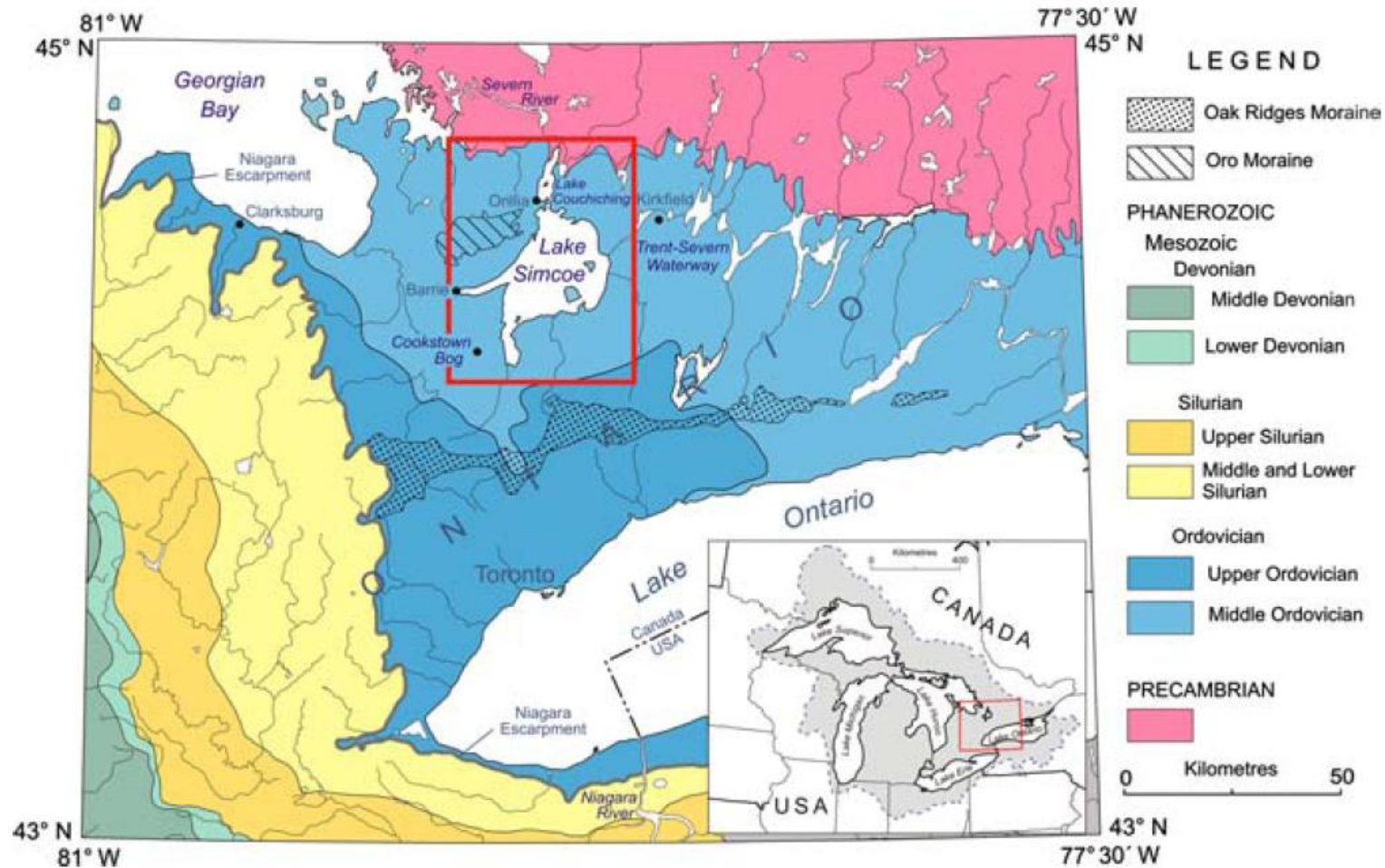




K2-NC186

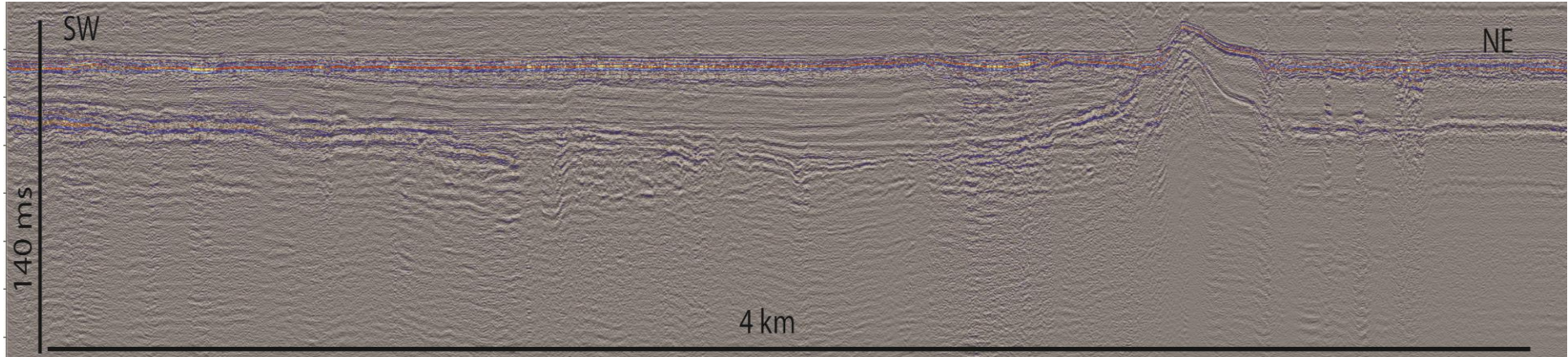


Geological map of the Lake Simcoe area showing the different types of basements and geological formations (after Todd et al. (2008)).



Complete view of seismic line SWNE in Lake Simcoe. The picture has been divided in two to fit this page, part 1 (above) shows the southernmost part of the lines, part 2 (below) shows the continuation of the line further north:

Part1:



Part 2:

